Hypoxia and Cell Signalling: Cardiovascular Remodelling, Glucose Homeostasis and Role of Calcium Channel Blocker (Cilnidipine)

Thesis submitted to
BLDE (Deemed to be University)
Vijayapur, Karnataka, India.

Faculty of Medicine

For the award of the degree of
DOCTOR OF PHILOSOPHY
in
Medical Physiology
By

Dr Shrilaxmi Bagali MBBS, MD

PhD Research Scholar
Registration No: 15PHD006

Laboratory of Vascular Physiology and Medicine,

Department of Physiology,

Shri B. M. Patil Medical College, Hospital and Research Centre,

BLDE (Deemed to be University),

Vijayapur, Karnataka, India

August 2019

DECLARATION BY THE CANDIDATE

I hereby declare that this thesis entitled *"Hypoxia and Cell Signalling: Cardiovascular Remodelling, Glucose Homeostasis and Role of Calcium Channel Blocker (Cilnidipine)"* is bonafide and genuine research work carried out by me under the supervision of Professor Kusal K. Das, (guide) Department of Physiology and Dr Akram A. Naikwadi, (co-guide) Department of Pharmacology, Shri B. M. Patil Medical College, Hospital and Research Centre, BLDE (Deemed to be University), Vijayapur, Karnataka, India. No part of this thesis has been formed the basis for the award of any degree or fellowship previously.

Signature of the Candidate

Dr Shrilaxmi Bagali MBBS, MD
PhD Scholar
Registration No: 15PHD006
Department of Physiology,
Shri B. M. Patil Medical College,
Hospital and Research Centre,
BLDE (Deemed to be University),
Vijayapur, Karnataka, India.

Date: 10.08.2019

BLDE (DEEMED TO BE UNIVERSITY)

Shri B. M. Patil Medical College, Hospital and Research Centre
Vijayapur, Karnataka, India.

Certificate

This is to certify that this thesis entitled *"Hypoxia and Cell Signalling: Cardiovascular Remodelling, Glucose Homeostasis and Role of Calcium Channel Blocker (Cilnidipine)"* is a bonafide research work carried out by Dr Shrilaxmi Bagali under our supervision and guidance in the Department of Physiology, Shri B. M. Patil Medical College, Hospital and Research Centre, BLDE (Deemed to be University), Vijayapur, Karnataka, India in the fulfilment of the requirements for the degree of Doctor of Philosophy in Physiology.

Signature of the guide

Kusal K. Das 10.8-2019

Prof. Kusal K. Das PhD, FRSB
Guide
Professor,
Laboratory of Vascular Physiology and Medicine,
Department of Physiology,
Shri B. M. Patil Medical College, Hospital and Research Centre,
BLDE (Deemed to be University),
Vijayapur, Karnataka, India.

Prof. Kusal K. Das PhD
Laboratory of Vascular Physiology & Medicine
Department of Physiology
BLDE(DU) Shri B M Patil Medical College
Vijayapur-586103 Karnataka India

Signature of the co-guide

Dr Akram Naikwadi, MD
Co-guide
Professor and Head
Department of Pharmacology,
Shri B. M. Patil Medical College, Hospital and Research Centre,
BLDE (Deemed to be University),
Vijayapur, Karnataka, India.

Professor & HOD
Dept. of Pharmacology
BLDEU's Shri B. M. Patil
Medical College VIJAYAPUR

BLDE (DEEMED TO BE UNIVERSITY)
Shri B. M. Patil Medical College, Hospital and Research Centre
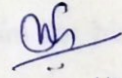Vijayapur, Karnataka, India.

Copyright

Declaration by the candidate
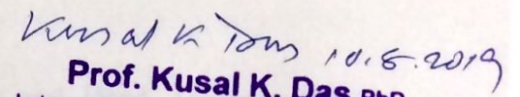
I hereby declare that the BLDE (Deemed to be University), Shri B. M. Patil Medical College, Hospital and Research Centre, Vijayapur, Karnataka, shall have the rights to preserve, use and dessiminate this declaration/thesis in print or electronic format for academic/research purpose.

© BLDE (Deemed to be University), Shri B. M. Patil Medical College, Hospital and Research Centre, Vijayapur, Karnataka, India.

Dr Shrilaxmi Bagali MBBS, MD
PhD Scholar
Registration No: 15PHD006
Department of Physiology,
Shri B. M. Patil Medical College,
Hospital and Research Centre,
BLDE (Deemed to be University),
Vijayapur, Karnataka, India.

10.08.2019

Prof. Kusal K. Das PhD, FRSB
Guide
Professor,
Laboratory of Vascular Physiology and Medicine,
Department of Physiology,
Shri B. M. Patil Medical College,
Hospital and Research Centre,
BLDE (Deemed to be University),
Vijayapur, Karnataka, India.
Date: 10.08.2019
Place: Vijayapur

Kusal K Das 10.8.2019

Prof. Kusal K. Das PhD
Laboratory of Vascular Physiology & Medicine
Department of Physiology
BLDE(DU) Shri B M Patil Medical College
Vijayapur-586103 Karnataka India

Index

LIST OF TABLES

LIST OF FIGURES

LIST OF ABBREVIATIONS

%	per cent
µl	microlitre
µM/L	Micro Moles per Litre
4-HNE	4-Hydroxynonenal
ABC	Avidin-Biotin-Peroxidase Complex
ACh	Acetylcholine
AGE	Advanced glycation end products
Akt	Protein kinase B
ANOVA	Analysis of Variance
ANS	Autonomic nervous system
ARNT	Aryl-Hydrocarbon-Nuclear Receptor-Translocator
ATP	Adenosine 5'-Triphosphate
AV	Atrioventricular
b. wt	Bodyweight
BAT	Brown adipose tissue
BH4	Tetrahydrobiopterin
BP	Blood Pressure
Ca^{2+}	Calcium
CB	Carotid body
CCA	Common carotid artery
CCB	Calcium channel blocker
cells/cumm	cells per cubic millimetre
CFU	Colony-forming unit
CH	Chronic hypoxia
CHER	Cholesterol esterase
CHOD	Cholesterol oxidase
Cil	Cilnidipine
CK-2	Casein kinase 2
Cm	Centimetre
CM	Chylomicron
COPD	Chronic obstructive pulmonary disease
CPCSEA	Committee for the Purpose of Control and Supervision of Experiments on animals
CUL 2	Cullin 2
$CuSO_4$	Copper sulphate
DBP	Diastolic blood pressure
DF	Degree of freedom
DNA	Deoxyribonucleic acid
ECA	External carotid artery
ECG	Electrocardiogram
ECP	Extracellular matrix
EDTA	Ethylenediaminetetracetic acid
EGF	Epidermal growth factor
ELISA	Enzyme-linked immunosorbent assay
eNOS	endothelial Nitric oxide synthase
Epo	Erythropoietin
ERKs	Extracellular signal regulated kinases
ET-1	Endothelin-1

ETA	Endothelin receptor type A
ETC	Electron transport chain
FAD	Flavin adenine dinucleotide
FBS	Fasting blood sugar
Fe^{2+}	Ferrous ion
FFA	Free Fatty Acids
FGF-2	Fibroblast growth factor -2
FMN	Flavin mononucleotide
g/dl	grams/decilitre
GLUT-4	Glucose Transporter-4
GND	Ground
H_2O_2	Hydrogen peroxide
H_2SO_4	Sulphuric acid
Hb	Haemoglobin
HCl	Hydrochloric acid
Hct	Hematocrit
HDL	High-density lipoprotein
HF	High frequency
HIFs	Hypoxia-Inducible Factors
HOMA-IR	Homeostatic model assessment for insulin resistance
HPE	Histopathological examination
HR	Heart rate
HRE	Hypoxia-responsive elements
HRP	Horseradish peroxidase
HRV	Heart rate variability
HSI	Hepatosomatic index
HVA	High voltage-activated
HVD	Hypoxic ventilatory decline
i.p	Intraperitoneal
ICA	Internal carotid artery
IF-kβ	Inhibitory factor-kappa beta
IH	Intermittent hypoxia
iNOS	inducible Nitric oxide synthase
IR	Insulin resistance
JNK1	c-Jun N-terminal kinase 1
K^+	Potassium channels
Kg	Kilogram
Km	Correction factor
LA	Lumen area
LCCA	Left common carotid artery
LDL	Low-density lipoprotein
LF	Low frequency
LVA	Low voltage-activated
m^2	meter square
MAP	Mean Arterial Pressure
MAPKs	Mitogen- activated protein kinases
MDA	Malondialdehyde
mg	milligram
mg/dl	milligram per decilitre
mg/kg	milligram per kilogram

mIU/L	Milli International Units per Litre
mm Hg	Millimetre of mercury
mm^3	cubic millimetre
MMPs	Matrix Metalloproteinases
N_2	Nitrogen
Na^+	Sodium
NaCMC	Sodium Carboxymethyl cellulose
NADPH	Nicotinamide adenine dinucleotide phosphate
NAFLD	Non-alcoholic Fatty Liver Disease
$NaNO_2$	Sodium nitrite
NaOH	Sodium hydroxide
NE	Norepinephrine
NF-kβ	Nuclear factor-kappa beta
NIBP	Non-invasive blood pressure
NIDMM	Non-insulin dependent diabetes mellitus
nm	Nanometre
nNOS	neuronal Nitric oxide synthase
NO	Nitric Oxide
nu	normalized units
NWI	Normalized wall index
O_2	Oxygen
OA	Occipital artery
OD	Optical density
ODDD	Oxygen dependent degradation domain
OGTT	Oral glucose tolerance test
OS	Oxidative stress
OSA	Obstructive sleep apnoea
P com A	Posterior communicating artery
p38 MAPK	p38 mitogen-activated protein kinases
PCA	Posterior cerebral artery
PCR	Polymerase chain reaction
PDGF	Platelet- derived growth factor
PEGME	Polyethylene- glycol- methyl ether
pg/ml	picogram per millimetre
PHDs	Prolyl hydroxylases
PI3-K	Phosphoinositide-3 kinase
PLGF	Placental growth factor
PO_2	Partial pressure of oxygen
PPA	Pterygopalatine artery
PSI	Pulmonosomatic Index
PUFAs	Polyunsaturated fatty acids
pVHL	von Hippel- Lindau tumour- suppressor protein
PVS	Polyvinyl sulfonic acid
RAAS	Renin Angiotensin Aldosterone System
RBC	Red Blood Cell
R_f	Respiratory frequency
RNS	Reactive nitrogen species
ROS	Reactive oxygen species
RR	Respiratory rate
SA	Sinoatrial

SBP	Systolic blood pressure
SD	Standard deviation
sec	seconds
SNS	Sympathetic nervous system
SOD	Superoxide dismutase
SPSS	Statistical Package for the Social Sciences
STA	Superior thyroid artery
TC	Total cholesterol
TG	Triglycerides
TMB	3,3',5,5'-Tetramethylbenzidine
TNF	Tumour necrosis factor
TVA	Total vessel area
VAH	Ventilatory acclimatization to hypoxia
VEGF	Vascular endothelial growth factor
VEGFR	Vascular endothelial growth factor receptors
VLDL	Very low- density lipoprotein
VSMCs	Vascular smooth muscle cells
V_T	Tidal volume
WA	Wall area
WAT	White adipose tissue
$ZnSO_4$	Zinc Sulphate
α-cells	Alpha-cells
β-cells	Beta-cells

ABSTRACT

Objective: The present study was undertaken to evaluate the cardiovascular autonomic functions and hypoxia signalling molecules after chronic hypoxia exposure and their impact on cardiovascular remodelling and glucose homeostasis and the role of cilnidipine, a dual L/N type calcium channel blocker. Further, the impact of unilateral common carotid artery occlusion on brain histopathology in experimental animals preconditioned to chronic hypoxia was assessed.

Methods: Twenty-four adult male Wistar strain albino rats (*Rattus Norvegicus*) were randomly allocated into four groups. Group 1: control; group 2: chronic hypoxia (10% O_2 and 90% N_2) exposed for 21 days; group 3: cilnidipine treated (2.0mg/kg/day); group 4: chronic hypoxia exposed (10% O_2 and 90% N_2) and cilnidipine treated (2.0mg/kg/day) for 21 days. All the experimental animals were subjected to gravimetry and % body weight gain was calculated after 21 days. Haematological parameters like RBC count (million cells/mm^3), Hb (g/dl) and Hct (%) were estimated. HRV analysis was done to assess cardiovascular autonomic balance. Hemodynamic parameters like heart rate and blood pressure were recorded. Oxidative stress and antioxidant defence were assessed by estimating MDA, vitamin C, vitamin E in the serum and MDA in heart, lung and liver tissue homogenate. Hypoxia signalling molecules like VEGF, NOS3 and NO were estimated in the serum. Glucose homeostasis was evaluated by estimation of fasting plasma glucose, oral glucose tolerance test (OGTT), fasting serum insulin. HOMA-IR was calculated as an index of insulin resistance. Cardiovascular remodelling was studied by calculation of cardiosomatic index, and histopathological examination of H&E stained sections of the ventricles, intramyocardial coronary artery, elastic artery and muscular artery. Further, the normalised wall index (NWI), was calculated for the coronary artery. Lipid profile was assessed. Histopathological examination of the lung and liver were also done.

To study the impact of unilateral common carotid artery (CCA) occlusion on brain pathophysiology in chronic hypoxia pre-exposed rats, the experimental animals were randomly assigned to one of the three groups: group 1: sham-operated; group 2: normoxia (21% oxygen), left CCA occlusion for 75 minutes and subsequent reperfusion for 12 hours; group 3: Hypoxia (10% O_2) pre-exposed for 21 days prior to left CCA occlusion for 75 minutes and reperfusion for 12 hours. After reperfusion for 12 hours, the experimental animals were assessed for neurologic deficits and then were sacrificed. The brain was dissected and subjected to histopathological examination.

Results: Chronic hypoxia resulted in lower % body weight gain, elevated hematocrit. HRV analysis revealed sympathetic overactivity and shift in the sympathovagal balance. Cardiovascular hemodynamics revealed decreased heart rate, increased mean arterial pressure (MAP). There were disturbances in oxidant-antioxidant balance indicating oxidative stress. VEGF, NOS3 were markedly elevated and NO significantly reduced. Glucose homeostasis was disturbed with increased fasting plasma glucose and HOMA-IR. HOMA-IR and fasting plasma glucose were positively correlated with the LF/HF ratio. There were features suggestive of cardiovascular remodelling. Further, NWI of the coronary artery was positively correlated with LF/HF ratio, heart tissue MDA, serum MDA and VEGF.

Cilnidipine treatment was able to 1) control sympathetic overactivity 2) reduce MAP 3) decrease oxidative stress 4) increase the bioavailability of NO 5) improve glucose homeostasis and 6) ameliorate cardiovascular remodelling resulting from chronic hypoxia exposure.

Brain histopathology in rats pre-exposed to chronic hypoxia and subjected to unilateral left common carotid artery occlusion demonstrated a reduction in brain oedema, a smaller infarct volume and lesser neurological deficits. This study demonstrates that rats pre-exposed to

chronic hypoxia could have reduced brain injury after focal ischemia as compared to normoxic (hypoxia unexposed) experimental animals.

Conclusion: The present study demonstrates that chronic hypoxia exposure is accompanied by altered hypoxia signalling mechanism, impaired oxidant/antioxidant balance and shift in the sympathovagal balance towards the increased sympathetic activity. These alterations further proceed to impact glucose homeostasis and induce cardiovascular remodelling. Cilnidipine, owing to its dual L/N type calcium channel blocking properties with additional antioxidant potential probably has a beneficial role in ameliorating chronic hypoxia-induced cardiovascular remodelling, disturbances in glucose homeostasis suggesting a possible therapeutic use of cilnidipine against hypoxia-related pathophysiology.

CHAPTER I

INTRODUCTION

1.0 INTRODUCTION

Oxygen is fundamental for cell survival. Any alterations in the oxygen levels both low and high disturb oxygen homeostasis and endanger cell survival. Most healthy organs live in 3-6% oxygen and conditions lower than 3% oxygen is referred to as hypoxia (Bhatia *et al*., 2013). Hypoxia could be acute or chronic and sustained or intermittent. In the clinical setting sustained hypoxia and intermittent hypoxia are observed in distinct clinical conditions. Sustained hypoxia is observed in chronic obstructive pulmonary diseases (COPD), cystic fibrosis and any lung parenchymal diseases impairing alveolar gas exchange. Intermittent hypoxia is associated with obstructive sleep apnea (OSA), central hypoventilation syndrome (Ramirez *et al*., 2012).

Since O_2 is crucial for life, the cells are equipped with mechanisms to detect and to respond to changes in the O_2 levels in the microenvironment. Important being hypoxia-inducible factor (HIF) which is fundamental for mammalian cell response to hypoxia. HIF has been considered as a 'master switch' for hypoxic gene expression. HIF transcriptionally activates more than 100 genes concerned with angiogenesis, nutrient and oxygen transport, metabolism, cell growth and proliferation (Qutub and Popel, 2008; Das and Saha, 2014). All these mechanisms allow the cells to adapt to the hypoxic microenvironment. However, these adaptive signalling mechanisms may be outweighed by the accompanying maladaptive consequences that may be deleterious to the organism (Essop, 2007).

Hypoxia may alter the autonomic nervous balance. Since the autonomic nervous system has a vital role in glucose homeostasis (Carnagarin, 2018) and is an important regulator of the cardiovascular system (Conde *et al*., 2014), autonomic dysregulation may be a major contributor to the onset and progression of cardiometabolic disorders like diabetes mellitus and hypertension in patients experiencing hypoxia (Malpas, 2010). Additionally disturbed

glucose homeostasis itself has important consequences on the cardiovascular system (Xiang *et al*., 2015).

Given the potential contribution of the autonomic nervous dysregulation in the initiation, development and progression of the cardiometabolic disorders, the need for a pharmacological approach for modulating the autonomic functions as an additional therapy to reduce the overall risk of diabetes and cardiovascular consequences in patients experiencing hypoxia seems logical. In view of the above background, cilnidipine could prove to be a promising drug. Cilnidipine belongs to the dihydropyridine class of the calcium channel blockers (CCB). It is a unique CCB owing to its dual L/N type calcium channel blocking actions. In addition to blocking L-type calcium channels on the vascular smooth muscle, it also blocks N-type calcium channels on the sympathetic nerve endings (Takahara, 2009). Due to its pharmacological profile, cilnidipine may have a vital role in affecting sympathetic neurotransmission.

With this background, the present study was undertaken to assess cardiovascular remodelling (ventricles and coronary artery, elastic artery and muscular artery) and glucose homeostasis in experimental Wistar rats exposed to chronic sustained hypoxia and the effect of treatment with L/N type CCB, cilnidipine.

CHAPTER II
REVIEW OF LITERATURE

2.1 HYPOXIA

All cells need a continuous supply of oxygen (O_2). ATP generation during oxidative phosphorylation in the mitochondria requires O_2. It acts as a final electron acceptor during the respiratory chain in the mitochondria. The function of the respiratory chain is ideal at physiological PO_2 and any deviations from normoxia leads to increased formation of reactive oxygen species (Samanta *et al*., 2017). The oxygen state of the tissues is determined by the balance between O_2 utilisation and supply. Different organs of the body are exposed to different oxygen environments depending on the location and the function of the cells in the organ. Most healthy organs reside in 3-6% O_2 and conditions lower than 3% O_2 is considered as hypoxia (Bhatia *et al*., 2013).

Depending on the duration of exposure, hypoxia can be acute (seconds to minutes) or chronic (days to years) (Pulgar-Sepulveda *et al*., 2018) and depending on the pattern of exposure can be sustained or intermittent (Nanduri and Nanduri, 2007).

Sustained hypoxia occurs when the concentration of oxygen falls to 8-12% from normal atmospheric concentration of 21%. Sustained hypoxia is observed during high altitude sojourns and in patients with chronic obstructive pulmonary disease and cystic fibrosis.

Intermittent hypoxia is characterised by alternating brief periods of hypoxia and normoxia. It occurs when O_2 levels fall for brief periods. Intermittent hypoxia is observed in patients with obstructive sleep apnea (Ramirez *et al*., 2012).

Hypoxia deranges oxygen homeostasis and endangers cell survival (Bhatia *et al*., 2013).

Since O_2 is crucial for life, the cells are equipped with mechanisms to detect and to respond to changes in the O_2 levels in the microenvironment. Table 2.1 represents the acute and chronic responses to hypoxia (Lopez-Barneo *et al*., 2016).

Table 2.1: Acute and Chronic Responses to Hypoxia (Lopez-Barneo *et al*., 2016)

Acute responses to Hypoxia (sec to minutes)	Chronic responses to hypoxia (hours to days)
1. Hyperventilation (airway and arterial chemoreceptors)	1. Activation of glucose metabolism and transport (most tissues)
2. Increase in cardiac output (peripheral chemoreceptors and heart muscle)	2. Erythropoiesis (Bone marrow)
3. Systemic arterial vasodilation (arterial endothelium and smooth muscle)	3. Angiogenesis and neovascularization (vascular endothelium, hypoxic or ischemic tissues)
4. Pulmonary vasoconstriction (Vascular endothelium, resistance vessel pulmonary myocytes)	4. Tissue hypertrophy and remodelling (pulmonary arterial wall, myocardium, carotid body)
5. Activation of glucose uptake (cardiac and skeletal muscle)	5. Production of vasodilators (vascular endothelium and smooth muscle)

2.1.1 Systemic responses to hypoxia

A) Role of Chemoreceptors

Exposure to hypoxia elicits immediate (within seconds to minutes) systemic responses that include respiratory and cardiovascular adjustments that enable the maintenance of oxygen supply to the vital organs like brain and heart. The chemoreceptors particularly the carotid bodies detect changes in the PO_2 and immediately stimulate the respiratory centre. Similarly, aortic bodies and neuroepithelial bodies are also included in the peripheral chemoreceptors. Neuroepithelial bodies are a group of cells in the airways that sense O_2 in the inspired air. Aortic bodies also contribute to cardiorespiratory adjustments but the response is weaker and the role of neuroepithelial bodies is not known (Lahiri, 2000).

Carotid bodies are tiny organs situated bilaterally at the bifurcation of the common carotid artery into internal and external carotid arteries. Carotid bodies (CB) demonstrate a

remarkable speed of response and sensitivity to hypoxia with only a 20% reduction in the arterial PO_2 eliciting the response within seconds (Samanta *et al*., 2017).

CB is composed of functional units called glomeruli. Glomeruli are made up of clusters of cells separated by a network of small capillaries and connective tissue. Each glomerulus is composed of two types of cells – 1) Glomus cells (Type I) and 2) Sustentacular cells (Type II). The CB also contains progenitors of glomus cells called the nestin-positive (nestin$^+$) cells. The glomus cells can be distinguished from sustentacular cells under electron microscopy by the presence of numerous mitochondria and small dense-core secretory vesicles. Glomus cells (type I) in the carotid body are excited and depolarize in response to hypoxemia in addition to hypercapnia and decrease in extracellular pH eliciting the chemoreceptor reflex. The chemoreceptor reflex induces hyperventilation and is accompanied by intense sympathetic stimulation to increase HR, BP and sympathetic drive (Lopez-Barneo *et al*., 2016). Hypoxia-induced increased sympathetic activity is considered as a defence mechanism to ensure O_2 supply to vital organs and to regulate the regional conductances. Increased sympathetic activity protects against the exaggerated vasodilation of the systemic blood vessels on exposure to hypoxia and prevents hypotension (Calbet, 2003; Samanta *et al*., 2017).

i) O_2 sensing by the glomus cells

Glomus cells contain K^+ channels which are closed under the influence of hypoxia. Closure of the K^+ channels reduces K^+ efflux and leads to membrane depolarization and opening of voltage-gated Ca^{2+} channels the L-type, with the resultant Ca^{2+} influx causing the exocytotic release of the transmitter to activate the afferent nerve endings to the brainstem respiratory centre. Among the various neurotransmitters present acetylcholine and adenosine triphosphate have been considered to be the excitatory transmitters in the pathway acting on the nicotinic acetylcholine receptors and P_2X receptors respectively on the chemosensory

afferents (Pulgar-Sepulveda *et al*., 2018). Mechanism underlying O_2 sensing by the carotid body still remains elusive although the role of mitochondria has been proposed. During hypoxia, mitochondrial complex I generate ROS and reduced pyridine residues that signal the closure of K^+ channels (Fernandez-Aguera *et al*., 2015).

ii) Carotid body and sustained hypoxia

The CB demonstrates plasticity and is observed to be larger in size in residents of high altitude and in patients with cardiopulmonary diseases. The greater size is due to neovascularisation, hyperplasia and hypertrophy of glomus cells contributing to its growth. The underlying mechanisms for these morphological alterations still remain unclear although the role of VEGF has been proposed (Prabhakar and Jacono, 2005). This unusual response observed in any neural organ leads to exaggerated electrical signals to the brain stem respiratory centre inducing hyperventilation (Lopez-Barneo *et al*., 2016). This enhanced sensitivity of the carotid body to O_2 may be due to alterations in the density of the ion current due to changes in the expression of K^+ and Na^+ channels (Pulgar-Sepulveda *et al*., 2018), neurotransmitter dynamics, recruitment of additional neuromodulators like endothelin-1 (ET-1) (Prabhakar and Jacono, 2005).

iii) Carotid body and intermittent hypoxia

There is evidence suggesting the role of CB in the development of adverse medical conditions in patients experiencing intermittent hypoxia. Intermittent periods of hypoxemia and hypercapnia in OSA leads to intense stimulation of the CB leading to strong activation of cardiovascular sympathetic reflexes. Long term IH leads to long term facilitation of the CB, a form of plasticity leading to CB overactivation during acute episodes of IH. The molecular mechanisms underlying the CB plasticity in IH largely remain unknown (Lopez-Barneo *et al*., 2016).

B) Vascular response to hypoxia

The vascular response to hypoxia is dilatation of systemic blood vessels and constriction of the pulmonary vasculature. Hypoxic pulmonary vasoconstriction is a fast response that diverts the blood from poorly ventilated to well-ventilated alveoli. It is observed in pulmonary arteries and veins but is greatest in small resistance arteries. Hypoxic vasodilatation of systemic vessels is another fast response that maintains the O_2 supply to vital organs like the brain and heart (Michiels, 2004).

2.1.2 Cellular responses to hypoxia

Cellular responses to hypoxia are initiated with the sensing of O_2 by the cells. All nucleated cells are capable of sensing and responding to lower O_2 levels acutely within minutes by activation of pre-existing proteins and chronically (within hours) through regulation of gene transcription (Michiels, 2004).

A) HYPOXIA SIGNALLING MOLECULES

1. Hypoxia-Inducible Factors (HIFs)

Hypoxia-inducible factors (HIFs) are transcriptional factors that govern the cell response to hypoxia. HIFs belong to the PAS (PER-ARNT (aryl hydrocarbon receptor nuclear translocator)-SIM) family of transcription factors that bind to DNA (Uchida *et al*., 2004; Rankin and Giaccia, 2008). They are heterodimers composed of α- and β-subunits. α-subunit is sensitive to oxygen. β-subunit also known as ARNT (Aryl-Hydrocarbon-Nuclear Receptor Translocator) is not sensitive to changes in the oxygen concentration and is thus constitutively expressed in all tissues under aerobic conditions (Uchida *et al*., 2004; Rankin and Giaccia, 2008).

Active HIF consists of α-subunit and a β-subunit. There are three types of α-subunits namely HIF-1α, HIF-2α and HIF-3α and accordingly, there are three subtypes of active HIFs: HIF-1,

HIF-2 and HIF-3. In all the three active forms of HIF, the β-subunit (ARNT) is common while HIF-1 has HIF-1α, HIF-2 has HIF-2α and HIF-3 has HIF-3α subunits (Nath and Szabo, 2012; Rankin and Giaccia, 2008).

Figure 2.1 depicts the regulation of HIF under normoxia and hypoxia. Under normoxia, α-subunit of HIF is rapidly hydroxylated by prolyl hydroxylases (PHDs). PHDs belong to a family of dioxygenases and are of three subtypes-PHD-1, PHD-2 and PHD-3 (El Guerrab *et al*., 2017). The PHDs hydroxylate two proline residues of oxygen-dependent degradation domain (ODDD) located in the central region of α-subunit in presence of dioxygen, Fe^{2+}, ascorbate and 2-oxoglutarate (Chun *et al*., 2002; Uchida *et al*., 2004). Hydroxylation of the proline residues allows the binding of α-subunit to the E3- ubiquitin ligase complex. E3-ubiquitin ligase complex contains pVHL(von Hippel Lindau tumour suppressor protein), elongin B and C, Cullin 2 (CUL 2) (Chun *et al*., 2002). pVHL is believed to be the substrate recognition component of E3 ubiquitin ligase complex (Rankin and Giaccia, 2008) which rapidly binds with the hydroxylated α-subunit of HIF followed by ubiquitination and degradation by the 26S proteasome (Chun *et al*, 2002).

Under hypoxia or alterations in the cellular redox state, HIF-α subunits are not hydroxylated because the major substrate dioxygen is not available (Nath and Szabo, 2012; Chun *et al*., 2002). Hence HIF-α is stabilized and moves to the nucleus, where it heterodimerizes with ARNT (HIF-β) and binds to hypoxia-responsive elements (HREs) in the promoter region of the HIF target genes bringing about their transcription (Rankin and Giaccia, 2008; Nath and Szabo, 2012). It has been demonstrated that stabilisation of HIF and its ability to bind DNA begins at an oxygen concentration of < 6% and peaks at 0.5% (Jiang *et al*., 1996; Rankin and Giaccia, 2008).
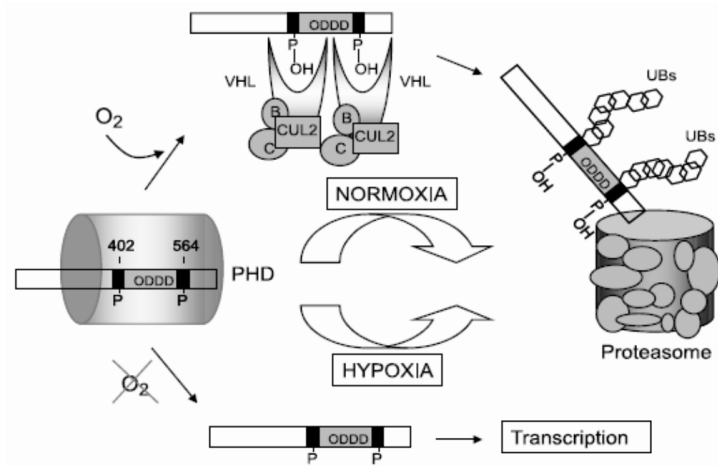
Figure 2.1: Regulation of HIF-1α under normoxia and hypoxia

Among the various HIFs, HIF-1 is crucial for cellular response to hypoxia since it is expressed in almost all cells and promotes the expression of numerous hypoxia-inducible genes. In contrast to HIF-1α, HIF-2α expression is limited to certain cell types that include endothelial cells, glial cells, type II pneumocytes, cardiomyocytes, fibroblasts of the kidney, interstitial cells of the pancreas and duodenum, and hepatocytes. The role of HIF-3 in the regulation of target gene expression during hypoxia is not clear (Rankin and Giaccia, 2008).

HIF-1α is supposed to be the 'master switch' of hypoxic gene expression inducing transcription of multiple genes (more than 100 genes) associated with angiogenesis, erythropoiesis, energy metabolism, nutrient transport, cell cycle and cell migration (Qutub, 2008). Figure 2.2 depicts the various genes induced by HIF-1α.
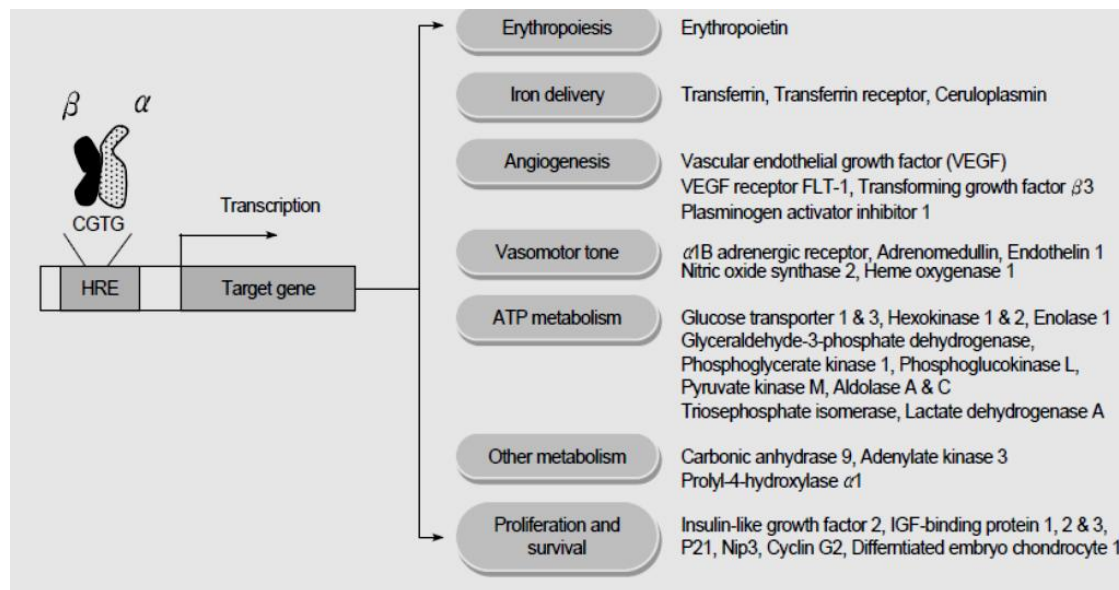
Figure 2.2: Identified HIF-1 target genes

α: HIF -1α; β: HIF - 1 β; HRE: hypoxia response *cis*-element

Source: Chun YS, Kim MS, Park JW. Oxygen-dependent and independent regulation of HIF-1alpha. J Korean Med Sci. 2002; 17(5): 583. DOI:10.3346/jkms.2002.17.5.581

2. Vascular Endothelial Growth Factor

Among the various HIF induced genes, vascular endothelial growth factor (VEGF) is an important transcriptional target of HIF-1 (Shibuya, 2011). VEGF regulates vasculogenesis, angiogenesis and lymphangiogenesis (Beeghly-Fadiel *et al*., 2011). Vasculogenesis is the term used for the development of new blood vessels from precursor cells observed during early embryogenesis. Angiogenesis is the formation of new blood vessels from pre-existing vessels at a later stage (Shibuya, 2011). In adults, vessel formation is by angiogenesis. The human VEGF family includes VEGF-A, -B, -C, -D, and placental growth factor (PLGF). The VEGF receptors are tyrosine kinases expressed in various vascular and extravascular tissues and are of three types: VEGFR-1, VEGFR-2, VEGFR-3 (Ramakrishnan *et al*., 2014). Of the three receptors, VEGFR-2 mainly mediates the cell growth and permeability action of VEGF (Kimura and Esumi, 2003). Under hypoxia, VEGF levels peak within 48 hrs and within 3 weeks return to basal levels. However, the effects of VEGF remain for many weeks to

months due to long term up-regulation of VEGF receptors (Adeoye OO *et al*., 2014). In addition to hypoxia, a number of other stimuli induce VEGF gene expressions like cytokines, hormones, phorbol esters, oncogenes, transitional metals and iron chelator. Nitric oxide has also been shown to regulate VEGF with optimal levels upregulating and excessive amounts of NO inhibiting VEGF (Kimura and Esumi, 2003).

3. **Endothelial Nitric Oxide Synthase (eNOS/NOS3) and Nitric Oxide (NO)**

NO, the smallest signalling molecule is produced by nitric oxide synthase (NOS). There are three isoforms of NOS 1) neuronal NOS (nNOS/NOS-1), 2) inducible NOS (iNOS/NOS-2) and 3) endothelial NOS (eNOS/NOS-3). All three isoforms are homodimers requiring the substrate L-arginine, co-substrates oxygen and NADPH, cofactors FAD, FMN and tetrahydrobiopterin (BH_4) for the NO production (Dweik, 2005; Umbrello *et al*., 2013).

eNOS is predominantly expressed in the endothelial cells. However, skeletal muscle, lung, liver, cardiac myocytes, platelets, certain neurons in the brain, syncytiotrophoblast of the human placenta also express eNOS (Forstermann and Sessa, 2012).

Actions of eNOS derived NO

1. NO released by the endothelium diffuses into the surrounding tissues and relaxes vascular smooth muscle cells and dilates all types of blood vessels

2. NO released towards the vascular lumen inhibits platelet adhesion and aggregation prevents the release of platelet-derived growth factor (PDGF) which stimulates the proliferation of VSMC and production of matrix molecules

3. eNOS is crucial for vascular remodelling secondary to chronic changes in flow

4. NO protects against the onset of atherogenesis by inhibiting adhesion of the leukocytes to the vessel wall

5. NO inhibits DNA synthesis, mitogenesis and proliferation of VSMC

6. NO prevents the formation of fibrous plaque which is a later step in atherosclerosis

7. NO has a role in collateral formation and angiogenesis post-ischemia

Endothelial dysfunction is a term used when the endothelium fails to produce sufficient amounts of bioactive NO and NO-mediated vasodilatation. Since NO is crucial for cardiovascular homeostasis endothelial dysfunction is involved in the pathophysiology of several cardiovascular diseases including hypertension and atherosclerosis (Janaszak-Jasiecka *et al*., 2018; Forstermann and Sessa, 2012).

Oxidative stress plays a crucial role in endothelial dysfunction. The enzymes that can generate ROS in the vessel wall are NADPH oxidase, xanthine oxidase, enzymes of the mitochondrial respiratory chain, and uncoupled eNOS. These enzymes are expressed by endothelial cells, smooth muscle cells and adventitia. Superoxide radical reacts with NO decreasing its bioavailability. Further, oxidative stress has also been implicated in NOS uncoupling. The generation of superoxide radical instead of NO by eNOS is termed NOS uncoupling. The underlying mechanisms for NOS uncoupling are oxidation of cofactor BH4, depletion of L-arginine and accumulation of endogenous methylarginine (Forstermann and Sessa, 2012).

Hypoxia and eNOS: HIF-1 transcriptionally induces eNOS in the early stages of hypoxia. However, prolonged hypoxia is associated with reduced bioavailability of NO due to the reduction of eNOS (Janaszak-Jasiecka *et al*., 2018).

2.1.3   Hypoxia and Oxidative stress

Reactive oxygen species (ROS) or reactive nitrogen species (RNS) are atoms or molecules having one or more unpaired electrons in the outer orbit and hence have the ability to react chemically (Lavie and Lavie, 2009). Free radical is unstable, short-lived and highly reactive due to the presence of an odd number of electrons. This high reactivity makes them pull away

electrons from other compounds to attain stability. The attacked molecules lose electrons and are converted to a free radical, setting a chain reaction which ultimately damages the cell (Phaniendra *et al*., 2015). The ROS/RNS act as a double-edged sword having both beneficial and adverse effects. At low to moderate concentrations they have various physiological functions like immune function, cell signalling pathways, mitogenic response and in redox regulation (Phaniendra *et al*., 2015; Bagali *et al*., 2018). At high concentrations both ROS/RNS potentially damage the biomolecules like lipids, proteins, carbohydrates, DNA and various cellular functions and alter the cell functions. However, the human body is well equipped with antioxidants that efficiently scavenge free radicals and defend against oxidative stress (Bagali *et al*., 2018). The antioxidants have been grouped into enzymatic and non-enzymatic antioxidants. Table 2.2 denotes major enzymatic and non-enzymatic antioxidants in the body (Birben *et al*., 2012). Normally there is a balance between ROS/RNS and antioxidants. Oxidative stress results when the ROS/RNS are produced in excess of the antioxidant defence ability resulting in the disruption of the redox signalling and/or inducing molecular damage (Debevec *et al*., 2017; Clanton, 2007). Both ROS and RNS are classified as radicals and non-radicals. Radicals contain at least one unpaired electron and are highly reactive. Non-radicals are not free radicals but can lead to free radical reactions in living organisms. Table 2.3 present list of ROS and RNS (both radicals and non-radical) produced during cellular metabolism (Phaniendra A *et al*., 2015). Among the various ROS, superoxide radical is an important one produced at mitochondrial complex I and III of the electron transport chain, and by enzymes like xanthine oxidase, lipooxygenase, cyclooxygenase, NADPH dependent oxidase, uncoupled eNOS (Lavie and Lavie, 2009; Phaniendra *et al*., 2015).

Table 2.2: Major enzymatic and non-enzymatic antioxidants

Enzymatic	Non-enzymatic
Superoxide dismutase	All trans retinol 2 (Vitamin A)
Catalase	Ascorbic acid (Vitamin C)
Glutathione peroxidise	α-Tocopherol (Vitamin E)
Thioredoxin	β-Carotene
Peroxiredoxin	Glutathione
Glutathione transferase	

Source: Birben E, Sahiner UM, Sackesen C, Erzurum S, Kalayci O. Oxidative stress and antioxidant defence. World Allergy Organ J. 2012; 5(1): 9-19. doi: 10.1097/WOX.0b013e3182439613.

Table 2.3: List of ROS and RNS

Reactive Oxygen Species		Reactive Nitrogen species	
Radicals	**Non radicals**	**Radicals**	**Non radicals**
Superoxide	Hydrogen radical	Nitric oxide	Peroxynitrite
Hydroxyl	Singlet Oxygen	Nitrogen dioxide	Nitrosyl cation
Alkoxyl Peroxyl	Ozone		Nitroxyl anion
	Organic Peroxide		Dinitrogen trioxide
	Hypochlorous acid		Dinitrogen tetraoxide
	Hypobromous acid		Nitrous acid
			Peroxynitrous acid
			Nitryl chloride

Source: Phaniendra A, Jestadi DB, Periyasamy L. Free radicals: properties, sources, targets, and their implication in various diseases. Indian J Clin Biochem. 2015; 30(1):11–26. Doi :10.1007/s12291-014-0446-0.

Although oxidative stress during hypoxia seems paradoxical, both acute (Magalhaes *et al*., 2004; Faiss *et al*., 2013) and chronic hypoxia exposure and hypobaric (high altitude) (Magalhaes *et al*., 2005) and normobaric hypoxia (simulated altitude) (Debevac *et al*., 2014) exposure induce oxidative stress (Dosek *et al*., 2007; Debevec, 2017). The precise mechanism underlying hypoxia-induced ROS/RNS generation is not clear. It has been proposed that although the hypoxic cell generates ATP by anaerobic glycolysis, the low levels of available O_2 continue the oxidative generation of ATP to some extent via

tricarboxylic acid cycle and electron transport chain (ETC). The electrons leaking from the ETC generate ROS and induce oxidative stress (Miyata *et al*., 2011).

2.2 Cardiovascular Remodelling

2.2.1 Cardiac remodelling

Cardiac remodelling is a term used to describe the molecular, cellular and interstitial changes that present clinically as alterations in size, mass, geometry and functions of the heart after any stressful event (Azevedo *et al*., 2016).

Hockman and Buckey first used the term 'remodelling' in 1982 to describe the replacement of infarcted tissue with scar tissue in a myocardial infarction model. Since then the term 'remodelling' was used in a number of scientific articles in various contexts to describe different clinical situations and pathophysiological changes. Therefore a consensus of the international forum on cardiac remodelling was published in 2000, which defined cardiac remodelling as a group of molecular, cellular and interstitial changes that clinically present as changes in size, shape and function of the heart resulting from cardiac injury (Azevedo *et al*., 2016).

Cardiac remodelling is initiated by ischemia (myocardial infarction), inflammation (myocarditis), hemodynamic overload (workload by volume or pressure) and neurohormonal activation (Dorsa Pontes *et al*., 2016).

At the cellular level, the various changes associated with cardiac remodelling are myocyte hypertrophy, necrosis, apoptosis, fibroblast proliferation, increased fibrillar collagen and fibrosis. At the macroscopic level, it presents as alterations in size, mass (hypertrophy or atrophy), the geometry of the heart (the chambers change shape from elliptical to spherical), and progressive left ventricular dysfunction. Further, there are associated abnormalities in

energy metabolism, altered expression or function of contractile proteins, electrophysiological alterations, and abnormalities in excitation-contraction coupling and changes in the extracellular matrix (ECM) (Dorsa Pontes *et al*., 2016; Roever *et al*., 2017).

Patients with cardiac remodelling demonstrate a progressive deterioration of cardiac function hence slowing or reversing of cardiac remodelling has been identified as an important goal in heart failure therapy (Cohn *et al*., 2000).
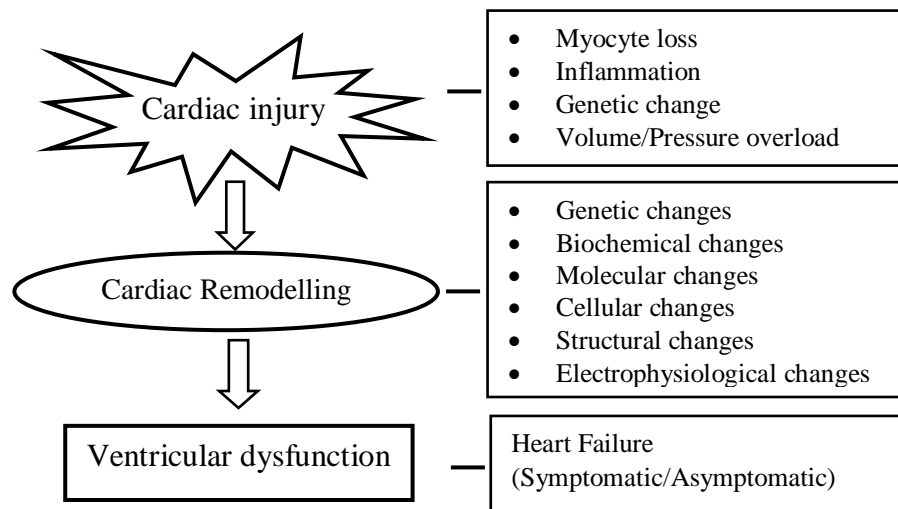
Figure 2.3: The sequence of events leading from cardiac injury to cardiac dysfunction

A) Oxidative stress and cardiac remodelling

Oxidative stress (OS) results when reactive oxygen species (ROS) are generated in excess of the antioxidant defences. The various sources of ROS in the heart are NADPH oxidase, xanthine oxidase, cyclooxygenase, cytochrome P450, glucose oxidase, lipoxygenase, catecholamine degradation, mitochondrial electron transport chain (Roever and Palandri Chagas, 2017). Oxidative stress results in lipid peroxidation, protein oxidation, DNA damage,

changes in proteins responsible for calcium transit, activation of signalling pathways for hypertrophy, cellular dysfunction, the proliferation of fibroblasts, activation of metalloproteinases, stimulation of apoptosis. Thus OS makes a significant contribution to the pathophysiology of cardiac remodelling (Azevedo *et al.*, 2016).

B) Neurohumoral activation and cardiac remodelling

Sympathetic nervous system and the renin-angiotensin-aldosterone system (RAAS) play a significant role in cardiac remodelling. Activation of both systems activates intracellular signalling pathways that stimulate the protein synthesis in myocytes and fibroblasts resulting in cellular hypertrophy and fibrosis. Other reported effects include activation of growth factors and metalloproteinases, hemodynamic overload by vasoconstriction and water retention, increase in oxidative stress and direct cytotoxic effect, leading to cellular death by necrosis or apoptosis. Blockage of these systems has an important role in the prevention or attenuation of cardiac remodelling secondary to stimuli (Azevedo *et al.*, 2016).

C) Altered glucose homeostasis and cardiac remodelling

Under normal physiological conditions, heart demonstrates considerable 'metabolic substrate flexibility' i.e. the heart can use different substrates to produce ATP. However, the preferred substrate is the free fatty acid accounting for 60-90% of the energy supply. Other substrates like glucose, lactate and ketone bodies and specific amino acids can also be utilized by the heart. Hyperglycemia and insulin resistance results in loss of this metabolic substrate flexibility. There is decreased glucose transport and increased transport of free fatty acids (FFA) across the sarcolemma. The oxidative phosphorylation is impaired and there is increased mitochondrial ROS generation. Increased free fatty acid uptake results in lipotoxicity. Besides oxidative stress and lipotoxicity, inflammation also triggers apoptosis. Upregulation of proinflammatory cytokines like tumour necrosis factor (TNF) and

interleukins 6 and 8, monocyte chemotactic protein 1 expression in the diabetic heart has been demonstrated. These cytokine affect cardiomyocytes, fibroblasts, endothelial cells and smooth muscle cells which all together contribute to pathological cardiac remodelling (Borghetti *et al*., 2018).

2.3 Vascular remodelling

The vascular system is highly dynamic, has several functions like transport, control of volume and blood pressure (vasoconstriction/dilation), immune function (leukocyte–vessel interactions), and mechanical function (erectile tissues). Vessels comprise three main layers: an inner endothelial layer, a middle vascular media, and an outer adventitia. Of the many cell types that make up the vascular wall, vascular smooth muscle cells are particularly important since they have a high degree of phenotypic variability (Touyz *et al*., 2014).

Blood vessels undergo structural changes in response to alterations in the endogenous and exogenous stimuli. These changes in cellular and extracellular structures of the blood vessel are known as remodelling and allow functional adaptation and specialization (Adeoye *et al*., 2016).

Vascular remodelling is a term used to describe the process of altering the structure and arrangement in blood vessels by cell growth, cell migration, cell death and production or degradation of extracellular matrix (Mittal *et al*., 2014).

Vascular remodelling is essential in some of the structures like endometrium in both pregnant and non-pregnant state (Adeoye *et al*., 2016). However, pathological remodelling is involved in the initiation and progression of cardiovascular diseases like hypertension, atherosclerosis, and aneurysm. Inflammation, injury, oxidative stress and hemodynamics are crucial in the process of vascular remodelling (Mittal *et al*., 2014).

There are multiple molecular mechanisms underlying vascular remodelling like activation of RAS, stimulation of growth signalling pathways, activation of tyrosine kinases, induction of proinflammatory responses, ROS and modification of the extracellular matrix (Touyz *et al*., 2014).

The flowing blood exerts a frictional force at the endothelial surface termed Shear stress. Shear stress is a vital signal for arterial remodelling. Under normal physiological conditions, changes in flow initiate arterial remodelling to restore normal shear stress and wall tension. Normal shear stress helps in the proper alignment of endothelial cells and maintain barrier function. It also promotes the expression of vasodilator and antithrombotic factors, suppresses growth and proinflammatory factors and maintains a state of vascular health (Zhao *et al*., 2013).

A) Sympathetic activity and vascular remodelling

Sympathetic hyperactivity leads to vasoconstriction and an increase in peripheral vascular resistance increasing blood flow velocity during systole. This increases luminal shear stress. A sustained increase in shear stress damages the vascular endothelial cells around the vascular lumen and promotes platelet aggregation. Sympathetic hyperactivity also promotes vascular smooth cell proliferation and increases the production of extracellular matrix proteins like elastin and collagen (Kontos *et al*., 2017).

B) Oxidative stress and vascular remodelling:

Oxidative stress plays a crucial role in the pathophysiology of vascular diseases. Macrophages have been thought to be the major source of ROS in the vessel wall. In addition, the endothelial cells, smooth muscle cells and adventitial cells contribute significantly in the production of ROS in response to various stimuli. Under normal physiological conditions, ROS have important roles in the vessel wall. They act as second

messengers, growth and survival of smooth muscle cells and endothelial cells, in the vessel wall remodelling. However, oxidative stress results when ROS production exceeds the antioxidant defence mechanisms. Among the several ROS, superoxide radical has key role in the context of oxidative stress. The various cellular sources of ROS particularly superoxide radical are NADPH oxidases, xanthine oxidases, lipooxygenases, mitochondrial oxidase, uncoupled nitric oxide synthase. ROS promote vascular remodelling by inducing growth, apoptosis and migration of vascular smooth cells, modulating endothelial functions, modification of extracellular matrix, endothelial cell expression of the proinflammatory phenotype. The brief outline of the contribution of oxidative stress in vascular remodelling and vascular diseases is given in figure 2.4 (Fortuno *et al.*, 2005).
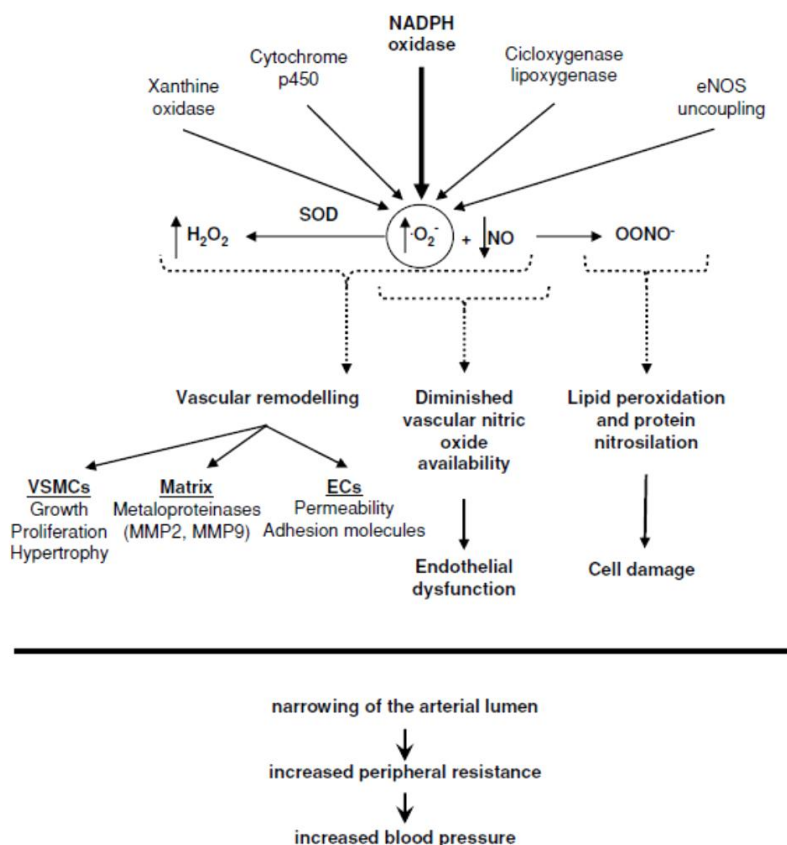
Figure 2.4: Outline of the oxidative stress induced vascular remodelling

Source: Fortuno A, San Jose G, Moreno MU, Diez J, Zalba G. Oxidative stress and vascular remodelling. Exp Physiol. 2005; 90(4): 457-62.

C) Altered glucose homeostasis and vascular remodelling

Insulin is crucial in maintaining vascular health. Insulin acts by two major signalling pathways – 1) Phosphoinositide-3- kinase (PI3-K)/Akt pathway, 2) Mitogen-activated protein kinase/extracellular signal-regulated kinase (MAPK/ERK) pathway. PI3-K/Akt pathway has a significant positive role in vascular health. This pathway stimulates endothelial NO production which is a potent vasodilator, inhibits platelet aggregation and restricts VSMC proliferation and migration. MAPK/ERK signalling pathway impacts adversely on vascular health by mediating inflammation, vasoconstriction and VSMC proliferation, increased levels of prothrombotic and proinflammatory markers and ROS. Under normal physiological conditions, PI3-K/Akt pathway predominates. However, the MAPK/ERK signalling pathway predominates during insulin resistance (Janus *et al*., 2016).

Hyperglycemia impairs insulin PI3-Akt signalling and inactivates eNOS (Musicki *et al*., 2005). It also promotes the formation of advanced glycation end products (AGE) formation which in turn stimulates ROS formation and impairs PI3-K/Akt pathway (Van Puyvelde *et al*., 2014)

2.4 GLUCOSE HOMEOSTASIS

The term glucose homeostasis refers to the neural regulatory and hormonal elements that regulate glucose uptake and utilisation. Glucose homeostasis maintains the plasma glucose concentration within a narrow range despite the physiological challenges that include fasting, postprandial state and during intense exercise (Carnagarin *et al*., 2018).

Glucose homeostasis is achieved by the coordinated interplay of several organ systems like liver, endocrine pancreas, skeletal muscle, adipose tissue and key areas in the central nervous system like hypothalamus and brain stem along with autonomic nervous system (Carnagarin *et al*., 2018).

2.4.1 Role of the liver in glucose homeostasis

Liver contributes to glucose homeostasis by altering its glucose uptake, storage and output guided by the varying blood glucose levels. The liver is a primary organ for glucose metabolism. Liver contributes to about 90% of the total circulating glucose that is not derived directly from the food.

Under fasting conditions, the liver generates glucose via glycogenolysis for other organs to utilize especially the brain, red blood cells and muscles. The increase in pancreatic hormone glucagon initiates glycogenolysis that causes the release of glucose from stored glycogen. The stored glycogen is sufficient to maintain blood glucose levels during an overnight fast. However, during long periods of fasting or starvation (~30 hours of fasting) the liver is depleted of its stored glycogen and de novo glucose synthesis or gluconeogenesis takes over that generates glucose to be utilized by other tissues. The major non-carbohydrate sources for gluconeogenesis are amino acids, lactate and glycerol.

In the postprandial state, with the elevated blood glucose and insulin, the liver shifts to storage organ which stores glucose in the form of glycogen that can be utilised during periods of reduced food intake (Han *et al*., 2016).

2.4.2 Role of the pancreas in glucose homeostasis

The pancreas has a vital role in glucose homeostasis. The pancreas secretes two vital hormones insulin and glucagon in response to alterations in the blood glucose concentration.

   A) Insulin:

Insulin is secreted by β-cells of the islet of Langerhans. It is secreted in response to elevated blood glucose concentration in the postprandial state to avoid postprandial hyperglycemia. Insulin reduces hepatic glucose output by inhibiting hepatic glucogenesis and glycogenolysis. It induces glycogenesis in the liver and muscle, increases glucose uptake by striated muscle

and adipose tissue. Glucagon is secreted by the β-cells of islets of Langerhans in response to hypoglycaemia.

B) Glucagon

Glucagon is secreted by α-cells of the islet cells of Langerhans in response to hypoglycemia. It stimulates hepatic glucose formation and releases to maintain blood glucose levels. It stimulates hepatic gluconeogenesis from amino acids and glycerol. It enhances the hepatic uptake of amino acids and release of glycerol from adipose tissue. It decreases glycogenesis and glycolysis. Higher glucagon to insulin ratio increases gluconeogenesis, β-oxidation of fatty acids and formation of ketone bodies (Szablewski, 2017).

2.4.3 Role of the kidneys in Glucose Homeostasis

The kidneys contribute to glucose homeostasis by the release of glucose into circulation, uptake of glucose from the circulation and reabsorption of glucose from the glomerular filtrate. Kidneys release approximately 20-25% of glucose into circulation after an overnight fast. The kidney participates in gluconeogenesis and lactate, glutamine and glycerol serve as the substrates for gluconeogenesis. Insulin stimulates the renal glucose uptake and decreases the renal release of glucose into the circulation by decreasing the renal gluconeogenesis and reducing the availability of gluconeogenic substrates. While adrenaline reduces renal glucose uptake and enhances renal gluconeogenesis (Szablewski, 2017).

2.4.4 Role of the sympathetic nervous system in glucose homeostasis

The autonomic nervous system (ANS) influences glucose homeostasis by direct neural actions and hormonal effects. The ANS controls the functions of important organs like liver, pancreas, adipose tissue and skeletal muscle thereby influencing glucose homeostasis. Both divisions of ANS innervate the liver, pancreas and skeletal muscle while adipose tissue receives only sympathetic nerves and has adrenergic receptors. The effects of parasympathetic stimulation are masked by the effects of sympathetic stimulation. The

consequences of sympathetic stimulation on glucose metabolism overtake and predominate over the effects of parasympathetic stimulation (Nonogaki, 2000).

The SNS mediates its effect on glucose metabolism by circulating epinephrine, glucagon and direct innervations of the liver, adipose tissue and skeletal muscle (Nonogaki, 2000).

A) Effects of sympathetic stimulation on the hepatic glucose handling

Stimulation of the sympathetic innervation to the liver increases hepatic glucose output by promoting glycogenolysis in fed states and gluconeogenesis in fasted states. In addition to the direct effects of sympathetic innervations, epinephrine released by the adrenal medulla also contributes to the increased hepatic glucose output. Circulating norepinephrine also contribute to hepatic glycogenolysis but less effective when compared to epinephrine (Nonogaki, 2000).

B) Effect of sympathetic stimulation on glucose uptake in skeletal muscles:

Skeletal muscle is an important site of insulin-stimulated glucose uptake and utilisation following an increase in blood glucose in the postprandial state (Carnagarin *et al*., 2018). However, sympathetic stimulation and muscle contraction cause glucose utilization by the skeletal muscle independent of insulin. Sympathetic stimulation activates alternate pathways of skeletal muscle glucose uptake. β-adrenergic receptor stimulation has been demonstrated to increase glucose uptake by skeletal muscle independent of GLUT 4 translocation and norepinephrine is involved in its signalling. In contrast to norepinephrine, epinephrine inhibits insulin-stimulated glucose uptake in skeletal muscle by β-adrenergic receptor mechanisms independent of glucose transport processes (Nonogaki, 2000).

C) Effect of sympathetic stimulation on glucose uptake in adipose tissue:

Adipose tissue is under autonomic control being innervated by the only sympathetic division of the ANS. The sympathetic stimulation mediates glucose uptake by both white adipose

tissue (WAT) and brown adipose tissue (BAT) predominantly mediated by norepinephrine via β-adrenergic receptors (Landsberg *et al*., 1992).

D) Effect of sympathetic stimulation on pancreatic secretion

Pancreas impacts glucose homeostasis by secreting glucagon and insulin by α-cells and β-cells of islets of Langerhans respectively. Stimulation of parasympathetic innervations of β-cells increases insulin while sympathetic stimulation decreases insulin secretion (Rodriguez-Diaz *et al*., 2012).

Figure 2.5 depicts the effects of sympathetic stimulation on glucose homeostasis
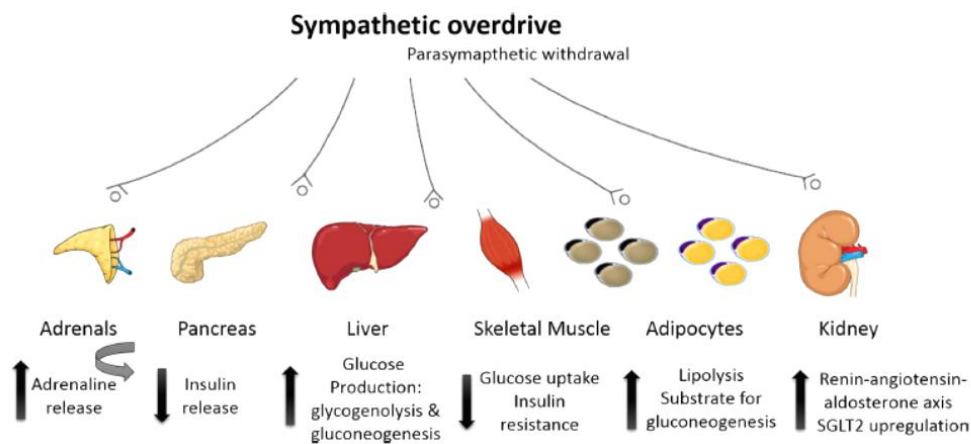
Figure 2.5: Effect of increased sympathetic drive on glucose homeostasis

Source: Carnagarin R, Matthews VB, Herat LY, Ho JK, Schlaich P. Autonomic regulation of glucose homeostasis: a specific role for sympathetic nervous system activation. Current Diabetes Reports 2018; 18: 107. Doi.org/10.1007/s11892-018-1069-2.

2.5 Insulin Resistance

 Insulin resistance sets in when the cells of the body become less responsive and resistant to insulin. Since insulin facilitates the entry of glucose into the cells particularly muscle, liver and adipose tissue, insulin resistance is characterized by increased blood glucose which triggers more secretion of insulin from the pancreas with resultant hyperinsulinemia. This long term overproduction of insulin exhausts the β-cells of islets of Langerhans off the

insulin and decreases their ability to release insulin. Over the years insulin resistance heralds the onset of type 2 diabetes.

2.5.1 Sympathetic Overactivity and Insulin Resistance

There is evidence suggesting the role of enhanced sympathetic activity in insulin resistance (Moreira *et al*., 2015). The most important tissues in insulin resistance are muscle and adipose tissue (Ceriello and Motz, 2004). Studies have revealed that insulin resistance occurs secondary to sympathetic overactivity (Baron *et al*., 1990; Julius *et al*., 1992). Increased skeletal muscle sympathetic nerve activity affects glucose metabolism primarily by reducing the blood flow to the skeletal muscle. Long term sympathetic overactivity can reduce skeletal muscle blood flow by alpha-adrenergic vasoconstriction decreasing postprandial glucose uptake by skeletal muscle and also stimulates additional insulin secretion by the pancreas leading to insulin resistance (Thorp and Schlaich, 2015). The brief outline of sympathetic overactivity induced insulin resistance is given in Figure 2.6.
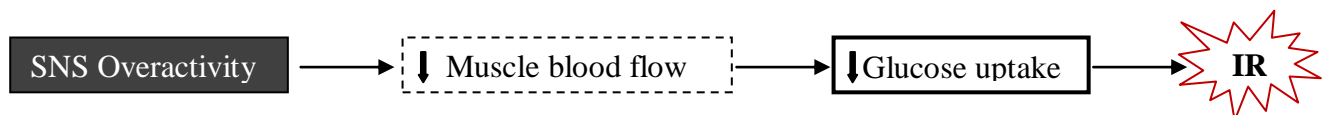
Figure 2.6: A brief outline of sympathetic overactivity induced insulin resistance

Source: Thorp AA, Schlaich MP. Relevance of sympathetic nervous system activation in obesity and metabolic syndrome. J Diabetes Res. 2015; 2015:341583. doi: 10.1155/2015/341583.

2.4.6 Oxidative stress and Insulin resistance

The mismatch between the formation of oxidants and the antioxidant defences with the resultant damage to the cells and the signal pathways is termed as oxidative stress (Sies, 2016). Oxidative stress has been recently linked to insulin resistance. ROS cause insulin resistance by affecting the insulin receptor signal transduction, resulting in the decreased expression of GLUT4 transporter on the cell membrane particularly of the skeletal muscle

resulting in desensitisation of the cell to glucose and positive feedback hyperinsulinemia (Hurrle and Hsu, 2017). Mechanism of oxidative stress-induced insulin resistance is depicted in Figure 2.7
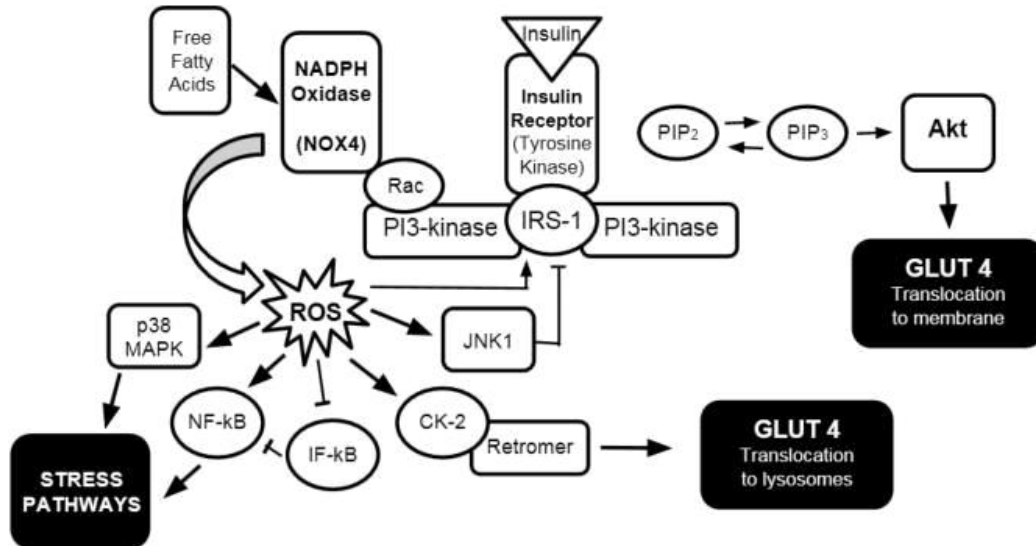
Figure 2.7: Mechanism of oxidative stress-induced insulin resistance

PIP2 and PIP3: phosphatidylinositol species; Rac: Rac GTPase; ROS: Reactive oxygen species; JNK1: c-Jun N-terminal kinase 1; CK-2: Casein kinase 2; NF-kβ: nuclear factor-kβ; IF- kβ: Inhibitory factor kβ; p38 MAPK: p38 mitogen-activated protein kinase; Akt: protein kinase B.

Source: Hurrle S, Hsu WH. The aetiology of oxidative stress in insulin resistance. Biomed J. 2017; 40(5):257–262. doi:10.1016/j.bj.2017.06.007

2.6 VOLTAGE- GATED Ca^{2+} CHANNELS

The voltage-gated calcium channels mediate the entry of calcium ions into the cells in response to membrane depolarization and action potential (Catterall, 2011). They belong to the family of multimeric transmembrane proteins. Six subtypes of Ca^{2+} channels have been identified namely L-, N-, P-, Q-, R- and T- types. Ca^{2+} channels are hetero-oligomeric composed of α_1, α_2-δ, β and γ subunits which are structurally dissimilar. The α_1 subunit is large and forms the calcium conduction pore. T-type Ca^{2+} channels are low voltage-activated (LVA), activated by small depolarisations while remaining ones are high voltage-activated Ca^{2+} channels (HVA) activated by larger depolarizations (Soderlund., 2010; Takahara, 2009).

The various physiological roles of voltage-gated calcium channels are as depicted in Figure 2.8 (Catterall, 2011).
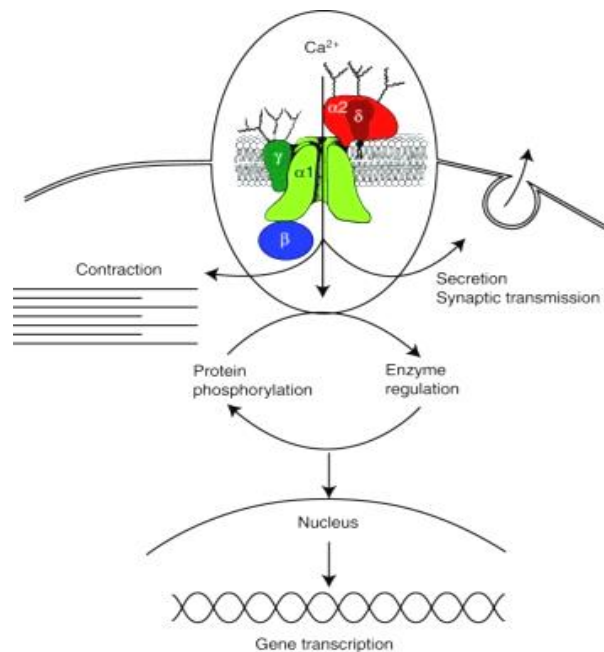
Figure 2.8: The Physiological role of voltage-gated Ca^{2+} channels

In the cardiovascular system, L-type Ca^{2+} channels are mostly present in the heart and blood vessels, regulating cardiac contractility, sinus nodal function, and vascular tone. N-type Ca^{2+} channels are localized at the nerve endings in the sympathetic and central nervous systems, regulating neurotransmitter release (Takahara, 2009).

Ca^{2+} channel blockers have been widely used in the pharmacological treatment of various cardiovascular diseases.

2.7 CALCIUM CHANNEL BLOCKERS (CCBs)

Most CCBs inhibit movement of Ca^{2+} ions across the membranes by blocking the L-type Ca^{2+} channels although some CCBs also block other Ca^{2+} channels. As a result, there is a reduced contraction of smooth and cardiac muscle, and cells within the sinoatrial (SA) and

atrioventricular (AV) nodes. Principle actions of the CCBs include dilatation of coronary and peripheral arteries, a negative inotropic, chronotropic and dromotropic actions. However, the actions of individual drugs vary depending on the degree of tissue selectivity demonstrated by the drug (McDonagh *et al*., 2005).

Based on the chemical structure, the CCBs are classified into three classes:

1. Benzothiazepines: Diltiazem

2. Phenylalkylamines: Verapamil

3. Dihydropyridines: Amlodipine, bepridil, felodipine, isradipine, nifedipine, nicardipine

Dihydropyridines demonstrate a greater selectivity for vascular smooth muscle compared to cardiac muscle since they block smooth muscle calcium channels at lower concentrations that are insufficient to produce significant cardiac effects. Hence, they have less negative inotropic effects than verapamil or diltiazem. Benzothiazepines and phenylalkylamines have a greater impact on the heart causing depression of SA and AV nodal conduction and have less selective vasodilator activity than dihydropyridines (McDonagh *et al*., 2005).

Among the various CCBs, dihydropyridines have been widely used in the management of cardiovascular diseases. Since their introduction in the 1960s, they have undergone several changes to improve efficacy and safety. There are four generations of dihydropyridines.

2.7.1 CILNIDIPINE

Cilnidipine is a fourth-generation dihydropyridine CCB. It is distinct due to its dual L/N type Ca^{2+} channel blocking properties. Since N-type Ca^{2+} channels are distributed along the sympathetic nerve endings they are demonstrated to inhibit the sympathetic nervous system (Chandra and Ramesh, 2013).
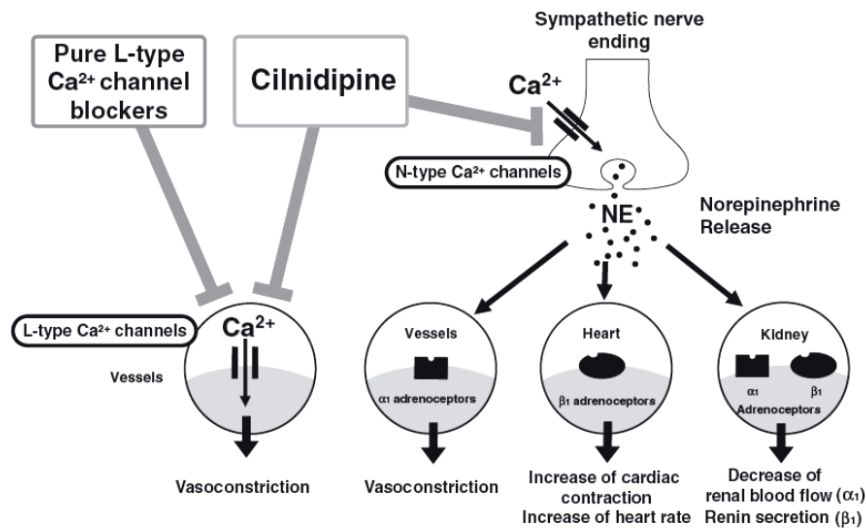
Figure 2.9: Dual L/N type Ca^{2+} channel blocking action of cilnidipine

Cilnidipine has a slow onset and long-lasting antihypertensive action. It is a potent coronary vasodilator and exhibits high vascular selectivity (Takahara, 2009).

Cilnidipine has been demonstrated to have a beneficial effect on glucose and lipid metabolism and renal function in hypertensive and type II diabetic patients (Takashi *et al*., 2011). It has been shown to improve insulin resistance in obese and in type II diabetes mellitus (Takeda et *al*., 1999; Ueshiba and Miyachi, 2002)

It has been demonstrated to reduce urinary albumin excretion in patients with hypertension (Rose and Ikebukoro, 2001). It has proven renoprotective and cardioprotective actions (Kojima *et al*., 2004; Tsuchihashi *et al*., 2005).

Cilnidipine is lipophilic and functions as a lipophilic chain-breaking antioxidant. When compared to other dihydropyridine CCBs, cilnidipine has been shown to be most lipophilic with the highest antioxidant actions (Hishikawa *et al*., 2009)

Cilnidipine has shown to enhance NOS3 expression and increase NO production in a human internal thoracic artery (Fan *et al*., 2011). Cilnidipine has been demonstrated to reduce endothelin -1 and endothelin ETA receptor expression and enhances NOS3 expression in the left ventricle thereby ameliorating cardiovascular remodelling in deoxycorticosterone acetate (DOCA)-salt hypertensive rats (Kobayashi *et al*., 2001).

CHAPTER III

AIM AND OBJECTIVES OF THE STUDY

3.1 AIM OF THE STUDY

The primary aim of the study was to evaluate the cardiovascular autonomic functions and hypoxia signalling molecules after chronic hypoxia exposure and their impact on cardiovascular remodelling and glucose homeostasis and the role of cilnidipine, a dual L/N type calcium channel blocker. To study the impact of unilateral common carotid artery occlusion on brain histopathology in experimental animals preconditioned to chronic hypoxia.

3.2 OBJECTIVES OF THE STUDY

1. To assess the impact of chronic sustained hypoxia on cardiovascular autonomic functions and the effect of treatment with cilnidipine.

2. To study the effect of chronic sustained hypoxia on cardiovascular remodelling and the effect of treatment with cilnidipine.

3. To evaluate the impact of chronic sustained hypoxia on glucose homeostasis and the effect of treatment with cilnidipine.

4. To study chronic hypoxia signalling pathways by quantitative assay of serum VEGF and serum NOS3.

5. To study the effect of unilateral common carotid artery occlusion on brain histopathology in chronic sustained hypoxia preconditioned rats.

3.3 HYPOTHESIS

We hypothesize that chronic hypoxia induces cardiovascular remodelling, impacts glucose homeostasis via hypoxia signalling and altering the cardiovascular autonomic functions. We further hypothesized that preconditioning to chronic hypoxia induces brain tolerance to subsequent acute brain ischemia/infarction.

CHAPTER IV

MATERIALS AND METHODS

4.0 MATERIALS AND METHODS

4.1. Experimental animals

The study involved laboratory-bred adult male Wistar strain albino rats (Rattus Norvegicus), weighing 180-250 g obtained from the animal house of Shri B. M. Patil Medical College, Hospital and Research Centre, BLDE (Deemed to be University), Vijayapur.

The experimental animals were maintained at 22-24^{0}C and exposed to 12 hours light and 12 hours dark cycle with food and water made available ad libitum. All the animals were acclimatized to the laboratory conditions for one week before initiating the experimental protocol.

4.2. Sample Size: The sample size was calculated using the resource equation approach (Affrin *et al*., 2017)

Sample Size= DF/k +1

DF=Degree of Freedom

k=No. of groups (4 in the present study)

Minimum n/group= 10/k+1=10/4+1=3.5

Maximum n/group=20/k+1=20/4+1=6

For the proposed study between 4-6 animals per group are required. A total of 16 to 24 animals are required to keep the degree of freedom within the range of 10-20.

4.3. Experimental groups:

The acclimatised animals were randomly allocated to one of the following four groups as depicted in table 4.1.

Table 4.1: Experimental groups

S. No.	Groups	Intervention
1.	Group 1 (Control)	Vehicle (0.5% NaCMC) by oral gavage for 21 days
2.	Group 2 (CH)	Chronic hypoxia (CH; 10% O_2, 90% N_2) for 21 days + Vehicle (0.5% NaCMC) by oral gavage for 21 days (Das *et al.*, 2015)
3.	Group 3 (Cil)	Cilnidipine (2.0mg/kg/day) in 0.5% Na CMC by oral gavage for 21 days (Nair and Jacob, 2016)
4.	Group 4 (CH+Cil)	Chronic hypoxia (CH; 10% O_2, 90% N_2) for 21 days + cilnidipine (2.0mg/kg/day) in 0.5% NaCMC by oral gavage for 21 days

CH-Chronic Hypoxia; Cil-Cilnidipine; CH+Cil-Chronic Hypoxia+Cil; NaCMC-Sodium Carboxymethylcellulose

4.4. Experimental Protocol: The experimental protocol followed in the study is depicted in figure 4.1
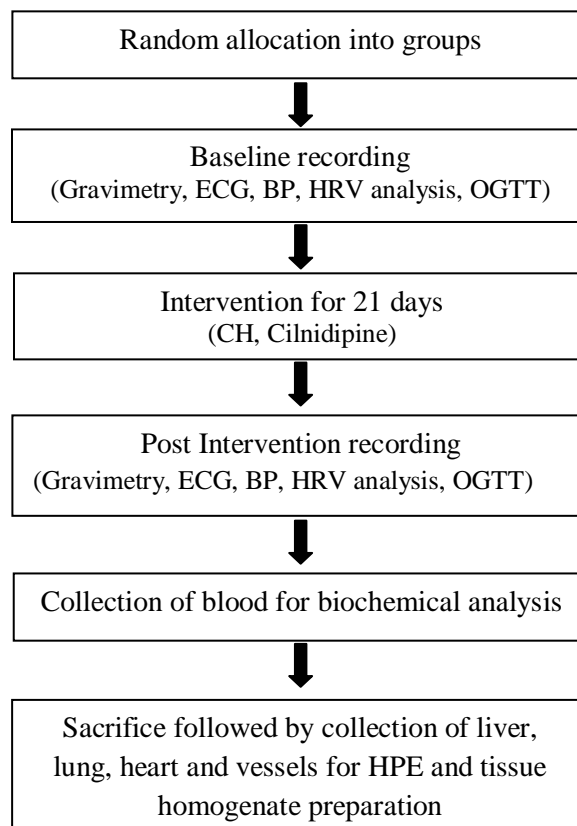
Figure 4.1: Summary of the experimental protocol

(CH: Chronic hypoxia)

4.5. Exposure of animals to chronic hypoxia: For chronic hypoxia exposure, caged rats (4 rats/cage) were placed in a 300-litre acrylic chamber that can accomodate 4 cages (16 rats). To induce normobaric hypoxia the experimental animals were exposed to inspired oxygen (10%) and nitrogen (90%). The hypoxic environment was created with an inflow of a mixture of room air and nitrogen. Soda-lime granules (27 granules) were used to absorb CO_2 and desiccator removed excess humidity. 24-26°C temperature was maintained. The chamber was opened two times a week for 1 hour to clean the cages and replenish food and water. In the present study rats were exposed to hypoxia for 21 days (Das *et al*., 2015).

4.6. Administration of drug cilnidipine: Cilnidipine was procured from LakshFine Chem Pvt. Ltd, Gujarat, India.

The dose of cilnidipine for rats was calculated using the formula given below (Nair and Jacob, 2016).

$$\text{Rat equivalent dose (mg/kg)} = \text{Human dose (mg/kg)} \times K_m \text{ ratio}$$

$$= \frac{20}{60} \times 6.2$$

$$\simeq 2.0 \text{ mg/kg/day}$$

K_m ratio is obtained by dividing human K_m factor by animal K_m factor or vice versa.

The K_m ratio for the rat is 6.2 and 0.162 obtained by dividing 37 (human K_m factor) by 6 (rat K_m factor) and vice versa respectively.

K_m - correction factor. It is estimated by dividing the average body weight (Kg) of species to its body surface area (m^2) (Nair and Jacob, 2016)

The dose of cilnidipine for each rat was calculated to be 2.0mg/kg/day.

Since cilnidipine is sparingly soluble in water, it was administered as a suspension in 0.5% sodium carboxymethylcellulose (NaCMC). The suspension was prepared afresh daily and was administered by oral gavage once every morning to group 3 (Cil) and group 4 (CH+Cil).

4.7. Method of data collection:

4.7.1. Gravimetry:

The body weight of all rats was recorded on day 0 of the experiment (initial body weight) and after 21 days of intervention (day 22, final body weight) (as the period of intervention was 21 days i.e. from day 1-day 21) with an electronic balance (Practum 1102-10IN, Sartorius Lab Instruments, Germany). Percentage change in body weight was calculated using the formula.

$$Change\ in\ body\ weight\ (\%) = \frac{Final\ body\ weight - Initial\ body\ weight}{Initial\ body\ weight} \times 100$$

The body weight of rats of all groups was matched at the onset of the experimental protocol.

4.7.2. Recording of Pneumogram:
The respiratory frequency was assessed by recording the abdominal movements during respiration by using the respiratory pad transducer (BioPac Student lab system). The respiratory rate was recorded twice – pre-intervention (day 1) and post-intervention (day 22) as the period of the intervention was from day 1-day 21 (total – 21 days intervention).

4.7.3. Evaluation of cardiovascular electrophysiology:

A) Recording of Blood Pressure
B) Recording of ECG
C) Heart rate variability (HRV) analysis

A) Recording of Blood Pressure

Blood Pressure was recorded noninvasively (NIBP) using a tail-cuff sensor (BioPac 200A) after placing the animal in a restrainer. Systolic blood pressure (SBP) and Diastolic blood pressure (DBP) were recorded. Three values were obtained and the average of the three readings was considered. Mean arterial pressure (MAP) was calculated using the formula.

$$\text{Mean Arterial Pressure} = DBP + \frac{1}{3}(SBP - DBP)$$

B) Recording of ECG

ECG was recorded using needle subcutaneous electrodes using MP45 Biopac instrument with a PC based BSL 4.1 (Biopac Student Lab 4.1) software. All the recordings were performed in the morning hours following overnight fasting. A 10 minute ECG was recorded in anaesthetized rats (ketamine, 60mg/kg b. wt., i.p and xylazine, 6mg/kg b. wt., i.p) in dorsal recumbency by inserting the needle electrodes in right (negative) and left (positive) front legs and right rear leg (GND). From the recorded ECG heart rate was obtained.

C) Heart rate variability analysis:

Heart functions as an effective pump. However, a healthy heart is not a metronome. There are oscillations in the time intervals between successive heartbeats. The analysis of such fluctuations in the interbeat intervals is termed heart rate variability analysis. HRV analysis is widely used as a non-invasive technique to assess cardiovascular autonomic functions. HRV analysis involves time and frequency domain indices. Frequency domain analysis of RR interval oscillations uses two major frequency bands a) low frequency (LF) band (0.04-0.15Hz) predominantly reflects sympathetic activity b) High frequency (HF) (0.15-0.4 Hz) band reflects the parasympathetic activity. LF/HF ratio is as an indicator of cardiac sympathovagal balance (Shaffer *et al*., 2017).

The recorded ECG was inspected offline for artefacts and ectopic beats that were manually deleted from the recording. RR intervals obtained from the recorded ECG were exported to Kubios software version 2.0 (developed by Department of Physics, University of Kuopio, Finland) for HRV analysis. Short term heart rate variability (HRV) analysis using 5 min ECG RR interval data was done to assess cardiac autonomic balance. Frequency-domain method of HRV analysis was used to assess the level of sympathetic activity, parasympathetic activity and sympathovagal balance.

Table 4.2: Components of the frequency domain method of HRV analysis

Sl. No	Component	Indicator
1.	Low-frequency component (LF) (nu)	Sympathetic activity
2.	High frequency component (HF) (nu)	Parasympathetic activity
3.	LF/HF ratio	Sympathovagal balance

- All the above parameters were recorded twice – pre-intervention (day 0) and post-intervention (day 22)

4.7.4. Collection of Blood:

Blood was collected on day 22 in overnight fasted rats. Blood was collected by cardiac puncture in anaesthetized rats in ethylenediaminetetraacetic acid (EDTA) and plain tubes for further haematological study and biochemical analysis respectively.

4.7.5 HAEMATOLOGICAL ANALYSIS:

About 1ml of blood was collected in commercial tubes containing about 40µl of potassium EDTA as an anticoagulant. The collected blood samples were analysed by an automated haematology cell counter (Sysmex K4500 Automated Haematology Analyzer) for determination of RBC count (million/mm^3), Hematocrit (%), Hemoglobin (g/dl).

4.7.6 BIOCHEMICAL ANALYSIS

A) Assessment of glucose homeostasis:

Assessment of glucose homeostasis was done by

1. Estimation of Fasting blood glucose
2. Estimation of Fasting Plasma Insulin
3. Oral Glucose Tolerance Test (OGTT)
4. Calculation of HOMA-IR

1. Estimation of fasting plasma glucose

Glucose was estimated by Trinder's method (glucose oxidase-peroxidase method) (Trinder, 1969) using a commercial kit (ERBA diagnostics, Mannheim GmBH,) according to the manufacturer's protocol. For this blood was collected from the overnight fasted rats. Fasting plasma glucose estimations were performed twice during the experimental protocol – preintervention (day 0) and post-intervention (day 22) in rats of all groups (as the period of the intervention was for 21 days i.e. from day 1-day 21).

Principle: Glucose in the sample is oxidized to yield gluconic acid and hydrogen peroxide in the presence of glucose oxidase. The enzyme peroxidase catalyses the oxidative coupling of 4-aminoantipyrine with phenol to yield a coloured quinoneimine complex, with the absorbance proportional to the concentration of glucose in the sample.

$$\beta\text{-D-Glucose} + H_2O + O_2 \xrightarrow{\text{Glucose oxidase}} \text{Gluconic acid} + H_2O_2$$

$$H_2O_2 + \text{Phenol} + 4AAP \xrightarrow{\text{Glucose Peroxidase}} \text{Red Dye} + 2H_2O$$
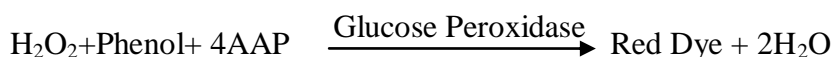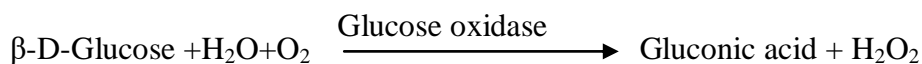
- **Reagent Composition**
  R1

  Phosphate Buffer   250 mmol/L

	Blank	Standard	Sample
Glucose oxidase		>25U/ml	
Peroxidase		>2 U/ml	
Phenol		5 mmol/L	
4-aminoantipyrine		0.5 mmol/L	

Glucose oxidase   >25U/ml

Peroxidase   >2 U/ml

Phenol   5 mmol/L

4-aminoantipyrine   0.5 mmol/L

R2

Glucose Standard – 100mg/dl

Procedure:

1. Three test tubes were taken and labelled as blank, standard and sample. The procedure of the assay was as follows

	Blank	Standard	Sample
Reagent 1	1000µl	1000µl	1000µl
Sample	--	--	10µl
Standard	--	10µl	--
Distilled Water	10 µl	--	--

2. The contents were mixed well and incubated at 37^0C for 5 -10 minutes.

3. The absorbance of the sample and standard was read against blank at 490-550nm maximum at 500nm by UV visible spectrophotometer (Shimadzu, Model: UV 1800).

Calculations

Glucose (mg/dl)$= \frac{OD\ of\ test}{OD\ of\ standard} \times concentration\ of\ standard\ (100 mg/dl)$

2. **Oral Glucose Tolerance Test**

OGTT was performed twice - preintervention (day 0) and post-intervention on the day of sacrifice (day 22). OGTT was performed in the morning hours in overnight fasted rats. The experimental rats were challenged with a glucose load of 2.0g/kg b.wt. administered by oral gavage. Fasting blood sample (0 min) was collected before administration of glucose load and subsequent samples were collected from the tail vein at 30min, 60min, 90min and

120min after administration of glucose load (Bowe *et al*., 2014). The glucose estimations were made with a commercial glucometer (ACCU-CHEK Active; Roche).

3. **Estimation of Fasting Plasma Insulin**

Fasting Plasma Insulin was estimated by ELISA using Rat Insulin ELISA kit (Catalog No: BEK1243, Chongqing Biospes Co., Ltd, Chongqing, China) following the protocol given in the product manual.

- **Principle of the Assay**: The kit is based on sandwich enzyme-linked immune sorbent assay technique. 96 well plates precoated with anti-Insulin monoclonal antibody was used. The HRP conjugated anti-Insulin polyclonal antibody was used as detection antibodies. The standards, test samples and HRP conjugated detection antibody were added to the wells subsequently, and washed with wash buffer. TMB substrates were used to visualize HRP enzymatic reaction. TMB was catalyzed by HRP to produce a blue colour product that changed into yellow after adding acidic stop solution. The density of yellow is proportional to the insulin amount of sample captured in plate. OD absorbance was read at 450nm in a microplate reader and then the concentration of insulin can be calculated.

- **Range**: 0µIU/ml-140µIU/ml
- **Sensitivity**: <5µIU/ml
- **Kit components**:
  1. One 96-well plate precoated with an anti-Rat Insulin antibody
  2. Lyophilized insulin standards: 5 tubes (8µIU/ml, 16µIU/ml, 32µIU/ml, 80µIU/ml, 140µIU/ml)
  3. HRP conjugated anti-rat Insulin antibody
  4. TMB substrate A
  5. TMB substrate B
  6. Stop solution
  7. Wash buffer

Protocol

- **Preparation of sample and reagents**

  1. *Sample*: Blood was collected in EDTA tube. Centrifuged for 30 min at 1000xg within 30 minutes of collection. Plasma was aliquoted and stored at -20^{0}C for further analysis.

  2. *Wash buffer:* The concentrated wash buffer was diluted 25-fold (1:25) with distilled water.

  3. *Standard:* Reconstitution of the lyophilized standards: The standards were first equilibrated to room temperature. 0.5ml of double distilled water was added into each vial of the corresponding standard and mixed thoroughly and kept at room temperature for 10 min for use.

- **Assay Procedure:**

1. Standard, test sample and control (zero) wells were set on the pre-coated plate respectively, and then, their positions were recorded. Each standard and sample was run in duplicate.

2. 50µl of 8µIU/ml, 16µIU/ml, 32µIU/ml, 80 µIU/ml, and 140µIU/ml of standard solutions were aliquoted into the standard wells. 50µl of sample diluent buffer was added into control well.

3. 50µl of the properly diluted sample (rat serum) was added into test sample wells.

4. 50µl of HRP conjugated anti-rat insulin antibody was added into above wells (except control wells) at the bottom of each well without touching the side well.

5. The plate was sealed with a cover and incubated at 37^{0}C for 60 min.

6. The cover was removed and the liquid of the wells discarded, the plate was clapped on the absorbent filter papers and not washed

7. The plate was washed three times with wash buffer using manual washing. Each well was completely filled with wash buffer and mildly vortexed for 2 min on ELISA shaker. The

contents were then aspirated from the plate and the plate was clapped on absorbent filter paper. The whole procedure was done 3 times.

8. 50µl of TMB substrate A was added into each well and then 50 µl of TMB substrate B was added. The plate was gently shaken by hand for 30 sec. the plate was covered and incubated in dark at 37^0C for 15 min. The shades of blue were observed in the first 3-4 wells with the highest concentration of rat insulin standard solutions, the other wells showed no obvious colour.

9. 50µl of stop solution was added into each well and mixed thoroughly. The colour changed to yellow immediately.

10. The OD absorbance was read at 450nm in a microplate reader (Model: Merilyzer EIAQUAN, Meril Diagnostics Pvt. Ltd.) within 30 min after adding the stop solution.

Calculations

Relative O.D. $_{450}$= (O.D.$_{450}$ of each well) – (O.D.$_{450}$ of Zero well).

The standard curve was plotted as the relative O.D.$_{450}$ of each standard solution (Y) vs. the respective concentration of the standard solutions (X). The rat insulin concentration of the samples was interpolated from the standard curve.

Standard curve

X	µIU/ml	0	8	16	32	80	140
Y	OD$_{450}$	0	0.084	0.1044	0.3405	0.986	2.034
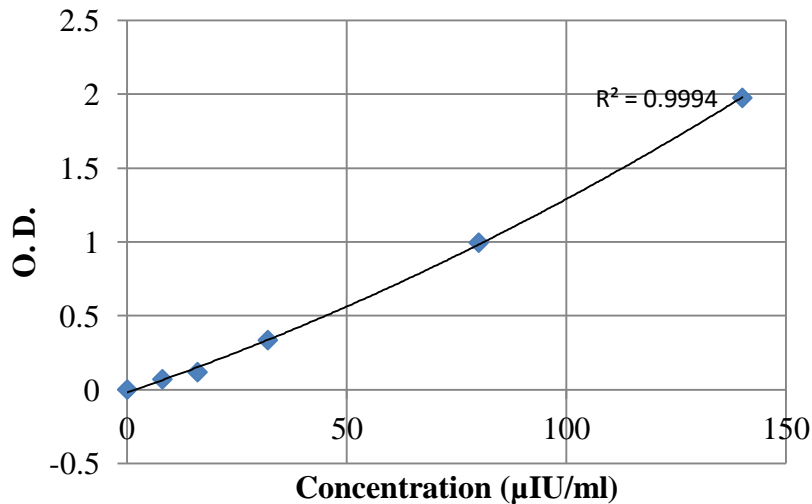
4. Calculation of HOMA - IR

Homeostasis Model Assessment of Insulin Resistance (HOMA-IR) a measure of insulin resistance was calculated by using formula (Das *et al*., 2016)

HOMA-IR = fasting plasma insulin (milliunits / liter) x fasting plasma glucose (millimoles / liter)/22.5

B) Assessment of Lipid Profile

a. Serum total cholesterol (TC), Serum triglycerides (TG), and High-density lipoprotein (HDL) were analyzed using a commercial diagnostic kit (Erba Diagnostic Mannheim GmBH).

b. LDL and VLDL levels were calculated using the Friedwald formula (Friedwald *et al*., 1972) as indicated below

- LDL (mg/dl)= Total cholesterol – HDL cholesterol - TG/5

- VLDL= TG/5

1. Estimation of Serum Total Cholesterol

Serum cholesterol was estimated by cholesterol oxidase – peroxidase enzymatic method (CHOD-POD) (Allain *et al*., 1974) using a commercial kit (Tranasia Bio-medicals Ltd, ERBA Diagnostics, Mannheim GmBH).

- **Principle**

Cholesterol esters were hydrolysed by cholesterol esterase to cholesterol and free fatty acids. Free cholesterol was oxidised by cholesterol oxidase to cholest-4-ene-3-one and hydrogen peroxide. This hydrogen peroxide combined with 4-aminoantipyrine to form chromophore (quinoneimine) dye which was measured at 505 nm.

- **Reagents**
1. Reagents
   - Good's buffer (50mmol/L)
   - Phenol (5mmol/L)
   - 4-aminoantipyrine (0.3mmol/L)
   - Cholesterol esterase ($\geq$200U/L)
   - Cholesterol oxidase ($\geq$50U/L)
   - Peroxidase (($\geq$3kU/L)
2. Cholesterol Standard : 200mg/dl

- **Procedure**

1. Three test tubes were taken and labelled as blank, standard and test. The procedure of the assay was as follows:

	Blank	Standard	Test
Sample	--	--	10µl
Standard	--	10µl	--
Reagent	1.0 ml	1.0 ml	1.0 ml
Distilled water	10µl	--	--

2. Mixed well and incubated at 37^0C for 10 minutes.

3. The absorbance of the test and standard was read against blank at 505nm by UV visible spectrophotometer (Shimadzu, Model: UV 1800).

- **Calculation:**

$$\text{Cholesterol (mg/dl)} = \frac{OD\ of\ test}{OD\ of\ standard} \times Concentration\ of\ standard\ (200mg/dl)$$

2. Estimation of Serum Triglycerides:

The serum triglycerides were estimated by glycerophosphate oxidase peroxidase (GOD-POD) method (Werner et al., 1981) using a commercially available kit (ERBA Diagnostics, Mannheim GmBH)

- **Methodology**

This reagent is based on the method of Wako and the modification by McGowan et al. and Fossati et al. (Fossati and Prencipe, 1982; McGowan *et al*., 1983;)

- **Principle**

Triglycerides were enzymatically hydrolyzed by lipase to glycerol and free fatty acids. The glycerol was subsequently measured by a coupled enzymatic reaction system. The glycerol released was phosphorylated to glycerol –3– phosphate by glycerol kinase. The glycerol –3– phosphate was oxidised by glycerol phosphate oxidase to produce dihydroxyacetone phosphate and hydrogen peroxide. Peroxidase catalyzed the reaction of hydrogen peroxide with 4-Aminoantipyrine and 3, 5-Dichloro-2-hydroxybenzene sulfonate. The absorbance of chromogen formed was measured at 505nm (500-540 nm).

$$\text{Triglycerides} + H_2O \xrightarrow{\text{LDL}} \text{Glycerol} + \text{Free Fatty acids}$$

$$\text{Glycerol} + ATP \xrightarrow[\text{Mg}^{+2}]{\text{GK}} \text{Glycerol-3-Phosphate} + ADP$$

$$\text{Glycerol-3-Phosphate} + O_2 \xrightarrow{\text{GPO}} \text{DAP} + H_2O_2$$

$$H_2O_2 + 4AAP + 3,5\ DHBS \xrightarrow{\text{Peroxidase}} \text{Quinoneimine dye} + 2H_2O$$
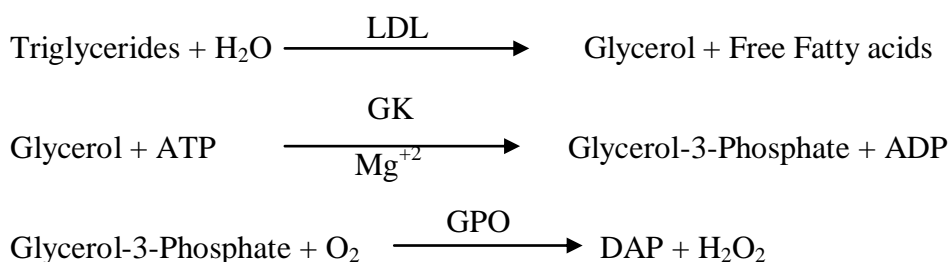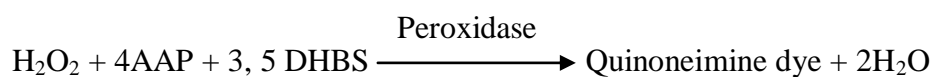
LPL-Lipoprotein Lipase

GK-Glycerol Kinase

GPO-Glycerol Phosphate Oxidase

DAP-Dihydroxyacetone phosphate

ATP-Adenosine triphosphate

4-ATP- 4 Aminoantipyrine

DHBS- 3, 5-Dichloro-2-hydroxybenzene sulfonate

The intensity of chromagen (Quinoneimine) formed is proportional to the triglycerides concentration in the sample when measured at 505nm (500-540nm).

- **Reagent Composition:**

Active Ingredient	Concentration
ATP	2.5 mmol/L
Mg^{+2}	2.5 m mol/L
4 Aminoantipyrine	0.8 mmol/L
3,5-DHBS	1mmol/L
Peroxidase	>2000U/L
Glycerol Kinase	>550U/L
GPO	>8000U/L
Lipoprotein Lipase	>3500U/L
Buffer (pH 7.0 ± 0.1 at 20^0C)	53mmol/L

Triglyceride Standard: 200 mg/dl (2.3mmol/L)

Reagent reconstitution: The reagent bottle and AQUA-4 (supplied in the kit) was allowed to attain room temperature (15-30^{0}C). The amount of AQUA-4 as indicated on the label was added to the contents of each vial. Swirled to dissolve and allowed to stand for 10 minutes at room temperature.

Sample: Serum or Plasma samples, free from hemolysis and collected after 12-16 hours fasting are suitable for triglyceride estimation.

- **Assay Procedure:**

Pipette into tube marked	Blank	Standard	Test
Working reagent	1000µl	1000µl	1000µl
Distilled water	10µl	-	-
Standard	-	10µl	-
Test	-	-	10µl

The above contents were mixed and incubated for 10 min at 37^0C. The absorbance of standard and each test was read at 505 nm on bichromatic analysers against reagent blank with UV visible spectrophotometer (Shimadzu, Model: UV 1800).

- **Calculations**

Triglycerides (mg/dl) $= \frac{Absorbance\ of\ Test}{Absorbance\ of\ Standard} \times Concentration\ of\ Standard\ (mg/dl)$

3. Estimation of HDL Direct

- **Principle**

The assay is based on a modified polyvinyl sulfonic acid (PVS) and polyethylene-glycol-methyl ether (PEGME) coupled classic precipitation method with the improvements in using optimized quantities of PVS/PEGME and selected detergents (Pisani *et al*., 1995). LDL, VLDL and chylomicron (CM) react with PVS and PEGME and the reaction results in inaccessibility of LDL, VLDL and chylomicron by cholesterol oxidase (CHOD) and cholesterol esterase (CHER). The enzyme selectively reacts with HDL to produce H_2O_2 which is detected through a Trinder reaction.

$$HDL + LDL + VLDL + CM \xrightarrow{\text{PVS, PEGME}} HDL + (LDL+VLDL+CM) + PVS/PEGME$$

$$HDL \xrightarrow{\text{CHOD, CHER}} \text{Fatty acid} + H_2O_2$$

$$2H_2O_2 + 4\text{-AA} + TODB \xrightarrow{\text{Peroxidase}} \text{Quinone} + 5H_2O$$
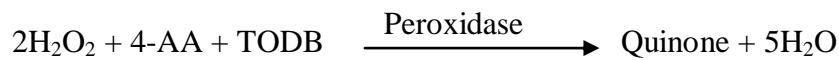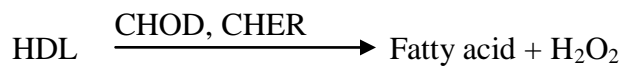
- **Reagent Composition**

R1

MES buffer
N, N-Bis (4-sulfobutyl)-3-methylaniline
Polyvinyl sulfonic acid
Polyethylene-glycol-methyl ester
$MgCl_2$

R2

MES buffer
Cholesterol esterase
Cholesterol oxidase
Peroxidase
4-aminopyrine
Detergent

R3 CAL

HDL/LDL calibrator

- **Reagent preparation**

Reagents R1 and R2 were liquid and ready to use.

Calibrator was reconstituted with 1ml of deionized water at 20-25^{0}C and mixed gently (avoid foaming) and allowed to stand for at least 30 minutes until complete reconstitution before use.

Sample: Serum or heparin plasma

- Assay Procedure

Pipette in Tube	Reagent blank	Sample/Calibrator
Reagent 1	750µl	750µl
D.D water	10µl	10µl
Mix and incubate at 37^0C for 5 min.		
Add Reagent 2	250µl	250µl
Mix and incubate at 37^0C for 5 min.		

The final absorbance was read at the specified wavelength against reagent blank by UV visible spectrophotometer (Shimadzu, Model: UV 1800).

CALCULATION

$$HDL\text{-}C = \frac{Abs.of\ Sample - Abs.of\ Sample\ Blank}{Abs.of\ Cal - Abs.of\ Cal.\ Blank} \times Concentration\ of\ Calibrator$$

4. LDL and VLDL levels were estimated by calculation using the Friedwald formula (Friedwald *et al*., 1972)

- LDL mg/dl = Total cholesterol-HDL cholesterol-Triglyceride/5

- VLDL = TG/5

C) OXIDATIVE STRESS ASSESSMENT:

1. Estimation of Serum MDA: By the method of Buege and Aust (Buege and Aust, 1978)

2. Estimation of Serum Vitamin C: By the method of Roe & Koether (Roe and Kuether, 1943)

3. Estimation of Serum Vitamin E: By the modified method of Jargar et al (Jargar *et al*., 2012)

4. Estimation of MDA in liver, lung, heart tissue homogenate: By the method of Buege and Aust (Buege and Aust, 1978)

1. **Estimation of Malondialdehyde**: By the method of Buege and Aust (Buege and Aust, 1978)

- **Introduction**

In the biological systems, malondialdehyde (MDA) is used as an indicator of oxidative stress. It is one of the end products of lipid peroxidation. It is formed by the degradation of polyunsaturated fatty acid (PUFA) by a free radical chain reaction. This compound is a reactive aldehyde and is one among the many reactive electrophile species causing oxidative stress.

- **Principle**

MDA formed by the breakdown of PUFA serves as a convenient index to determine the extent of lipid peroxidation. It reacts with thiobarbituric acid (TBA) giving a pink colour which is read at 535nm.

- **Sample**: serum, saliva, tissue homogenate

- **Chemicals required**:
    1. Trichloroacetic acid (TCA)

    2. 2-Thiobarbituric acid (TBA)

    3. Hydrochloric acid (HCl)

    4. Malonaldehydebis (dimethyl acetal)

- **Preparation:**

1. *TCA-TBA-HCl reagent*

    0.25 N HCl: 2.21 ml of concentrated HCl was made up to 100 ml with distilled water (DW). 15% TCA and 0.375% TBA was dissolved in 100ml of 0.25N HCl. The reaction mixture was warmed to dissolve the contents and stored at 4^0C.

2. *MDA standard (stock-164µg/ml)*

   16.4µl of standard MDA solution was taken and made up to 100 ml using distilled water.

3. *MDA working standard (working- 1.64µg/ml)*

   100µl of the stock was made up to 10 ml using distilled water.

- **The procedure for standardization:**

Standardisation (Range 2-10µM/L)

The standardization was carried out referring to the table and all the reagents were added according to the values given in the table

S.No.	Vol. of MDA (ml)	Vol. of DW (ml)	Conc. of MDA (µM/L)	TBA-TCA-HCl (ml)	
B	0.0	1	0.0	1	Keep in boiling water bath for 15 min
1	0.2	0.8	2.0	1	
2	0.4	0.6	4.0	1	
3	0.6	0.4	6.0	1	
4	0.8	0.2	8.0	1	
5	1	-	10.0	1	

Read O.D. absorbance at 535nm. The optical densities were plotted against the concentration on a graph.

- **Standard Curve**
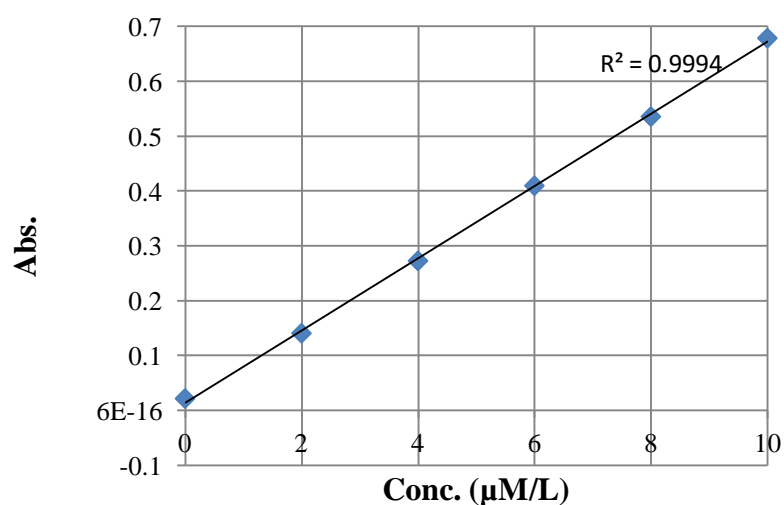
Estimation of MDA in the sample:

- Sample preparation:

Serum: 100µl serum was diluted to 500µl with distilled water

Tissue Homogenate: 500 µl of 10% tissue homogenate was taken

(Tissue homogenate preparation: 10% tissue homogenate was prepared by adding 500 mg of tissue to 5ml of 0.1M phosphate buffer, homogenized for a few minutes, centrifuged and the supernatant was used in the estimation).

- **Procedure**

1. To the diluted sample 1ml of TCA-TBA-HCl reagent was added.
2. The samples were kept in a boiling water bath for 15 minutes.
3. The reaction mixture was cooled and centrifuged.
4. The supernatant was taken and the optical densities of the pink colour formed were read at 535nm by UV visible spectrophotometer (Shimadzu, Model: UV 1800).
5. The concentration of MDA in the sample was determined by plotting the obtained absorbance against the standard graph. The optical density of pink colour formed was directly proportional to the concentration of MDA in the given sample.

- **Calculations**

The optical densities of the test samples were directly proportional to the concentration of MDA in the sample and calculated by plotting against the standard graph and multiplied by the respective dilution factors. The final concentration was expressed as µM/L.

2. Estimation of Vitamin C

By Roe and Kuther method (Roe and Kuether, 1943)

Vitamin C assay includes standardization of chemicals and estimation of vitamin C in the sample.

- **Standardization of Vitamin C:**

Principle: The ascorbic acid is oxidized to diketogluconic acid in presence of strong acid solution which reacts with 2, 4, dinitrophenylhydrazine to form diphenylhydrazone which dissolves in strong H_2SO_4 solution to produce red colour which can be measured at 505nm (range of vitamin C 500-520nm) spectrophotometrically.

- **Reagents**

  1. TCA (10%): 10gm of trichloroacetic acid (TCA) was dissolved in distilled water and the volume was made up to 100ml.

  2. 2,4, dinitrophenylhydrazine (2,4, DNPH): 2gm of 2,4, dinitrophenylhydrazine was dissolved in 9N H_2SO_4 and volume was made up to 100ml.

  3. Thiourea: 10gm of Thiourea was dissolved in 100ml of 50% ethanol

  4. $CuSO_4$: 1.5 gm of $CuSO_4$ was dissolved in distilled water up to 100ml.

  5. Combined color reagent (prepared fresh at the time of assay): 5ml 2,4 DNPH + 0.1 ml of $CuSO_4$ + 1ml Thiourea.

  6. 85% H_2SO_4: 85 ml of H_2SO_4 was added in distilled water to make up to 100ml.

  7. Stock Solution: 1gm of vitamin C dissolved in distilled water and made up to 100ml.

  8. Working Standard: 1ml of stock solution was made up to 100ml with distilled water.

- The procedure of standardization:

S.No.	Conc. of Vit C (mg/dl)	Vol. of working standard Ml	DW (ml)	TCA (ml)	Colour reagent (ml)			85% H_2SO_4 (ml)
B	0	0	0.5	0.5	0.4	Mix well and keep in a warm water bath at 56^0C for 1 hour	Cooled in an ice bath for 5 min	2
S1	0.2	0.1	0.4	0.5	0.4			2
S2	0.4	0.2	0.3	0.5	0.4			2
S3	0.6	0.3	0.2	0.5	0.4			2
S4	0.8	0.4	0.1	0.5	0.4			2
S5	1.0	0.5	-	0.5	0.4			2

20 minutes after adding 2ml of chilled 85% H_2SO_4 the reading was taken at 505nm by UV visible spectrophotometer (Shimadzu, Model: UV 1800). The optical densities were plotted against the concentration on a graph.
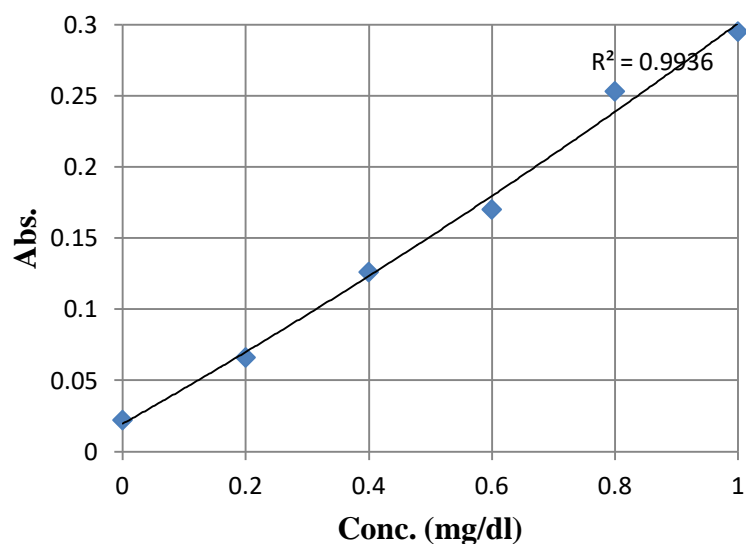
Estimation of Vitamin C in the sample

- **Sample preparation:**

1. For plasma/serum: 500µl of the sample was added to 500 µl of 10% TCA. Mixed well for 10-15 sec. Centrifuged for 10min at 3500rpm and supernatant taken.

2. For Tissue: To 500µl of supernatant, 500µl of 10% TCA was added and centrifuged for 10 min at 3500 rpm and the supernatant was taken.

(Preparation of tissue homogenate: 500mg of tissue in 5ml of 0.9% NaCl was taken and homogenized for a few minutes. Centrifuged and the supernatant was used for estimation).

- **Procedure**

Following sample preparation, 500µl of supernatant was taken, 0.4ml of a colour reagent was added and placed in water bath at 56^0C for 1 hour. Then cooled and 2ml of chilled 85% H_2SO_4 was added and after 20 minutes the readings were taken at 505nm spectrophotometrically (Shimadzu, Model: UV 1800).

- **Calculations**

Concentration of serum vitamin C

$$= \frac{OD\ of\ Test}{OD\ of\ Std} \times \frac{Conc.of\ Std}{Volume\ of\ Test} \times 100$$

=.....................mg/dl

3. Estimation of Vitamin E

By Jameel Jargar and Das method (Jargar JG *et al.*, 2012)

- **Reagents**

  Absolute ethanol (aldehyde free)

  N-propanol

  Xylene (extra pure)

  Ferric chloride (0.12%)

  Distilled water

  DL-α-tocopherol acetate

  2, 2'-Bipyridyl

- **Reagent preparation**

  1. Stock Standard (0.27% w/v): 270 mg of α-tocopherol acetate was diluted in 100ml of absolute ethanol and mixed thoroughly.

  2. 2, 2' – Bipyridyl (0.12% w/v): 120 mg of 2, 2' bipyridyl dissolved and made volume up to 100 ml in n-propanol and kept in a brown bottle.

  3. Ferric Chloride: (0.12% w/v): 120 mg of ferric chloride dissolved in 100 ml absolute ethanol and kept in a brown bottle.

  4. Working Standard: (27μg/ml): 1ml of the stock standard was diluted to 100ml with absolute ethanol to obtain a concentration of 27μg/ml.

- **The procedure of standardisation**

6 centrifuge tubes were taken and labelled as B (Blank), S1, S2, S3 S4 and S5. 0, 150, 300, 450, 600 and 750µl of the working standard were added in respective tubes and the volume adjusted to 750µl using absolute ethanol. These solutions S1-S5 were equivalent to 4, 8, 12, 14, 16 and 20 μg/ml of α-tocopherol respectively using these solutions in the routine procedure as shown in the following table. The absorbance was read by using 200 µl of solutions prepared above including blank on plain ELISA microplate (non-antibody-coated)

and read in ELISA reader at 492nm. A standard curve absorbance vs α-tocopherol (µg/ml) was plotted.

The Procedure of standardisation

| S.No | Working Standard | | Ethanol (µl) | Distilled Water | Xylene µl | | 2,2'-Bipyridyl (µl) | FeCl₃ (µl) |
	α-tocopherol µl	Conc. µg/ml						
B	0	0	750	750	750	Centrifuge for 10 min at 3000 rpm. Take 500µl of xylene layer	500	100
S1	150	4	600	750	750		500	100
S2	300	8	450	750	750		500	100
S3	450	12	300	750	750		500	100
S4	600	14	150	750	750		500	100
S5	750	16	0	750	750		500	100

After 2 minutes, OD was read at 492 nm using UV visible spectrophotometer (Shimadzu, Model: UV 1800). The curve was drawn to determine the extent of adherence to the Beer-Lambert Law with various photoelectric instruments.

- **Standard Curve**
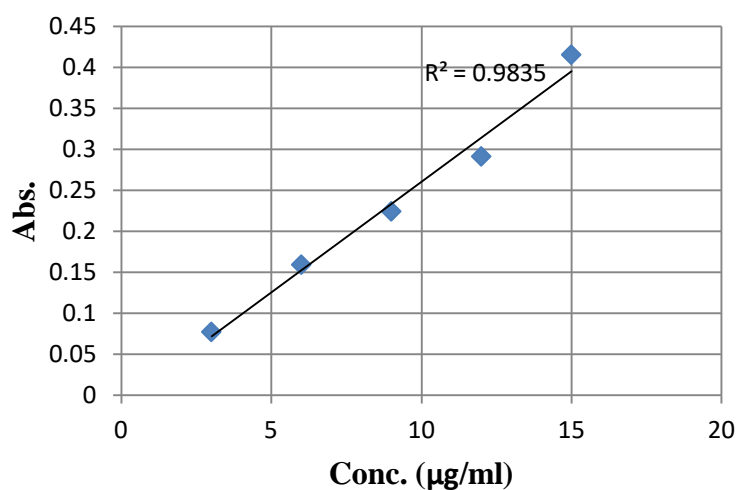
Analysis of serum α-tocopherol:

- Sample preparation: Allow 3ml of blood to clot in a centrifuge tube for 2 hours at room temperature and centrifuge at 3000rpm for 15 minutes to get the serum. Serum for α-tocopherol estimation should be protected from sunlight and undue agitation. α-tocopherol darkens on exposure to light and slowly gets oxidised by atmospheric oxygen.

α-tocopherol was found to be stable in collected serum at 25^0C for 1 day, at 4^0C for 2 weeks and at -20^0C for 2 months.

- **Procedure**

STEP 1: Two centrifuge tubes labelled as S and B (i.e sample and blank). To the sample tube, add 750µl absolute ethanol and 750 µl serum. Add the serum slowly with shaking to obtain a finely divided protein precipitate. To the blank add 750 µl of DW and 750 µl absolute ethanol. Stopper the tubes tightly by wrap paper and shake vigorously for at least 30 sec. To all the tubes add 750 µl of n-heptane. Again stopper the tubes tightly by wrap paper and shake vigorously for at least 30 sec and centrifuge all the tubes for 10 min at 3000rpm.

STEP 2: Transfer 500µl of xylene layer (supernatant) into properly labelled clean small size test tubes. To each tube add 500µl of 2, 2'-bipyridyl and 100µl of $Fecl_3$ solution and wait for 2 min.

STEP 3: Transfer 200µl solution from these tubes to plain microplate respectively. Readings are taken in ELISA reader at 492nm within 4 min.

- **Calculations**

Concentration of Vit E (µg/ml)$= \frac{OD\ of\ test - OD\ of\ Blank}{Slope} \times Dilution\ factor$

Slope$=\frac{y2-y1}{X2-X1}$, *X* and *Y* are concentration and absorbance of standard respectively

D) Hypoxia signalling molecules

1. Estimation of serum VEGF: Rat VEGF Elisa Kit (Chongqing Biospes Co., Ltd, Chongqing, China)

2. Estimation of serum NOS3: Rat NOS3 Elisa Kit (Chongqing Biospes Co., Ltd, Chongqing, China)

3. Estimation of serum Nitric Oxide (NO): By Greiss reaction

1. Estimation of serum VEGF

Serum VEGF was estimated by ELISA using Rat VEGF ELISA Kit (Catalog No.: BEK1228 Chongqing Biospes Co., Ltd, Chongqing, China) following the protocol given in the product manual.

- **Principle**

This kit is based on sandwich enzyme-linked immune-sorbent assay technique. 96 well plates pre-coated with Anti-VEGF polyclonal antibody were used. The biotin-conjugated anti-VEGF polyclonal antibody was used as detection antibodies. The standards, test samples and biotin conjugated detection antibody were added to the wells and washed with wash buffer. The avidin-biotin-peroxidase complex was added and unbound conjugates were washed away with wash buffer. TMB substrates were used to visualize Avidin-Biotin-Peroxidase complex enzymatic reaction. TMB was catalyzed by Avidin-Biotin-Peroxidase to produce a blue colour product that changed into yellow after adding acidic stop solution. The density of yellow is proportional to the VEGF amount of sample captured in plate. O.D. absorbance was read at 450nm in a microplate reader, and then the concentration of VEGF can be calculated.

- **Range:** 15.6pg/ml-1000pg/ml
- **Sensitivity**<1pg/ml

- **Kit components:**

  1. One 96-well plate precoated with an anti-RatVEGF antibody

  2. Lyophilized rat VEGF standards (10ng/tube)

  3. Sample/Standard diluents buffer

  4. Biotin conjugated anti-rat VEGF antibody (1:100)

  5. Antibody diluent buffer

  6. Avidin-Biotin-Peroxidase Complex (ABC) (1:100)

  7. ABC diluents buffer

  8. TMB substrate

  9. Stop solution

  10. Wash buffer (25X)

- **Protocol**

Preparation of sample and reagents

1. *Sample***:** The blood was collected in plain tubes and allowed to coagulate at room temperature (about 4 hours). Centrifuged at approximately 1500 x g for 15 min. The serum was aliquoted and stored at -20^{0}C.

2. *Wash buffer: T*he concentrated Wash buffer was diluted 25-fold (1:25) with distilled water.

3. *Standard:* Reconstitution of the lyophilized rat VEGF: the standard solution was prepared no more than 2 hours prior to the experiment.

a. 10,000pg/ml of a standard solution: 1ml of Sample/Standard diluents buffer was added into one Standard tube and kept at room temperature for 10 min and mixed thoroughly.

b. 1000pg/ml of standard solution: 0.1ml of the above 10ng/ml standard solution was added into 0.9ml of sample diluents buffer and mixed thoroughly.

c. 500pg/ml of standard solution to 15.6pg/ml of standard solutions: 6 Eppendorf tubes were labelled with 500pg/ml, 250pg/ml, 125pg/ml, 62.5pg/ml, 31.2 pg/ml, 15.6pg/ml, respectively. 0.3ml of Sample/Standard diluents buffer was aliquoted into each tube. To this 0.3ml of the above 1000pg/ml of standard solution was added into the 1st tube and mixed thoroughly. 0.3ml from the 1st tube was transferred into 2nd tube and mixed thoroughly. 0.3ml form the 2nd was transferred to 3rd tube and mixed thoroughly and so on.

4. **Preparation of biotin-conjugated anti-rat VEGF antibody working solution:** Prepared no more than 2 hours before the experiment.

a. Calculation of the total volume of working solution: 0.1ml/well x quantity of wells.

b. Biotin conjugated anti-rat VEGF antibody was diluted with antibody diluent buffer at 1:100 and mixed thoroughly i.e. 1µl of Biotin conjugated anti-rat VEGF antibody was added into 99µl of antibody diluent buffer.

5. **Preparation of Avidin-Biotin-Peroxidase Complex (ABC) working solution:** Prepared no more than 1 hour before the experiment.

a. Calculation of the total volume of working solution: 0.1ml/well x quantity of wells.

b. Avidin-Biotin-Peroxidase Complex (ABC) is diluted with ABC diluents buffer at 1:100 and mixed thoroughly i.e 1µl of Avidin-Biotin-Peroxidase Complex (ABC) is added into 99µl of ABC diluent buffer.

- **Assay Procedure**

Before adding to the wells the ABC working solution and TMB substrate are equilibrated at room temperature for at least 30 min.

1. Standard, test sample, and control wells are set on pre-coated plate respectively and their positions are recorded.

2. 0.1ml of 1000pg/ml, 500pg/ml, 250pg/ml, 125pg/ml, 62.5pg/ml, 31.2pg/ml, 15.6pg/ml standard solutions are aliquoted into standard wells.

3. 0.1ml of sample/standard diluents buffer was added into control (zero) well.

4. 0.1ml of properly diluted sample was added into test sample wells.

5. The plate is sealed with a cover and incubated at 37^0C for 90min.

6. The cover is removed and the plate contents are discarded and the plate is claped on the absorbent filter paper. Care should be taken not to let wells to dry at any time. The plate must not be washed.

7. 0.1ml of biotin-conjugated anti-rat VEGF antibody working solution was added into above wells (standard, test samples and zero wells). The solution was added at the bottom of each well without touching the sidewall.

8. The plate was sealed with a cover and incubated at 37^0C for 60 min.

9. The cover is removed and the plate was washed with wash buffer by manual washing. For this, the solution in the plate was discarded without touching the sidewalls. The plate was claped on absorbent filter paper. Each well was filled completely with wash buffer and vortexed mildly on ELISA shaker for 2min, the contents of the plate were aspirated. The plate was claped on absorbent filter paper. The same procedure was repeated two more times for a total of three washes.

10. 0.1ml of ABC working solution was added into each well. The plate was covered and incubated at 37^0C for 30 min.

11. The cover was removed and the plate was washed 5 times with wash buffer and each time the wash buffer was allowed to stay in wells for 1-2min.

12. 90µl of TMB substrate was added into each well. The plate was covered and incubated in dark for 25-30 min at 37^0C. The shades of blue could be seen in the first 3-4 wells (with

most concentrated rat VEGF standard solutions), the other wells showed no obvious colour.

13. 0.1ml of stop solution was added into each well and mixed thoroughly. The colour changed to yellow immediately.

14. The O.D. absorbance was read at 450nm in a microplate reader (Model: Merilyzer EIAQUAN, Meril Diagnostics Pvt. Ltd.) within 30 min after adding the stop solution.

- **Calculations**

Relative $O.D._{450}$ = (O.D. $_{450}$ of each well) – (O.D. $_{450}$ of Zero well). The standard curve was plotted as the relative O.D. $_{450}$ of each standard solution (Y) *vs.* the respective concentration of the standard solutions (X). The Rat VEGF concentration of the samples was interpolated from the standard curve.

Standard Curve:

X	pg/ml	0	15.6	31.2	62.5	125	250	500	1000
Y	OD_{450}	0	0.0415	0.1	0.1769	0.358	0.7458	1.456	2.5123
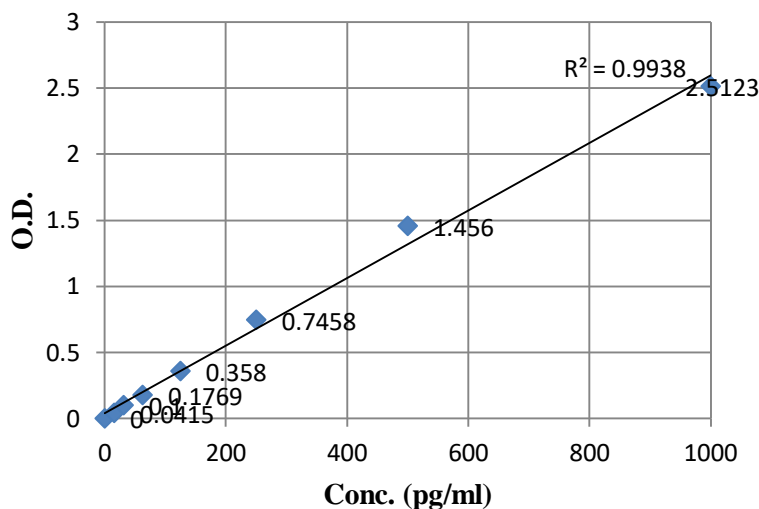
2. Estimation of serum NOS3

Serum NOS3 was estimated by ELISA using Rat NOS3 ELISA Kit (Catalog No.: BYEK2703 Chongqing Biospes Co., Ltd, Chongqing, China) following the protocol given in the product manual.

- **Principle of the Assay**

This kit works on technique of sandwich enzyme-linked immune-sorbent assay. 96 well plates precoated with the purified anti-NOS3 antibody are used. The anti-NOS3 antibody conjugated with HRP was used as detection antibodies. The standards, test samples and HRP conjugated detection antibody were added to the wells, mixed and incubated, and then unbound conjugates are washed away with wash buffer. TMB substrates (A&B) are used to visualize HRP enzymatic reaction. HRP catalyzes TMB to produce a blue colour product that changes into yellow after adding acidic stop solution. The density of yellow is proportional to the amount of NOS3 in the sample captured in plate. O.D. absorbance was read at 450nm in a microplate reader, and the concentration of NOS3 is calculated.

- **Range**: 3pg/ml-120pg/ml
- **Kit components:**

c. One 96-well plate pre-coated with anti-rat NOS3 antibody

d. Standard (180pg/ml)

e. Standard diluent buffer

f. Wash buffer (30X): Dilution (1:30)

g. Sample diluent buffer

h. HRP conjugated anti-rat NOS3 antibody

i. Stop solution

j. TMB substrate A

k. TMB substrate B

l. Plate sealer

m. Hermetic bag

- **Protocol**

  Preparation of sample and reagents

1. **Sample:** The collected blood is allowed to coagulate at room temperature for 10-20 min, and then centrifuged at the speed of 2000-3000rpm for 20 min to collect the supernatant. The supernatant is aliquoted and stored at -20^0C. Multiple freeze-thaw cycles were avoided.

2. **Wash buffer:** Concentrated wash buffer was diluted 30 fold (1:30) with distilled water.

3. **Standard:** Dilution of the standard: 10 standard wells were set on the pre-coated plates and 100µl of the standard was added to the 1st and 2nd well. 50µl of the standard diluent buffer was then added to the above two wells and thoroughly mixed. 100µl from the 1st and 2nd were transferred to the 3rd and 4th well respectively. 50µl of the standard diluent buffer was added to the 3rd and 4th well and mixed thoroughly. 50µl was taken from the 3rd and 4th well and discarded and 50µl was transferred to 5th and 6th well. 50µl of the standard diluent buffer was added to 5th and 6th well and mixed thoroughly. 50µl was transferred from 5th and 6th well to 7th and the 8th well. 50µl of standard diluents buffer was added to 7th and 8th well and mixed thoroughly. 50µl from 7th and 8th well was transferred to 9th and 10th well. 50µl of standard diluents buffer was added to 9th and 10th well and mixed thoroughly. 50µl was taken out from 9th and 10th well and discarded. After diluting, the loading volume for each well was 50µl and the concentrations were 120pg/ml, 80pg/ml, 40pg/ml, 20pg/ml, 10pg/ml.

- **Assay Procedure**

1. Equilibrate kit components for 15-30 min at room temperature

2. Standard, test sample and control (zero) were set in the wells on pre-coated plate respectively. Their positions were recorded. 50µl of diluted standards (120pg/ml,

80pg/ml, 40pg/ml, 20pg/ml, 10pg/ml) were added into standard wells. 50μl of the standard diluent buffer was added into control (zero) well.

3. For test sample wells, 40μl of sample diluents buffer was added and then 10μl of the sample was added. The solution was added at the bottom of each well without touching the side well. The plate was mildly shaken to mix thoroughly.

4. The plate was covered with a plate sealer and incubated at 37^0C for 30 min.

5. The sealer was removed and the plate was washed manually. For this, the solution in the plate was discarded without touching the sidewalls. The plate was claped on absorbent filter paper. Each well was filled completely with wash buffer (1x) and vortexed mildly on ELISA shaker for 2 min, the contents of the plate were then aspirated. The plate was claped on absorbent filter paper. The same procedure was repeated four more times for a total of five washes.

6. 50μl of HRP conjugated anti-NOS3 antibody was added into each well (except control well).

7. The plate was covered with a plate sealer and incubated at 37^0C for 30min.

8. The sealer was removed and the plate was washed.

9. 50μl of TMB substrate A was added into each well, followed by 50μl of TMB substrate B. The plate was gently shaken by hand for 30 sec and incubated in dark at 37^0C for 15 min. The shades of blue were seen in the wells.

10. 50μl of Stop solution was added into each well and mixed thoroughly. The colour changed into yellow immediately.

11. The O.D. absorbance was read at 450nm in a microplate reader (Model: Merilyzer EIAQUAN, Meril Diagnostics Pvt. Ltd.) within 15 min after adding the stop solution.

- **Calculations**

Relative O.D.$_{450}$= (O.D. $_{450}$ of each well) – (O.D. $_{450}$ of Zero well). The standard curve was plotted as the relative O.D. $_{450}$ of each standard solution (Y) vs. the respective concentration of the standard solutions (X). The NOS3 concentration of the samples was interpolated from the standard curve.

Standard Curve

X	pg/ml	0	10	20	40	80	120
Y	OD$_{450}$	0	0.0567	0.0935	0.1568	0.2737	0.3812
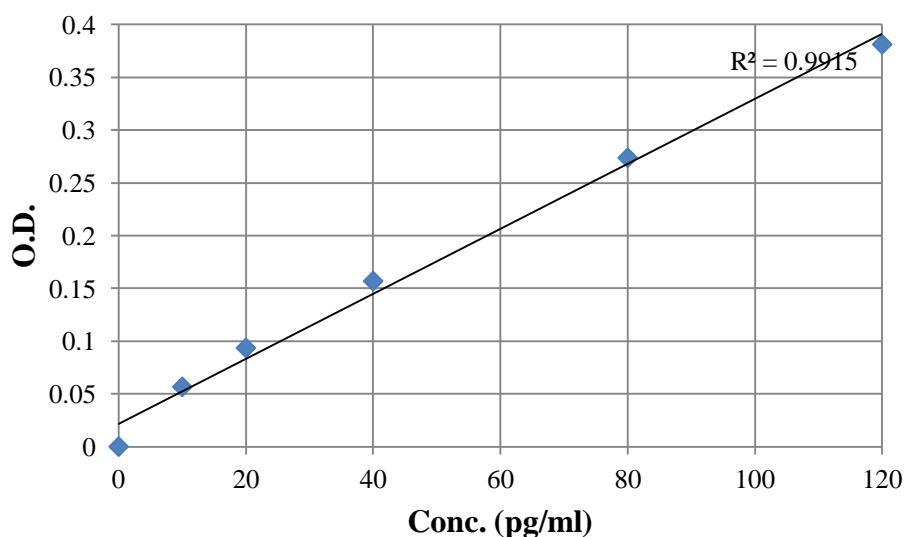
3. **Estimation of serum Nitric Oxide concentration:**

By Greiss Reaction (Moshage Han et al., 1995; Cortas and Wakid, 1990; Green et al., 1982)

- **Principle**

Nitrate, the stable product of nitric oxide was reduced to nitrite by cadmium reduction method after deproteination and coupling to N-naphthylethylene diamine. The coloured complex produced was measured at 540nm in a spectrophotometer.

- **Reagents**

1. Cadmium granules: 2.5-3gm granules stored in 0.1M/L H_2SO_4

2. Glycine-NaOH buffer (pH-9.7): 7.5gm of glycine was dissolved in 200ml distilled water. The pH was then adjusted to 9.7 by 2M NaOH and was diluted to 500ml by distilled water.

3. Sulfanilamide: 2.5gm of sulfanilamide was dissolved in 250ml of warm 3M/L HCl and allowed to cool.

4. N-Naphthylethylene diamine: 50mg N-Naphthylethylene diamine was dissolved in distilled water and the volume was adjusted to 250ml.

5. Standard sodium nitrite solution:

   a. *Stock standard (0.1mol/L)*

   690 mg of sodium nitrite was dissolved in 100ml of 10mmol/L sodium borate solution.

   b. *Working standard (10μmol/L)*

   10μl of stock sodium nitrite ($NaNO_2$) was diluted up to 100ml with 10mmol/L sodium borate solution.

6. ZnSO4 solution (75mmol/L)

7. NaOH solution (55mmol/L)

8. H_2SO_4 solution (0.1mol/L)

9. $CuSO_4$ solution (5mmol/L)

   125mg of $CuSO_4$ was dissolved in 100ml of glycine-NaOH buffer.

- **Procedure**

a. *Deproteinization:*

 In clean, dry centrifuge tube 0.5ml of serum was taken. To this 2.0 ml of 75mmol/L ZnSO4 solution was added and mixed. To this 2.5 ml of 55mmol/L of NaOH reagent was

added and mixed well and centrifuged for 10 minutes. The supernatant was treated as a protein-free filtrate.

b. *Activation of cadmium granules:*

Cadmium granules that were previously stored in 0.1mol/L H_2SO_4 solution, were rinsed three times with distilled water at the time of assay. The granules were then swirled in 5mmol/L $CuSO_4$ solution for 1-2 minutes. The copper-coated granules were drained and washed by the glycine-NaOH buffer. These activated granules were used within 10min after activation. The granules after use were washed by distilled water and stored in 0.1mmol/L H_2SO_4 solution. The same procedure of activation of granules was followed each time.

c. *Nitrite Assay:*

1. Three Erlenmeyer flasks were taken and labelled as Blank (B), Test (T) and Standard (S).

2. 1ml of glycine-NaOH buffer was added to each Erlenmeyer flask. To the flasks labelled B (Blank), T (Test), S (Standard) 1ml of deionised water, 1ml of deproteinized sample and 1ml of the working standard were added respectively.

3. With a spatula, 2.5-3gm of freshly activated cadmium granules was added to each flask.

4. The contents of all the flasks were stirred to swirl the granules.

5. After 90min the mixture in all three flasks was diluted to 4ml with distilled water.

6. 2ml of this solution from respective flasks were pipette in 3 clean dry test tubes labelled B, S, T respectively.

7. 1ml of sulfanilamide followed by 1ml of N-napthylethylene diamine solution were added to each tube.

8. All the three tubes were shaken well and after 20 min OD of S, T was read against blank at 540nm on a spectrophotometer.

- **Calculations**

$$\text{Serum Nitric Oxide (μmol/L)} = \frac{OD\ of\ Sample}{OD\ of\ Standard} \times conc.\ of\ standard \times DF$$

4.7.7 The sacrifice of animals and collection of tissues:

The animals were sacrificed after completion of 21 days of intervention i.e. on day 22 by an overdose of ketamine (150 mg/kg, i.p.) after the collection of blood. Rats were carefully dissected. Liver, heart and lungs were separated. The individual organs were immediately weighed. The organosomatic index was calculated for each organ.

$$\text{Organosomatic index} = \frac{Organ\ weight}{Body\ weight} \times 100$$

Part of the tissues was fixed in 10% neutral buffered formalin for subsequent histopathological examination (HPE) and the remaining was stored at -20^0 C for tissue homogenate preparation. To study the vascular system, thoracic aorta (elastic artery) and femoral artery (muscular artery) were also carefully dissected and fixed in 10% neutral buffered formalin for further histopathological study.

4.7.8 Histopathological examination:

The liver, heart, lungs, thoracic aorta and femoral artery that were fixed in 10% neutral buffered formalin were embedded in paraffin blocks, sectioned with a microtome (3-5µm thickness) and finally stained by Haematoxylin & Eosin (H&E) and were subjected to histopathological examination.

4.7.9 Study of cardiovascular remodelling:

The heart particularly the ventricles and the vasculature (coronary artery, elastic artery, muscular artery) were evaluated for changes in the architecture to assess chronic hypoxia-induced cardiovascular remodelling and the effect of treatment with cilnidipine.

The histological images of the coronary artery were processed with Image J software (https://imagej.nih.gov/ij/). Lumen area (LA) and total vessel area (TVA) of the coronary artery was manually traced and values were obtained using the software. Wall area was calculated using the formula given below (Harteveld *et al*., 2018).

Wall area (WA) =Total vessel area (TVA)-Lumen Area (LA)
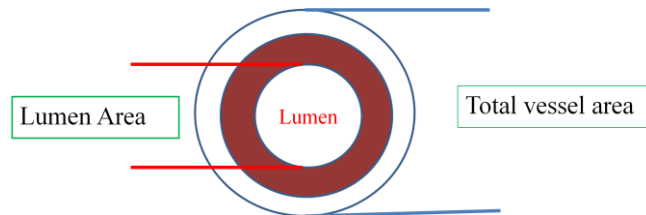
Figure 4.2 Schematic diagram depicting lumen area and total vessel area

- **Normalized wall index (NWI):**

Normalized wall index indicates the percentage of the wall area of the total vessel area (Harteveld *et al*., 2018). NWI is considered a measure of arterial remodelling (Zhu *et al*., 2010). Normalized wall index (NWI) for coronary artery was calculated as follows (Patil *et al*., 2019; Harteveld *et al*., 2018)

NWI=Wall area/Total vessel area

4.7.10 Cerebrovascular Physiology: Hypoxia and Cerebral Ischemia

To study the effect of unilateral common carotid artery occlusion on brain histopathology in chronic hypoxia preconditioned rats

- **Experimental Protocol** (Das *et al*., 2018)

Table 4.3 depicts the random allocation of experimental rats into groups

Table 4.3: Random assignment of experimental animals into 3 groups

Sl. No	Groups	Experimental protocols
1.	Group 1	Sham-operated (surgical incision at the carotid triangle, no occlusion and immediate allow or instant reperfusion
2.	Group 2	Normoxia, 21% oxygen (75 minutes left CCA occlusion and subsequent reperfusion for 12 hours)
3.	Group 3	Hypoxia (10% oxygen) preconditioned for 21 days prior to 75 minutes left CCA occlusion and reperfusion for 12 hours

CCA-common carotid artery occlusion

- **Left Common Carotid Artery Occlusion**

Figure 4.3 depicts the site of unilateral left common carotid artery occlusion (LCCAO). Left common carotid artery (LCCA) was occluded at the level of the carotid triangle in anaesthetized rats (ketamine-60mg/kg b.wt. i.p. and xylazine – 6mg/kg b.wt. i.p.). After the carotid artery was traced it was occluded for 75 minutes in group 2 (Normoxia) and group 3 (hypoxia preconditioned). After 75 minutes the occlusion was slowly released, a surgical incision was closed and allowed for reperfusion for 12 hours till sacrifice. In group 1 (sham) all surgical steps were followed except for occlusion of LCCA and allowing for instant reperfusion. The utmost post-operative care was taken for each rat.
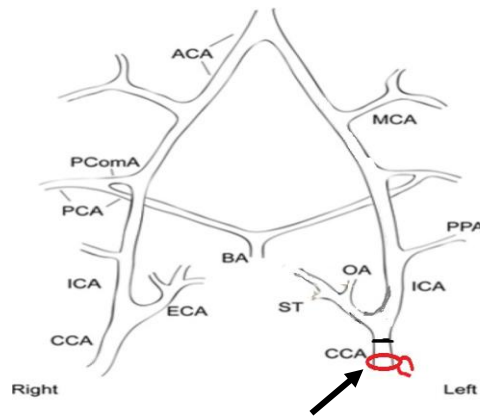
Figure 4.3 The site of unilateral left common carotid artery occlusion

CCA, common carotid artery; ECA, external carotid artery; ICA, internal carotid artery; MCA, middle cerebral artery; OA, occipital artery; PCA, posterior cerebral artery; P ComA, posterior communicating artery; PPA, pterygopalatine artery; ST, superior thyroid artery

Source: Das KK, Yendigeri SM, Patil BS, Bagoji IB, Reddy RC, Bagali S et al. Subchronic hypoxia pretreatment on brain pathophysiology in unilateral common carotid artery occluded albino rats. Indian J Pharmacol 2018; 50(4): 185-191. DOI:10.4103/ijp.IJP_312_17.

- **Examination of rats for neurologic deficits**

Following unilateral left common carotid artery occlusion, the experimental rats of all groups were assessed for neurological deficits as depicted in table 4.4. The neurologic findings were scored on a five-point scale: score 0-indicated no neurologic deficit; score 1- failure to extend affected forepaw fully (mild focal neurologic deficit); score 2- circling (moderate focal neurologic deficit); score 3- falling (severe focal neurologic deficit); score 4- inability to walk spontaneously and a depressed level of consciousness (Longa *et al*., 1989; Das et al., 2018).

Table 4.4: Neurological deficit score

Neurological Signs	Score (0-5 scale) for each rat
Failure to extend affected forepaw fully	1
Circling	2
Falling	3
Inability to walk spontaneously	4
Grand Total Score	10x6 =60 (for n=6)

- **Sacrifice followed by collection of the brain**

After 12 hours reperfusion, the experimental animals were euthanized with an overdose of ketamine (150 mg/kg, i.p.). The brain was carefully dissected out and fixed in 10% neutral buffered formalin and later was subjected to histopathological examination (Das *et al*., 2018).

4.8 STATISTICAL ANALYSIS

- SPSS 16.0 (SPSS Inc., Chicago, USA) was used for statistical analysis.

- All the parameters are presented as Mean $\pm$ SD. One-way analysis of variance (ANOVA) was used for statistical significance of data across multiple groups followed by post hoc test to determine the significant difference between groups.

- Paired t-test was performed for within-group analysis.

- Pearson's correlation was done to establish a relationship between a pair of variables.

- p-value $\leq$ 0.05 was considered as statistically significant.

4.9 ETHICAL STATEMENT

The experimental protocol was approved by the Institutional Animal Ethics Committee (IAEC) (vide letter: BLDE/BPC/641/2016-2017 dated 21.10.2016). All the experimental procedures were performed according to the guidelines laid by the Committee for the Purpose of Control and Supervision of Experiments on Animals (CPCSEA), Government of India.

CHAPTER V
RESULTS AND DISCUSSION

5.1 GRAVIMETRY

5.1.1 RESULTS

Table 5.1.1: Comparison of gravimetry among groups of experimental animals (n=6 in each group)

Parameter	Group 1 (Control)	Group 2 (CH)	Group 3 (Cil)	Group 4 (CH+Cil)	ANOVA	
					F value	P-value
Initial body wt (gm, Day 1)	194.833 ± 3.43	197.50 ± 4.63	203.00 ± 9.59	196.00 ± 6.35	1.89	0.164
Final body wt (gm, Day 22)	246.80 ± 6.23	219.74 ± 6.97^a	257.57 ± 11.71^b	223.57 ± 6.79^{ac}	29.45	0.000*
% body wt gain	26.66 ± 1.11	11.25 ± 1.83^a	26.89 ± 1.46^b	14.08 ± 1.63^{abc}	172.26	0.000*

Values are presented as mean$\pm$SD. One way ANOVA followed by Post Hoc Tukey's multiple comparison tests. Superscript a, b, c indicates a significant difference between groups. 'a' depicts comparison with Group 1, 'b' depicts comparison with group 2, 'c' depicts comparison with group 3. *p$\leq$0.05. Wt: weight
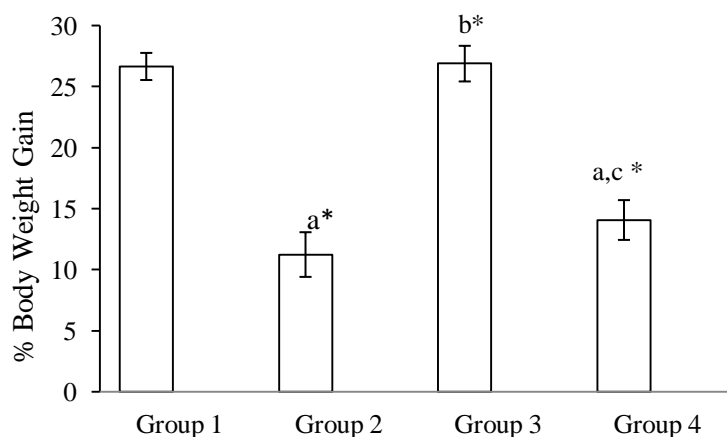
Figure 5.1.1: Comparison of % body weight gain among groups (n=6 in each group)

Superscript a, b, c indicates a significant difference between groups. 'a' depicts a comparison with Group 1, 'b' depicts a comparison with group 2, 'c' depicts a comparison with group 3. *p<0.05

Table 5.1.1 depicts within groups and between groups comparison of initial body weight (Day 1), final body weight (Day 22) and % body weight gain. The rats of all groups were matched for body weight at the onset of the experimental protocol. Accordingly, initial body weight was not significantly different between groups. After 21 days, there was a significant increase in mean body weight in rats of all groups as demonstrated by paired t-test. One way ANOVA revealed significant differences in the final body weight between groups indicating

a non-uniform increase in body weight. On further statistical analysis, % body weight gain was significantly different between groups. Although all groups of rats demonstrated an increase in body weight, % body weight gain was smaller in group 2 (CH) and group 4 (CH+Cil) compared to age-matched group 1(control). When group 2 (CH) and group 4 (CH+Cil) were compared, a lower % body weight gain was observed in group 2.

5.1.2 DISCUSSION

Energy expenditure is one of the key factors influencing body weight. Autonomic nervous system by influencing energy expenditure controls body weight. Particularly sympathetic activation increases energy expenditure that in turn reduces body weight (Messina *et al*., 2013). In our study magnitude of weight gain was lower in chronic hypoxia exposed rats (group 2 (CH), group 4 (CH+Cil) indicates alteration of autonomic nervous balance in favour of increased sympathetic activity following chronic hypoxia exposure. Interestingly cilnidipine treated chronic hypoxia exposed group (group 4) demonstrated a better % body weight gain when compared to only chronic exposed group 2 (CH). This could be due to the action of drug cilnidipine. Cilnidipine blocks N-type calcium channels present on the sympathetic nerve terminals thereby reducing sympathetic neurotransmission and consequently sympathetic drive (Takahara, 2009). By virtue of this action, cilnidipine might probably influence sympathetic activity and consequently body weight.

Barton *et al*. also recorded a similar lower magnitude of weight gain in experimental animals subjected to chronic hypoxia (Barton *et al.,* 2003).

In contrast to our findings, Corno *et al.,* Luneburg *et al*., and Siques *et al*. observed gradual weight loss in chronic hypoxia exposed rats at the end of intervention period of 15 days, 30 days, 46 days respectively (Luneburg *et al*., 2016; Siques *et al.,* 2014; Corno *et al.,* 2002).

5.2 HEMOGRAM

5.2.1 RESULTS

Table 5.2.1: Comparison of haematological parameters among groups of experimental animals

Parameter	Group 1 (control)	Group 2 (CH)	Group 3 (Cil)	Group 4 (CH+Cil)	ANOVA F-value	P-value
RBC count (million/cumm)	7.69 ± 0.177	9.10 ± 0.22^a	7.75 ± 0.10^b	8.91 ± 0.44^{ac}	18.83	0.000*
Hb (g/dl)	13.57 ± 0.88	16.25 ± 0.42^a	13.60 ± 0.5^b	15.47 ± 0.68^{ac}	15.55	0.000*
Hematocrit (%)	43.30 ± 0.50	50.12 ± 1.53^a	42.63 ± 3.29^b	48.90 ± 1.78^{ac}	13.59	0.001*

Values are presented as mean$\pm$SD. One way ANOVA followed by Post Hoc Tukey's multiple comparison tests. Superscript a, b, c indicates a significant difference between groups. 'a' depicts comparison with Group 1, 'b' depicts comparison with group 2, 'c' depicts comparison with group 3. *$p\leq0.05$

Table 5.2.1 shows the comparison of haematological parameters among groups. RBC count, haemoglobin and hematocrit were significantly higher in group 2 (CH) and group 4 (CH+Cil) compared to group 1 (control).

5.2.2 DISCUSSION

Since oxygen is indispensable for life, the lack of O_2 poses a significant threat to cell survival. Accordingly, the cells mount a significant defence in face of O_2 lack. Increased red blood cells (RBCs), haemoglobin and hematocrit are among the several physiological responses to hypoxia attempting to maintain adequate O_2 supply to the tissues.

The results of the present study show the expected increase in RBC count, Hb, and Hct after chronic hypoxia exposure.

Walsh and Marshall studied the early effects of chronic hypoxia on the cardiovascular system in experimental rats exposed to chronic hypoxia (12% O_2) of varying duration - 1 day (1CH), 3 days (3CH) or 7 days (7CH). There were no changes in Hct in 1CH rats. Hct increased in 3CH and 7CH exposed rats with a similar increase in Hct in the two groups. The increase in

Hct in rats exposed to chronic hypoxia for 1-5 days was attributed to a reduction in plasma volume and release of RBCs and reticulocytes from the spleen, while in 7CH rats erythropoiesis contributes to increased Hct (Walsh and Marshall, 2006).

In a study by Corno *et al.* demonstrated increased RBCs, haemoglobin and hematocrit in experimental animals exposed to chronic hypoxia for 2 weeks (Corno *et al*., 2004). Siques *et al.* also reported increased Hct in rats exposed to chronic sustained hypoxia for 46 days (Siques *et al.,* 2014).

Similar results were also observed by Kang *et al.,* Fan *et al.* in experimental animals exposed to chronic hypoxia (Kang *et al.,* 2016; Fan *et al*., 2005).

Increased RBC formation and consequently Hct are among the several vital physiologic responses to hypoxia. The increase in hematocrit begins by day 3 and reaches 80% of the maximum in a week (Xu and Lamanna, 2006). Hypoxia-inducible factor (HIF) concerts this response with the resultant enhanced production of erythropoietin (Epo) by the liver and kidney, increased iron uptake and consumption, changes in the microenvironment of the bone marrow that promote erythroid progenitor maturation and proliferation. Studies have now clarified the predominant role of HIF-2 in regulating Epo production in vivo. Levels of Epo correlate with the severity of hypoxia increasing to several hundred folds. The prime role of Epo is to promote the survival of Epo-dependent colony-forming unit-erythroid (CFU-cells) and erythroblasts that are yet to start haemoglobin synthesis (Haase, 2013).

5.3   RESPIRATORY RATE

5.3.1   RESULTS
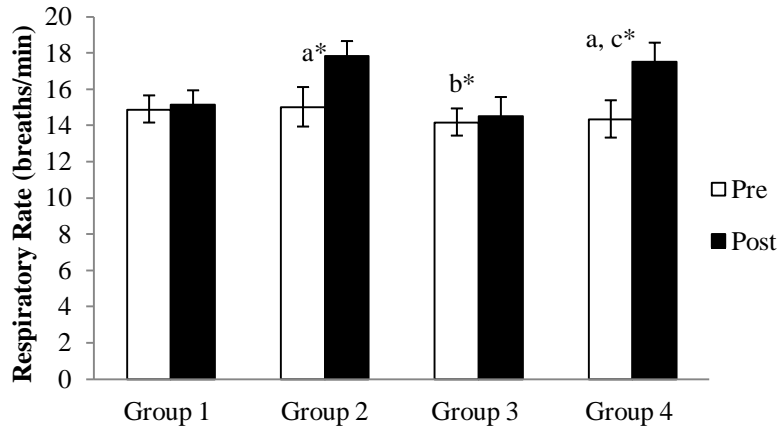
Figure 5.3.1: Comparison of respiratory rate among groups of experimental animals

Superscript a, b, c indicates a significant difference between groups. 'a' depicts a comparison with Group 1, 'b' depicts a comparison with group 2, 'c' depicts a comparison with group 3.* Statistically significant paired t-test. *$p \leq 0.05$

Fig. 5.3.1 depicts within and between-group comparisons of respiratory rate (RR). The initial respiratory rate (day 1) is comparable between groups. The final respiratory rate (day 22) is significantly different between groups. It is raised in group 2 (CH) and group 4 (CH+Cil) compared to group 1 (control). In addition, paired t-test revealed significantly increased final RR compared to initial RR in group 2 (CH) and group 4 (CH+Cil). However, the two were comparable in group 1 (control) and group 3 (Cil).

5.3.2   DISCUSSION

Exposure to low oxygen microenvironment induces respiratory adaptations within seconds attempting to make for the discrepancy between supply and demand of O_2 of the tissues. Hypoxia reduces the arterial partial pressure of oxygen (PO_2) stimulating the peripheral chemoreceptors particularly the 'carotid body' triggering the chemoreceptor reflex and

increasing the respiratory frequency and tidal volume (Lahiri *et al.,* 2006). Interestingly the ventilatory response to acute hypoxia and chronic hypoxia differ. In acute hypoxia, a biphasic response is observed with an initial increase in the pulmonary ventilation followed by a gradual decline in the ventilatory response termed 'hypoxic ventilatory decline' (HVD) (Powell *et al.,* 1998). Upon exposure to chronic hypoxia resting ventilation progressively increases. This phenomenon is termed ventilatory acclimatization to hypoxia (VAH), commonly observed in high altitude sojourner (Powell *et al.,* 2000). Sensitization of the peripheral chemoreceptor reflex pathway and adjustments in the neuronal network in the brainstem involved in related to respiratory response to peripheral chemoreceptor reflex activation has been proposed as a mechanism of VAH (Bisgard, 2000; Kaab *et al.,* 2005; Zhang *et al.,* 2009).

In our study, experimental animals exposed to chronic sustained hypoxia revealed increased respiratory frequency. Similar findings in cilnidipine treated chronic hypoxia exposed experimental animals suggest no possible role of drug cilnidipine in chronic hypoxia-induced respiratory changes.

Walsh and Marshall reported the effects of sustained hypoxia on ventilation in rats exposed to hypoxia for 1day, 3 days and 7 days. Regardless of the duration of exposure, a similar increase in ventilation in all the groups resulting from a higher respiratory frequency (R_f) and tidal volume (V_T) was documented (Walsh and Martin, 2006). On the contrary, Olson and Dempsey demonstrated a differing V_T-R_f relationship driving the ventilatory responses depending on the duration of exposure. Beyond 7 days of hypoxic exposure, the R_f and V_T progressively increased contributing to higher ventilation and below 7 days of hypoxia exposure, R_f made a major contribution to the higher ventilation (Olson and Dempsey, 1978). Reeves *et al*. also demonstrated a higher R_f and V_T after 30 days of chronic sustained hypoxia exposure.

5.4 Heart rate variability analysis: frequency-domain analysis

The impact of chronic hypoxia and the effect of treatment with drug cilnidipine on chronic hypoxia-induced changes on cardiovascular autonomic control were done by HRV analysis.

5.4.1 RESULTS

a. LF (nu) component

Table 5.4.1 depicts within the group (paired t-test) and between-group (ANOVA) comparisons of LF (nu) among groups.

Table 5.4.1: Comparison of LF (nu) among groups of experimental animals
(n=6 in each group)

Parameter		Group 1 (Control)	Group 2 (CH)	Group 3 (Cil)	Group 4 (CH+Cil)	ANOVA F value	P-value
Pre intervention	LF (nu)	47.26 ± 1.73	49.14 ± 2.16	47.12 ± 2.08	48.26 ± 2.08	0.87	0.483
Post intervention	LF (nu)	45.59 ± 1.87	61.39 ± 2.52^a	33.17 ± 2.09^{ab}	53.24 ± 2.99^{abc}	99.02	0.000*
Paired t - test		0.088	0.0008*	0.0002*	0.0055*		

Values are expressed as mean$\pm$SD. One way ANOVA followed by Post Hoc Tukey's multiple comparison tests. Superscript a, b, c indicates a significant difference between groups. 'a' depicts comparison with Group 1, 'b' depicts comparison with group 2, 'c' depicts comparison with group 3. *p$\leq$0.05

Within each group, a comparison was made between pre-intervention and post-intervention LF component of HRV analysis. In group 1 (control) the pre-intervention (day 0) and post-intervention (day 22) values were similar indicating no alterations in the sympathetic activity over time. In group 3 (Cil) post-intervention (day 22) LF was significantly reduced compared to pre-intervention (day 0) values. In group 2 (CH) and group 4 (CH+Cil) post-intervention LF is significantly increased compared to pre-intervention LF.

One way ANOVA was performed to compare LF between groups. Pre-intervention (day 0) LF was comparable between groups. Post-intervention (day 22) LF was increased in group 2 (CH) and group 4 (CH+Cil) and decreased in group 3 (Cil). Also, post-intervention LF was significantly higher in group 2 (CH) compared to group 4 (CH+Cil).

Group 2 (CH) demonstrated increased sympathetic activity, decreased parasympathetic activity and shift in the sympathovagal balance towards the sympathetic activity. Group 4 (CH+Cil) demonstrated a smaller increase in sympathetic activity and no differences in the parasympathetic activity and sympathovagal balance when compared to group 1 (control).

b. HF (nu) component

Table 5.4.2 represents within the group and between-group comparisons of the HF component of HRV analysis.

Table 5.4.2: Comparison of HF (nu) among groups of experimental animals (n=6 in each group)

Parameter		Group 1 (Control)	Group 2 (CH)	Group 3 (Cil)	Group 4 (CH+Cil)	ANOVA F value	P-value
Pre intervention	HF (nu)	53.53 ± 2.63	51.15 ± 2.70	$52.69 + 2.89$	51.72 ± 3.35	0.522	0.675
Post intervention	HF (nu)	55.18 ± 2.41	37.79 ± 2.04^a	$58.03 + 3.58^b$	49.85 ± 2.53^{bc}	43.73	0.000*
Paired t – test		0.08	0.004*	0.001*	0.38		

Values are expressed as mean$\pm$SD. One way ANOVA followed by Post Hoc Tukey's multiple comparison tests. Superscript a, b, c indicates a significant difference between groups. 'a' depicts comparison with Group 1, 'b' depicts comparison with group 2, 'c' depicts comparison with group 3 *p$\leq$0.05.

Within each group, post-intervention (day 22) HF was compared with pre-intervention (day 0) values. Both the values were comparable in group 1 (control) and group 4 (CH+Cil). In group 2 (CH) post-intervention HF was significantly decreased and in group 3 (Cil) it was significantly increased.

Between groups, comparisons were made by one way ANOVA. Pre-intervention (day 0) HF was comparable between groups. Post-intervention HF was significantly different between groups. It was significantly reduced in group 2 (CH) compared to group 1 (control). In group 4 (CH+Cil) the values were comparable with group 1 (control).

c. LF/HF Ratio

Table 5.4.3 presents within the group and between-group comparisons of the LF/HF ratio.

Table 5.4.3: Comparison of LF/HF ratio among groups of experimental animals
(n=6 in each group)

Parameter		Group 1 (Control)	Group 2 (CH)	Group 3 (Cil)	Group 4 (CH+Cil)	ANOVA F value	P-value
Pre intervention	LF/HF	0.88 ± 0.05	0.95 ± 0.05	0.88 ± 0.042	0.93 ± 0.07	1.65	0.228
Post intervention	LF/HF	0.84 ± 0.02	1.62 ± 0.13^a	0.55 ± 0.05^{ab}	0.96 ± 0.15^{bc}	73.89	0.000*
Paired t - test		0.06	0.002*	0.000*	0.59		

Values are presented as mean$\pm$SD. One way ANOVA followed by Post Hoc Tukey's multiple comparison tests. Superscript a, b, c indicates a significant difference between groups. 'a' denotes comparison with Group 1, 'b' denotes comparison with group 2, 'c' denotes comparison with group 3. *p$\leq$0.05

Within-group comparison between pre-intervention (day 0) and post-intervention (day 22), LF/HF revealed no significant differences in group 1 (control) and group 4 (CH+Cil). In group 2 (CH) post-intervention, LF/HF was significantly increased and group 3 (Cil) was significantly reduced when compared to pre-intervention values.

Between groups, the comparison revealed similar pre-intervention LF/HF among groups. Post-intervention LF/HF was significantly different between groups. It was increased in group 2 (CH) and decreased in group 3 (Cil) when compared to group 1 (control). Group 4 (CH+Cil) was comparable with group 1 (Control).

- **Correlation between frequency domain indices of HRV analysis and serum MDA**

Pearson's correlation was done to know the correlation between LF, HF and LF/HF ratio with systemic oxidative stress as assessed by estimating serum MDA. We observed a statistically significant positive correlation between LF (nu) and LF/HF ratio with serum MDA (Figure 5.4.1 and 5.4.3) and statistically significant negative correlation between HF and serum MDA (Figure 5.4.3).
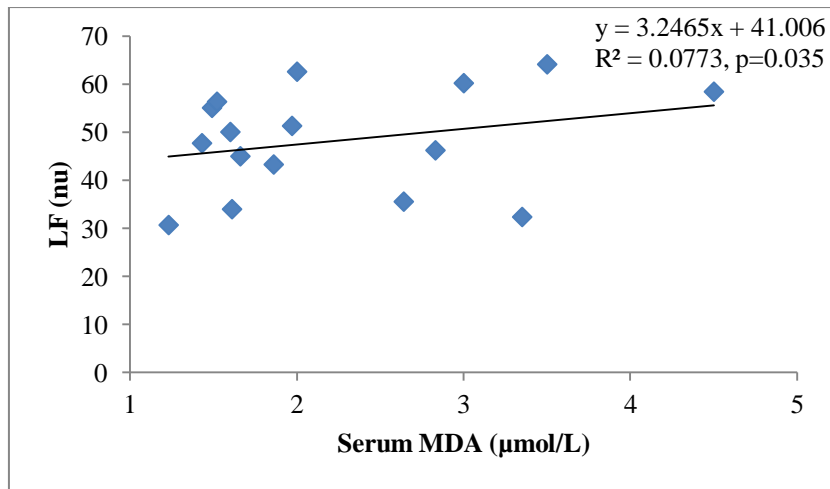
Figure 5.4.1: Correlation between LF (nu) and serum MDA (µmol/L)
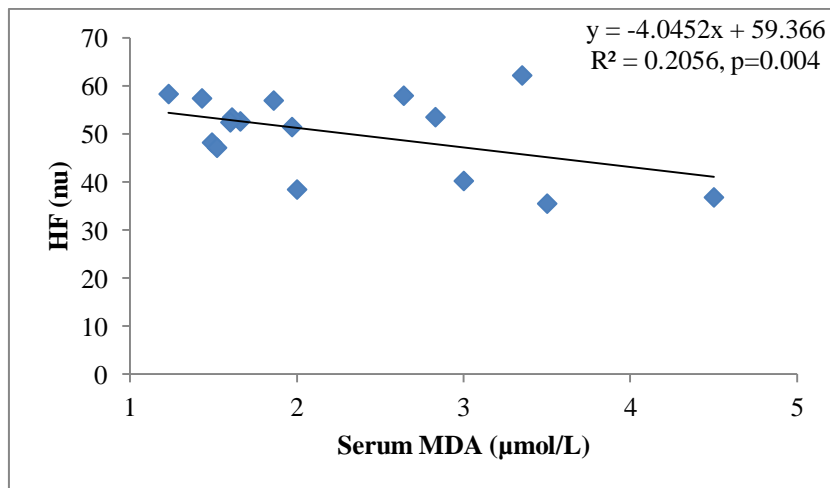
Figure 5.4.2: Correlation between HF (nu) and serum MDA (µmol/L)
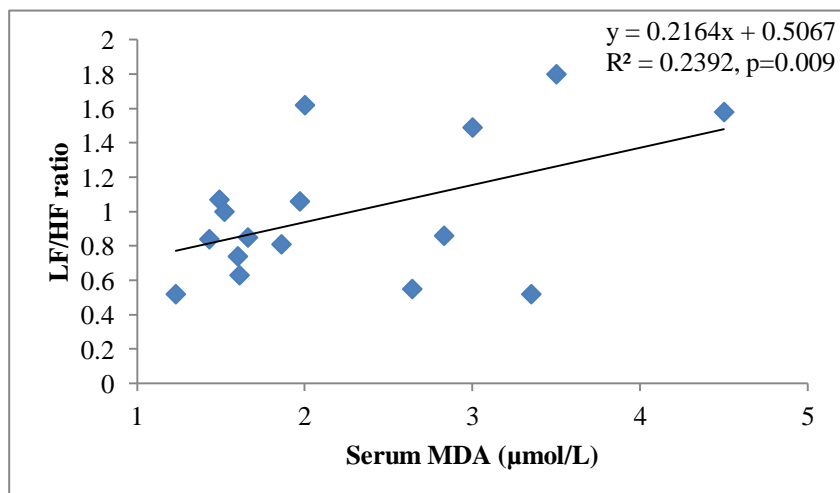
Figure 5.4.3: Correlation between LF/HF and serum MDA (µmol/L)

5.4.2 DISCUSSION

Heart functions as an effective pump. However, a healthy heart is not a metronome. There are oscillations in the time intervals between successive heartbeats. The analysis of such fluctuations in the interbeat intervals is termed heart rate variability analysis. HRV analysis is widely used as a non-invasive technique to assess cardiovascular autonomic functions. HRV analysis involves time and frequency domain indices. Frequency domain analysis of RR interval oscillations uses two major frequency bands a) low frequency (LF) band (0.04-0.15Hz) predominantly reflects sympathetic activity b) High frequency (HF) (0.15-0.4 Hz) band reflects the parasympathetic activity. LF/HF ratio is as an indicator of cardiac sympathovagal balance (Shaffer *et al.*, 2017).

In our study chronic hypoxia exposed rats (group 2) exhibited an increased sympathetic activity (increased LF), decreased parasympathetic activity (decreased HF) and shift in the sympathovagal balance (increased LF/HF). Exposure to chronic sustained hypoxia activates the carotid body eliciting the chemoreceptor reflex. The peripheral chemoreceptor reflex in addition to inducing respiratory changes to ensure adequate tissue oxygenation also mediates the modulation of the autonomic nervous functions to optimize tissue perfusion (Moraes, 2014) by adjusting cardiac output and vascular conductances (Pulgar-Sepulveda *et al.*, 2018). Further, there appears to be a need for the sympathetic tone to be increased since hypoxia may directly or indirectly through its metabolic effects induce vasodilatation in most vascular beds with potential for exaggerated vasodilatation and hypotension (Calbet, 2003).

Moraes *et al.* demonstrated persistent elevation of baseline sympathetic activity in rats exposed to sustained hypoxia for 24 hours. Further, they attributed this increase in sympathetic activity in the causation of elevated arterial pressure. The elevated arterial pressure maintains the blood flow to crucial organs, especially to the brain. They also

observed that the increase in sympathetic activity was coupled with the occurrence of respiratory changes especially to active expiration (Moraes *et al.*, 2014).

There is evidence indicating the role of NO and ROS in sympathetic overactivity (Campese *et al.*, 2004; Hirooka *et al.*, 2011; Macarthur *et al.*, 2008). Because NO exerts a tonic inhibition of central sympathetic nervous activity, increased ROS by decreasing the bioavailability of NO may contribute to enhanced sympathetic activity (Campese *et al.*, 2004). The positive correlation between serum MDA and LF and LF/HF ratio observed in our study are also in favour of the role of systemic oxidative stress in enhancing sympathetic activity. Thus oxidative stress may induce sympathetic overactivity that in turn may also escalate oxidative stress thus setting up a vicious cycle that adversely affects the cardiovascular system (Lavie and Lavie, 2009).

5.5 Cardiovascular Hemodynamics: Hemodynamic Parameters

5.5.1 RESULTS

Table 5.5.1 represents within the group and between-group comparisons of hemodynamic parameters.

a. Heart Rate

Within each group, pre-intervention heart rate (day 0) was compared with post-intervention heart rate (day 22) by paired t-test. After 21 days of intervention (post-intervention), there was a significant decrease in the heart rate across all groups.

One way ANOVA was done to compare heart rate across groups. Pre-intervention heart rate was similar between groups. Interestingly even post-intervention heart rate was comparable between groups.

% decrease in the heart rate was calculated which also revealed a decrease in the heart rate across all groups after 21 days, with the highest decrease in group 3 (Cil) and least decrease in group 2 (CH).

Table 5.5.1: Comparison of hemodynamic parameters among groups of experimental animals (n=6 in each group)

Parameters		Group 1 (Control)	Group 2 CH	Group 3 Cil	Group 4 CH+Cil	ANOVA F value	P-value
Heart Rate (beats/min)	Pre	321.61$\pm$42.80	290.00$\pm$22.44	314.75$\pm$28.36	323.66$\pm$15.82	1.331	0.314
	Post	294.29$\pm$49.49	284.52$\pm$20.33	262.95$\pm$8.37	306.00$\pm$14	1.489	0.271
	Paired t-test	0.004*	0.04*	0.0002*	0.01*		
% decrease in HR		8.65$\pm$3.22	2.74$\pm$1.51[a]	16.38$\pm$1.07[ab]	5.44+1.87[c]	27.62	0.00*
MAP (mm Hg)	Pre	91.25$\pm$2.69	92.37$\pm$4.78	93.00$\pm$3.16	91.00$\pm$2.58	0.306	0.821
	Post	96.75$\pm$1.70	108.50$\pm$6.60[a]	99.75$\pm$2.87[b]	84.00$\pm$4.32[abc]	23.395	0.00*
	Paired t-test	0.001*	0.01*	0.002*	0.02*		
% change in BP		6.05$\pm$1.22	17.54$\pm$6.63[a]	7.26$\pm$1.76[b]	-6.61$\pm$1.70[b]	9.309	0.002*

Values are expressed as mean$\pm$SD. Paired t-test for comparisons within each group. One way ANOVA followed by Post Hoc Tukey's multiple comparison tests. Superscript a, b, c indicates a significant difference between groups. 'a' denotes comparison with Group 1, 'b' denotes comparison with group 2, 'c' denotes comparison with group 3. *p$\leq$0.05.

b. Mean Arterial Pressure (MAP)

Within each group, the pre-intervention MAP was compared with post-intervention MAP. There was a significant increase in the mean arterial pressure after 21 days (post-intervention) except for group 4 (CH+Cil). In group 4 (CH+Cil) we noted a significant decrease in the post-intervention MAP.

One way ANOVA was done to compare the MAP between groups. Pre-intervention MAP was comparable between groups. There were significant differences in the post-intervention MAP. It was significantly increased in group 2 (CH) and decreased in group 4 (CH+Cil) compared to control. There were no significant differences between group 3 (Cil) and group 1 (control).

% Change in MAP was calculated and compared in each group. Group 1 (control) rats exhibited a 6.05$\pm$1.22% increase in MAP. Groups 2 (CH) exhibited an increase by 17.54$\pm$6.63 % which was significantly higher compared to group 1 (Control). Group 4 (CH+Cil) showed a decrease in MAP by 6.61$\pm$1.70 %.

5.5.2 DISCUSSION

The hemodynamic evaluation was done to study the effect of chronic hypoxia exposure on the cardiovascular system and the effect of treatment with drug cilnidipine on chronic hypoxia-induced alterations.

The hemodynamic evaluation demonstrated a decrease in heart rate after 21 days (post-intervention) across all groups. Interestingly even chronic hypoxia exposed rats (group 2), demonstrated a small decrease in heart rate after 21 days of an intervention despite the enhanced sympathetic drive (as reflected by LF component and LF/HF ratio of HRV analysis). This decrease in heart rate could be due to the direct depressive action of hypoxia

on the heart that surpassed the stimulatory effects of the enhanced sympathetic drive (Walsh and Marshall, 2006) or may be due to hypoxia-induced down-regulation of cardiac β-adrenergic receptors (Kacimi *et al.,* 1985). Kacimi *et al.,* evaluated effects of chronic hypoxia exposure of varying duration (1, 3, 7, 15, 21 days) on cardiac β-adrenergic receptor density. Wistar rats exposed to 1-15 days hypoxia demonstrated no changes in cardiac β-adrenergic receptor density. While hypoxia exposure for 21 days induced a decrease in the β-adrenergic receptor density in the hypertrophied left ventricle and desensitization of the β-adrenergic receptor in the hypertrophied right ventricle. The decreased density of cardiac β-adrenergic receptor may be due to chronically elevated levels of circulating or neurally released catecholamines. The down-regulation of β-adrenergic receptors has been thought to be a part of the physiological homeostatic mechanisms to maintain myocardial PO_2 to normal levels on long term exposure to hypoxia (Richalet, 1990).

Chronic hypoxia exposures for 21 days lead to an increase in MAP. There are multiple factors contributing to a higher MAP in this group. In our study, there are three important factors contributing to higher MAP, crucial being increased sympathetic drive as reflected by HRV analysis (vide chapter:5.4; Table:5.4.1, 5.4.2). Other factors that may contribute to increased MAP include increased viscosity secondary to raised hematocrit (vide chapter: 5.2; Table: 1), decreased the bioavailability of NO causing endothelial dysfunction (vide chapter: 5.9; table: 5.9.1) (Calbet, 2003). NO by its potent vasodilator action plays a vital role in the maintenance of arterial blood pressure. It also acts as a counter-regulatory factor opposing the vasoconstrictor effects of endothelin, angiotensin II and renal sympathetic nerve activity. NO, in addition, has a role in pressure natriuresis (Barton *et al.*, 2003).

Chronic hypoxia exposed cilnidipine treated rats (group 4) demonstrated a greater decrease of heart rate ($5.44\pm1.87\%$ in group 4 versus $2.74\pm1.51\%$ in group 2) and a decreased MAP in contrast to increased MAP in group 2 (CH). The observed decrease in heart rate and

MAP in group 4 (CH+Cil) may be due to the administration of drug cilnidipine, a dual L and N-type Ca^{2+} channel blocker. Cilnidipine brings about vasorelaxation by blocking the L-type Ca^{2+} channels present on the vascular smooth muscle and reduces the sympathetic drive by blocking the N-type Ca^{2+} channels on the sympathetic nerve endings. Further, it also blocks the release of neurotransmitter from sympathetic nerve endings (Takahara, 2009). Thus overall action of cilnidipine is to reduce the heart rate and blood pressure. Hence it may be stated that hypoxia has a critical role in the pathogenesis of hypertension and cilnidipine may possibly have a potentially beneficial role in its management.

5.6 GLUCOSE HOMEOSTASIS

5.6.1 RESULTS

- **Oral Glucose Tolerance Test (OGTT)**

Glucose Tolerance Test is a simple and widely used test to assess glucose homeostasis in rodents.
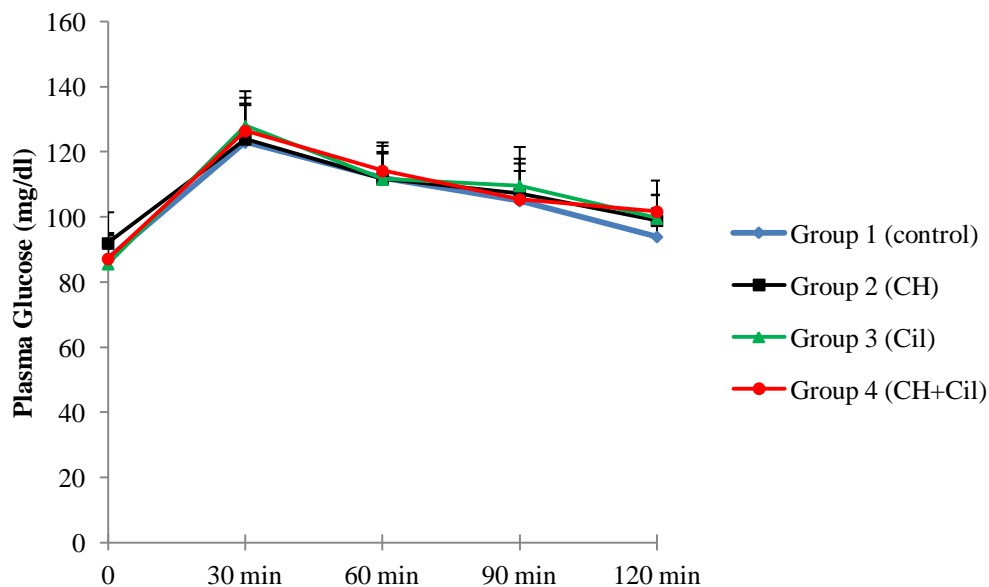
Figure 5.6.1: Comparison of pre-intervention OGTT among groups (n=6 in each group)

Figure 5.6.1 depicts a comparison of pre-intervention (day 0) OGTT among groups. Fasting blood glucose levels (0 min) were comparable between groups. Following administration of an oral glucose load, glucose levels peaked at 30 min, subsequently, there was a gradual decline in the glucose levels at 60 min, 90 min to reach near fasting levels at 120 min. A similar pattern was observed in all four groups.
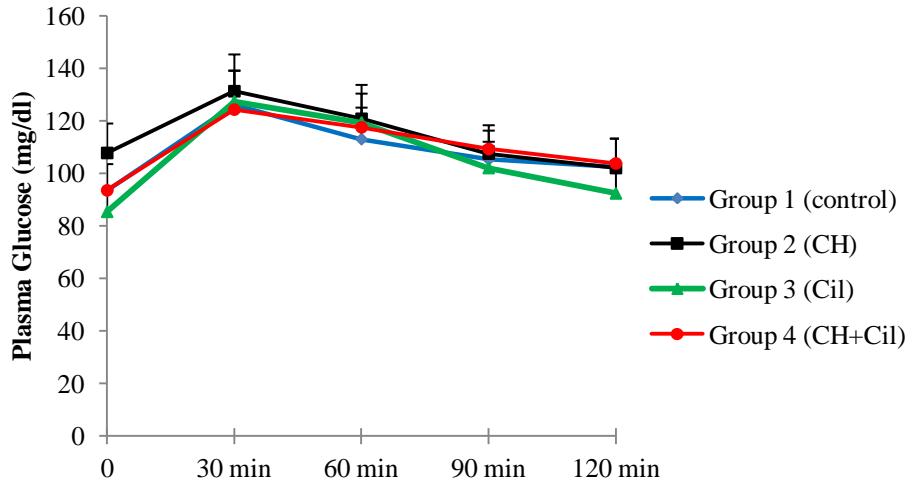
Figure 5.6.2: Comparison of post-intervention OGTT among groups (n=6 in each group)

Figure 5.6.2 depicts a comparison of post-intervention (day 22) OGTT among groups. Fasting blood glucose levels (0 min) was significantly increased in group 2 (CH) compared to group 1 (Control) after 21 days of chronic hypoxia exposure. However, in group 4 (CH+Cil) fasting blood glucose levels were comparable to that of group 1 (Control). The time course of blood glucose after an oral glucose challenge is comparable among groups.
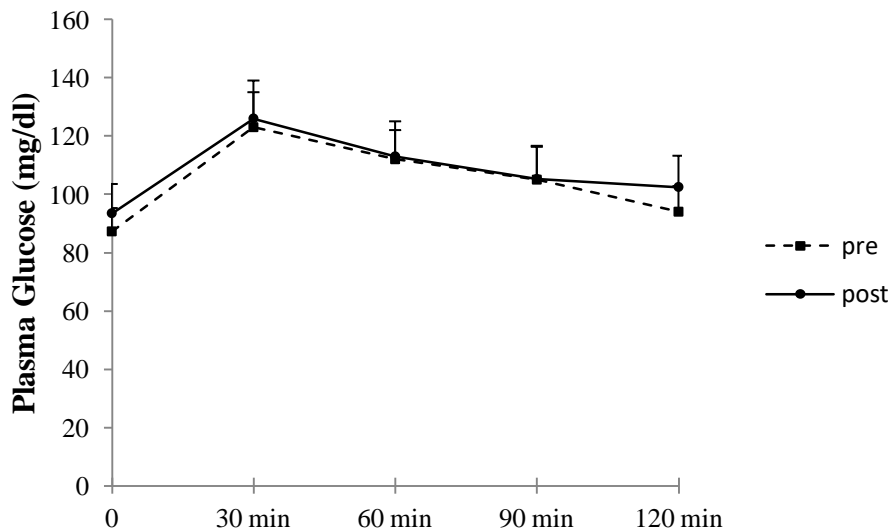
Figure 5.6.3:Pre-intervention *vs.* post-intervention OGTT in group 1 (control)
(n=6 in each group)

Figure 5.6.3 represents a comparison of pre-intervention OGTT (day 0) with the post-intervention (day 22) OGTT in group 1 (control) which appears to be similar.
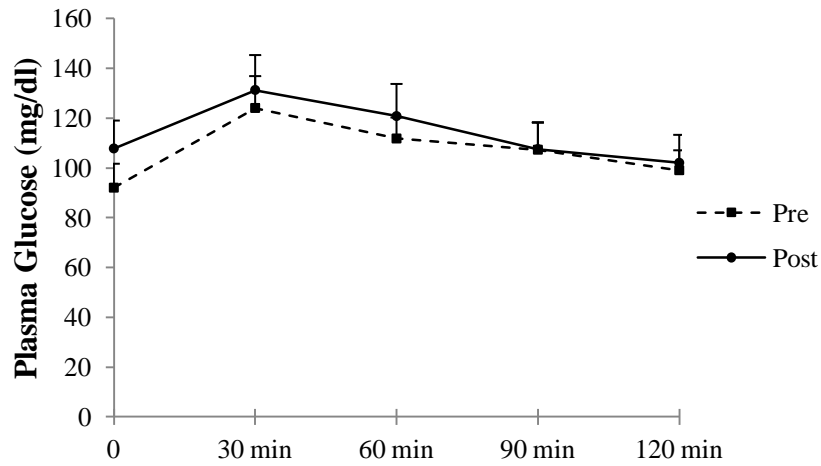
Figure 5.6.4: Pre-intervention *vs.* post-intervention OGTT in group 2 (CH)
(n=6 in each group)

Figure 5.6.4 depicts a comparison of pre-intervention OGTT (day 0) with the post-intervention OGTT (day 22) in group 2 (CH). Fasting blood glucose was increased after 21 days of chronic hypoxia exposure (post-intervention, day 22). However, the time course of blood glucose after an oral glucose challenge was comparable to pre-intervention (day 0) and post-intervention (day 22).
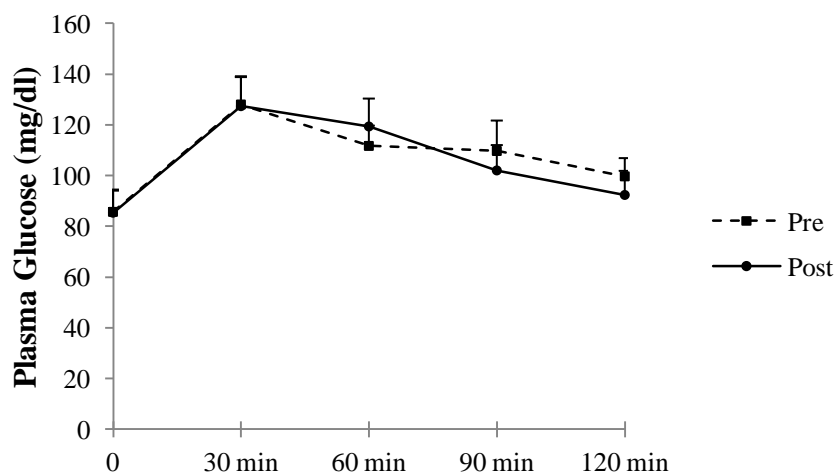
Figure 5.6.5: Pre-intervention *vs.* post-intervention OGTT in group 3 (Cil)
(n=6 in each group)

Figure 5.6.5 represents a comparison of pre-intervention OGTT (day 0) with the post-intervention OGTT (day 22) in group 3 (CH+Cil). The time course of blood glucose levels after an oral glucose challenge appear to be comparable.
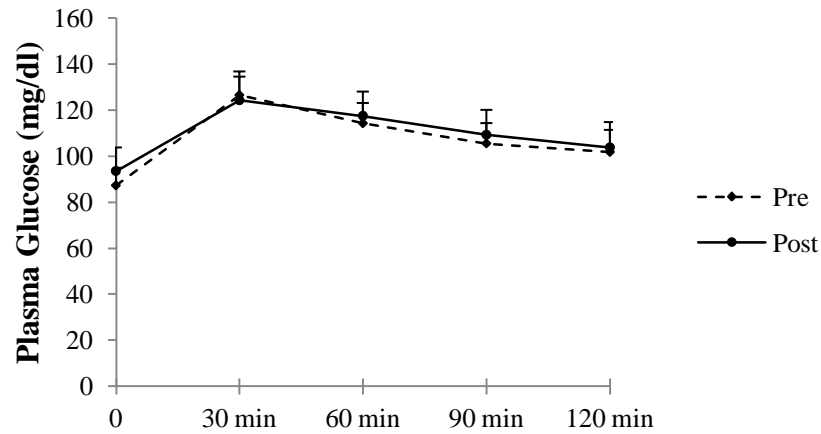
Figure 5.6.6: Pre-intervention *vs.* post-intervention OGTT in group 4 (CH+Cil)

Figure 5.6.6 depicts the time course of blood glucose levels after an oral glucose challenge in group 4 (CH+Cil) on day 0 (pre-intervention) and day 22 (post-intervention). Fasting blood glucose levels were comparable and the two curves appeared similar.

Table 5.6.1 represents a comparison of glucose homeostasis parameters among groups.

Table 5.6.1: Comparison of glucose homeostasis parameters among groups (n=6 in each group)

Parameters	Group 1 (Control)	Group 2 (CH)	Group 3 (Cil)	Group 4 (CH+Cil)	ANOVA F value	P-value
Fasting blood glucose (mg/dl) (day 22)	93.5± 6.75	107.75± 6.75[a]	85.33± 3.81[b]	93.50+3.10[b]	10.421	0.002*
Serum Insulin (mIU/L) (day 22)	28.77± 1.26	30.88 ± 2.91	28.29 +1.29	29.02 ± 1.36	1.509	0.262
HOMA-IR (day 22)	7.0 ± 0.16	8.46+0.20[a]	6.55+0.45[b]	6.02+0.75[b]	20.69	0.000*

Values are expressed as mean±SD. One way ANOVA followed by Post Hoc Tukey's multiple comparison tests. Superscript a, b, c indicates a significant difference between groups. 'a' denotes comparison with Group 1, 'b' denotes comparison with group 2. *$p \leq 0.05$.

- **Fasting blood glucose**

Table 5.6.1 depicts significantly higher fasting blood glucose in group 2 (CH) compared to group 1 (control). In group 4 (CH+Cil) it was significantly lower when compared to group 2 (CH).

- **Serum Insulin**

Table 5.6.1 shows no significant differences in serum insulin among groups.

- **HOMA-IR**

Table 5.6.1 shows significantly higher HOMA-IR in group 2 (CH). HOMA-IR in groups 1 (control), 3 (Cil) and 4 (CH+Cil) was comparable.

- **Correlation of glucose homeostasis parameters and cardiac autonomic functions**

Pearson's correlation was done to know the correlation between glucose homeostasis parameters like fasting blood glucose, HOMA-IR and LF/HF ratio an indicator of sympathovagal balance.
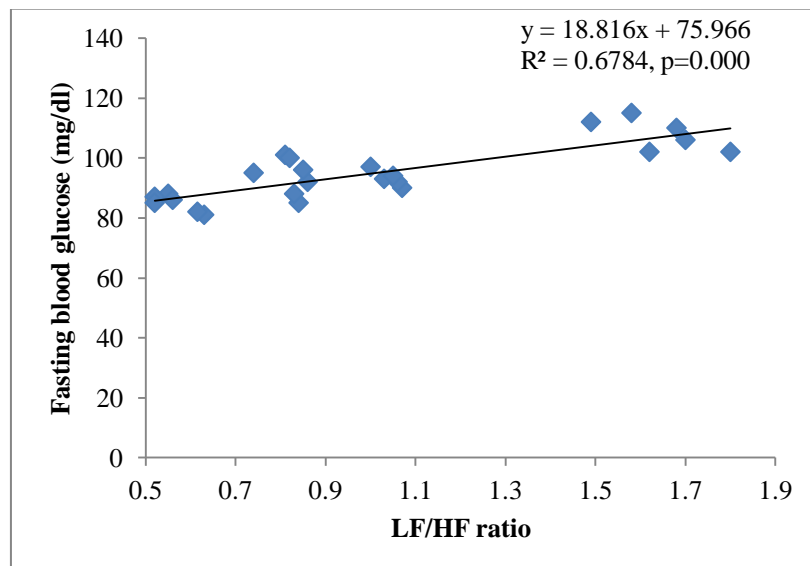
Figure 5.6.7: Correlation between fasting blood glucose and LF/HF ratio

Figure 5.6.7 represents a statistically significant positive correlation between fasting blood glucose and LF/HF ratio, an indicator of sympathovagal balance.

Graph showing correlation between HOMA-IR (y-axis, 0 to 10) and LF/HF ratio (x-axis, 0.5 to 1.9). Trend line with equation y = 1.7778x + 5.1061, R² = 0.4609, p=0.000.
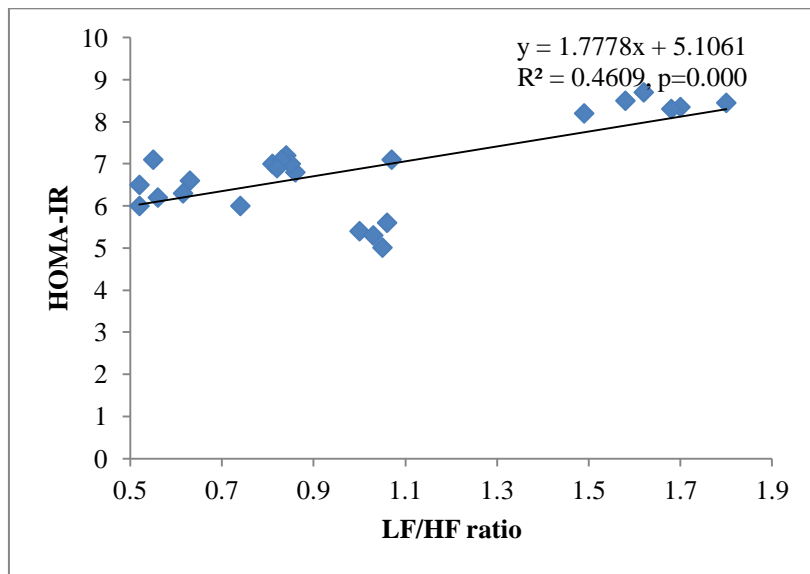
Figure 5.6.8: Correlation between HOMA-IR and LF/HF ratio

Figure 5.6.8 depicts a statistically significant positive correlation between HOMA-IR and LF/HF ratio an indicator of sympathovagal balance.

5.6.2 DISCUSSION

Oxygen is vital for various metabolic processes. Exposure to hypoxia triggers multiple pathways at the cellular and organ level to restore oxygen homeostasis (*Cao et al.*, 2014). In the present study, we evaluated the effect of chronic hypoxia exposure on glucose homeostasis by OGTT, serum insulin, HOMA-IR.

The results of our study reveal normal glucose tolerance, normal serum insulin levels, increased fasting blood glucose and increased HOMA-IR suggestive of impaired glucose homeostasis following chronic hypoxia exposure. Pearson's correlation revealed a significant positive correlation between LF/HF ratio, fasting blood glucose and HOMA-IR pointing towards the role of the sympathetic nervous system and sympathovagal balance in glucose homeostasis.

Increased fasting blood glucose levels on chronic hypoxia exposure could be explained by increased sympathetic activity. The significant positive correlation between FBS and LF/HF are also in support of the same. The sympathetic nervous system (SNS) stimulates hepatic glucose output by accelerating gluconeogenesis in fasting state and glycogenolysis in the postprandial state. In addition, SNS regulates hepatic glucose output via pancreatic hormones. In rats, sympathetic stimulation via α_2-adrenergic receptor activation favours glucagon secretion and suppresses insulin secretion. Although SNS via β_2-adrenergic receptors transiently stimulates insulin secretion, inhibition of insulin secretion by α_2-adrenergic receptor predominates. In addition to the liver and pancreas, sympathetic stimulation as well affects skeletal muscle glucose metabolism. Sympathetic stimulation in skeletal muscle induces glycogenolysis by β-adrenergic receptor activation releasing lactate into circulation. Lactate is channelled into the liver for further hepatic gluconeogenesis. Thus the sympathetic nervous system increases blood glucose levels by its actions on the liver, skeletal muscle and pancreas (Nonogaki, 2000).

HOMA-IR is increased in chronic hypoxia exposed experimental animals (group 2) suggestive of insulin resistance. The positive correlation between HOMA-IR and LF/HF ratio (elevated in group 2) is indicative of a causal relationship between the sympathetic nervous system and insulin resistance. There is evidence that sympathetic overactivity precedes the development of insulin resistance (Flaa *et al*., 2008). Sympathetic overactivity reduces skeletal muscle blood flow via α-adrenergic receptor-mediated vasoconstriction. This reduces the postprandial increase in skeletal muscle blood flow impairing glucose uptake by skeletal muscle (Thorp and Schlaich, 2015). Since skeletal muscle is a principal site of insulin-stimulated glucose uptake and a major site of blood glucose utilisation, reduced glucose utilisation by skeletal muscle leads to insulin resistance (Nonogaki, 2000). Insulin resistance is followed by a compensatory increase in insulin secretion by the pancreas. Hence insulin

resistance is usually accompanied by hyperinsulinemia. However in our study serum insulin levels in chronic hypoxia exposed rats were similar to control rats. This may be related to the duration of hypoxia exposure. The results must be further evaluated by increasing the duration of hypoxia exposure.

Cilnidipine treated chronic hypoxia exposed rats displayed better glucose homeostasis. These findings are suggestive of a role of cilnidipine in alleviating the chronic hypoxia-induced impaired glucose homeostasis. These actions of cilnidipine are probably mediated by its N-type calcium channel blocking actions. N-type calcium channels are located on the sympathetic nerve endings and mediate sympathetic neurotransmission. Cilnidipine by blocking N-type calcium channels reduces sympathetic neurotransmission thereby lowering the hypoxia-induced enhanced sympathetic drive (Takahara, 2009).

Harada et al. evaluated the effect of cilnidipine treatment on insulin sensitivity in an experimental rat model of NIDDM. They reported significant improvement in insulin sensitivity without any effect on serum glucose or insulin levels in addition to its antihypertensive action (Harada *et al*., 1999).

5.7 LIPID PROFILE

5.7.1   RESULTS

Table 5.7.1 represents a comparison of lipid profile among groups. After 21 days of intervention total cholesterol, triglycerides, HDL, LDL and VLDL were estimated and were found comparable between groups.

Table 5.7.1: Comparison of lipid profile among groups of experimental animals (n=6 in each group)

Parameter	Group 1 (control)	Group 2 (CH)	Group 3 (Cil)	Group 4 (CH+Cil)	ANOVA F value	P-value
Total Cholesterol	62.78±2.12	64.12±1.63	59.63±3.27	63.66±3.51	1.628	0.258
Triglycerides	49.00±2.00	55.00±3.00	52.00±2.64	55.33±3.05	3.59	0.066
HDL	32.24±2.46	28.00±2.00	29.00±1.00	27.33±2.08	3.708	0.061
LDL	20.81±1.87	25.12±1.18	20.33±3.78	25.23±3.98	2.43	0.14
VLDL	9.80±0.40	11.00±0.60	10.40±0.52	11.06±0.61	3.591	0.066

Values are expressed as mean±SD. One way ANOVA followed by Post Hoc Tukey's multiple comparison tests.

5.7.2   DISCUSSION

Our study revealed no significant differences in the lipid profile among groups after 21 days of intervention indicating no effect of chronic hypoxia (CH) exposure on lipid metabolism.

Siques *et al*. evaluated the lipid profile in rats exposed to chronic hypobaric hypoxia for 30 days. They observed increased triglycerides and VLDL-cholesterol after 15 days of CH exposure which persisted at 30 days of CH exposure. While total cholesterol and LDL-cholesterol were transiently elevated and HDL-cholesterol was decreased after 15 days of CH exposure which were comparable to normoxia control rats at 30 days of CH exposure (Siques *et al*., 2014).

Das *et al*. evaluated the lipid profile in experimental animals exposed to chronic hypoxia for 21 days. They observed elevated HDL cholesterol and higher HDL/LDL ratio and decreased LDL and VLDL (Das *et al*., 2015).

Xu *et al*. evaluated the lipid profile in experimental animals exposed to hypobaric hypoxia for 30 days. They reported lower triglyceride compared to control. Total Cholesterol, LDL and HDL were comparable with control after 30 days of hypobaric hypoxia exposure (Xu *et al*., 2016).

5.8 Oxidative Stress

5.8.1   RESULTS

Table 5.8.1 depicts a comparison of oxidative stress parameters among all groups.

Table 5.8.1: Comparison of oxidative stress among groups of experimental animals (n=6 in each group)

Parameter	Group 1 (control)	Group 2 (CH)	Group 3 (Cil)	Group 4 (CH+Cil)	ANOVA F value	P-value
Serum MDA (µmol/L)	1.69 ± 0.98	4.76 ± 1.03^a	1.71 ± 0.51^b	3.12 ± 1.20^{abc}	31.42	0.00*
Serum Vit C (mg/dl)	1.65 ± 0.04	1.35 ± 0.06^a	1.64 ± 0.07^b	1.58 ± 0.10^b	14.523	0.000*
Serum Vit E (µg/ml)	1.81 ± 0.32	1.11 ± 0.27^a	1.68 ± 0.25	1.66 ± 0.29	4.653	0.022*
Ventricular tissue MDA (µmol/gm of tissue)	10.81 ± 0.48	13.80 ± 0.21^a	10.73 ± 0.46^b	10.73 ± 0.37^b	28.80	0.004*
Liver MDA (µmol/gm of tissue)	27.27 ± 3.68	43.68 ± 3.50^a	28.36 ± 3.94^b	41.31 ± 1.81^{ac}	32.91	0.000*
Lung MDA (µmol/gm of tissue)	27.01 ± 2.97	37.12 ± 2.57^a	28.88 ± 3.33^b	31.74 ± 5.40	6.95	0.003*

Values are expressed as mean$\pm$SD. One way ANOVA followed by Post Hoc Tukey's multiple comparison tests. Superscript a, b, c indicate a significant difference between groups. 'a' denotes comparison with Group 1, 'b' denotes comparison with group 2, 'c' denotes comparison with group 3. *p$\leq$0.05.

a. Lipid Peroxidation Product:

Malondialdehyde (MDA) is a lipid peroxidation product and a commonly used marker of oxidative stress. MDA was estimated in the serum as well as in the tissue homogenate of liver, lung and heart.

Table 5.8.1 depicts a significant increase in serum MDA levels in group 2 (CH) compared to group 1 (control). Further, group 2 (CH) also demonstrated significantly increased MDA levels in liver, heart and lung tissue homogenate.

Group 4 (CH+Cil) revealed an increase in serum MDA compared to group 1(control). However, when compared to group 2 (CH), the rise in serum MDA was significantly lower in group 4 (CH+Cil). MDA in liver and lung tissue homogenate were increased in Group 4 (CH+Cil) and comparable to group 2 (CH). But MDA in heart tissue homogenate was significantly reduced in group 4 (CH+Cil) in comparison to group 2 (CH).

b. Exogenous non-enzymatic antioxidants:

Serum Vit C and Vit E were significantly lower in group 2 (CH) compared to group 1 (control). In group 4 (CH+Cil) the values were comparable with group 1 (control)

5.8.2 DISCUSSION

Oxidative stress results when the oxidants are produced in excess and beyond the scavenging capacity of the antioxidants resulting in the disruption of the redox signalling and/or inducing molecular damage (Clanton, 2007). Among the various consequences of oxidative stress are the oxidative damage of biomolecules of lipids, proteins, carbohydrates and nucleic acids ultimately leading to cell death in severe oxidative stress (Ryan, 2010) (Hanna Ali H, 2012). Lipid peroxidation results when the free radicals or the non-radical species attack lipids containing carbon-carbon double bond, especially the polyunsaturated fatty acids (PUFA) resulting in the production of lipid peroxyl radicals (LOO*) and hydroperoxides (LOOH). Lipid peroxidation produces a wide variety of oxidation products. The primary products of lipid peroxidation are lipid hydroperoxides and the secondary products are different aldehydes like malondialdehyde (MDA), propanal, hexanal, 4-hydroxynonenal (4-HNE) (Ayala *et al*., 2014). MDA is a product of peroxidation of omega-3 and omega-6 fatty acids (Ayala *et al*., 2014) and has frequently been used as an indirect biomarker of oxidative stress (Buege and Aust, 1978). Antioxidants like vitamin C and E are known to prevent lipid peroxidation (Huang, 2002). Vitamin E is fat-soluble and acts as a chain-breaking

antioxidant. Vitamin C is a non-enzymatic water-soluble antioxidant having free radical scavenging action and can directly react with superoxide radical, hydroxyl radical and various lipid hydroperoxides (Trimbake, 2013).

In this study, systemic oxidative stress was assessed by estimating MDA in serum and tissue oxidative stress by estimating MDA in liver, heart and lung tissue homogenate as well as non-enzymatic antioxidants vitamin C and E in the serum. We observed elevated MDA in the serum and in the liver, lung and heart tissue homogenate in chronic hypoxia exposed rats (group 2, group 4) as compared to control rats (group 1) pointing towards oxidative stress in the former. Hypoxia results in the paradoxical release of reactive oxygen species from complex III and to a lesser extent from complex II of the mitochondrial electron transport chain (Giaccia et al., 2004). Oxidative stress results when the production of ROS exceeds the antioxidant defence mechanisms.

Among the liver lung and heart, the highest oxidative stress was noted in the liver and least in the the heart. These results suggest that the liver experiences greater brunt of hypoxia induced oxidative stress despite the fact that it has an abundant antioxidant reserve. There are multiple factors contributing to this. Vital organs like heart and brain are supply dependent and organs like kidneys, skin, resting muscle and splanchnic area are supply independent (Bryan, 1988). In the event of exposure to any stressful condition like hypoxia, the blood flow is diverted to vital organs like heart and brain at the cost of the visceral organs (Jun et al., 2008). In addition, ROS formation is promoted by free iron, hemoproteins and polyunsaturated fatty acids (PUFAs). The liver has more iron and free iron reacts with hydrogen peroxide via Fenton reaction producing hydroxyl radicals. Further, heme released from the hemoproteins enhances the formation of ROS via the Fenton reaction. High levels of cytochrome P450 in the liver also contributes to ROS formation (Kammer et $al.,$ 2011). Thus hepatic oxidative stress induced by exposure to low O_2 microenvironment may have a vital role in the

pathogenesis of liver diseases in patients experiencing hypoxia. There are studies reporting a higher prevalence of Non-alcoholic Fatty Liver Disease (NAFLD) in patients suffering from a chronic obstructive pulmonary disease (COPD) (Viglino *et al*., 2017).

Lungs are the gateway for oxygen between the cells of the body and the environment. Hence, lungs may be one of the earliest organs to encounter adverse consequences of hypoxia. However, in the present study lungs demonstrated lower oxidative stress in comparison to the liver. This could be due to the inherent tolerance exhibited by the alveolar epithelial cells to hypoxia due to which they can maintain adequate cellular ATP on exposure to prolonged hypoxia (Smita *et al*., 2015).

In the present study, serum vitamin C and E were reduced in chronic hypoxia exposed experimental rats (group 2) due to their utilization in scavenging lipid peroxides.

Cilnidipine belongs to the dihydropyridine class of calcium channel blockers (CCB) with a dual L/N type calcium channel blocking property (Takahara, 2009). Cilnidipine is lipophilic and acts as a lipophilic chain-breaking antioxidant. When compared to other dihydropyridine CCBs, cilnidipine has been demonstrated to be highly lipophilic with the strongest antioxidant actions (Hishikawa *et al*., 2009). In our study cilnidipine treated chronic hypoxia exposed rats have shown reduced oxidative stress supporting the antioxidant property of cilnidipine.

Luneburg *et al*. also demonstrated higher oxidative stress and a 2-fold increase in MDA in lung tissue homogenates in rats exposed to chronic hypoxia for 30 days (Luneburg *et al*., 2016).

Xu *et al*. evaluated oxidative stress in experimental animals exposed to hypobaric hypoxia for 30 days. They reported increased MDA in serum and liver tissue homogenate which are in accordance with results of the present study (Xu *et al*., 2016).

The results of Nakanishi *et al*. corroborate with the results of our study. They reported significantly increased MDA in serum, heart, lung, liver and kidney in experimental animals exposed to hypobaric hypoxia for 21 days (Nakanishi *et al*., 1995). Sarada *et al*. reported an increase in plasma MDA in experimental animals exposed to hypoxia for 7 days (Sarada *et al*., 2002). Jusman *et al*. evaluated MDA in the liver tissue homogenate in experimental animals exposed to hypoxia for 1, 3, 7 and 14 days. They reported a gradual increase in MDA in liver tissue homogenate from day 1-14 with peak values in rats exposed to hypoxia for 3 days. Thereafter MDA levels remained elevated irrespective of the duration of exposure (Jusman *et al*., 2010). Smita *et al*. assessed MDA in lung tissue homogenate in rats exposed to hypoxia for 2hr, 4hr, 8hr, 12hr, 16hr, 24hr, 48 hr. MDA levels were raised in rats exposed to hypoxia for 12 hr, 16 hr, 24 hr, 48 hr (Smita *et al*., 2015).

5.9 HYPOXIA SIGNALLING MOLECULES

5.9.1 RESULTS

Table 5.9.1: Comparison of hypoxia signalling molecules between groups of experimental animals (n=6 in each group)

Parameter	Group 1 (control)	Group 2 (CH)	Group 3 (Cil)	Group 4 (CH+Cil)	ANOVA F value	P-value
Serum VEGF (pg/ml)	60.00$\pm$9.93	110.82$\pm$7.61[a]	60.50$\pm$11.47[b]	89.33$\pm$7.02[abc]	27.32	0.000*
Serum NOS3 (pg/ml)	16.59$\pm$2.86	35.04$\pm$6.62[a]	12.67$\pm$2.36[b]	31.54$\pm$2.99[ac]	26.69	0.000*
Serum NO (µmol/L)	11.21$\pm$2.63	6.95$\pm$1.76[a]	10.04$\pm$1.25[b]	9.38$\pm$1.81	3.24	0.056

Values are presented as mean$\pm$SD. One way ANOVA followed by Post Hoc Tukey's multiple comparison tests. Superscript a, b, c indicates a significant difference between groups. 'a' denotes comparison with Group 1, 'b' denotes comparison with group 2, 'c' denotes comparison with group 3. *p$\leq$0.05.

Table 5.9.1 represents a comparison of hypoxia signalling molecules between groups.

Group 2 (CH) demonstrated increased serum VEGF, serum NOS3 with significantly decreased serum NO compared to group 1 (control).

Group 4 (CH+Cil) also revealed elevated serum VEGF and serum NOS3 accompanied by a normal serum NO when compared to group 1 (control). However, when compared to group 2 (CH), the increase in serum VEGF and serum NOS3 was significantly lower in group 4 (CH+Cil).

5.9.2 DISCUSSION

Since O_2 is crucial for cell survival, the cells are equipped with mechanisms to detect and to respond to alterations in the O_2 levels in the microenvironment (Giaccia *et al*., 2004). There are specialized chemoreceptors that detect alterations in the PO_2 and initiate systemic responses (ventilatory, autonomic and cardiovascular) within seconds to make up for the changes. In addition, every single nucleated cell is equipped to detect the changes in the O_2

levels and to respond immediately (within minutes) by activation of proteins already present and chronically (within hours) through regulation of gene expression (Michiels, 2004).

Hypoxia-inducible factor (HIF) is a transcription factor plays a vital role in the molecular response of the cells to hypoxia. HIF-1, a 'master switch' for hypoxic gene expression transcriptionally activates more than 100 genes associated with angiogenesis, erythropoiesis, glucose uptake and metabolism, energy metabolism, cell proliferation and apoptosis. Among the several HIF-1 target genes, transcription of vascular endothelial growth factor (VEGF) and endothelial nitric oxide synthase (eNOS/NOS3) are crucial for the cardiovascular responses to hypoxia. VEGF is a key molecule governing the angiogenic response to hypoxia (Rodriguez-Miguelez *et al*., 2015) (Dulak and Jozkowicz, 2003). It promotes endothelial mitosis, induces the widespread formation of collateral blood vessels to achieve the supply of oxygen to the tissues (Yin *et al*., 2016). VEGF also stimulates the production of NO by NOS3 (Le Moine *et al*., 2011). Vascular endothelial cells, cardiac endothelial cells, ventricular cardiomyocytes express NOS3. NO, a potent vasodilator brings about dilation of the systemic arteries increasing blood flow to peripheral tissues (Yoon *et al*., 2016). Further, NO at appropriate concentration induces VEGF through HIF-1. VEGF, in turn, potentiates NO production by NOS3. However, excessive amounts of NO can inhibit HIF-1 activity and reduce VEGF levels (Rodriguez-Miguelez *et al*., 2015).

In our study chronic hypoxia exposure resulted in an increase in serum VEGF and serum NOS3. Interestingly serum NO was significantly reduced despite elevated NOS3. Lower NO points towards reduced bioavailability of NO. The reduced bioavailability of NO may be due to the destruction of NO by the generated ROS particularly superoxide radicals or due to uncoupling of NOS3. Uncoupled NOS3 induced by peroxynitrite produces superoxide radicals instead of NO (Siques *et al*., 2014). The reduced NO in chronic hypoxia induces

nitrosative damage that may be responsible for increased mean arterial pressure observed in the group and may also possibly induce cardiovascular remodelling.

It has been demonstrated that hypoxia-induced increases in VEGF peaks at 48 hrs after hypoxia exposure and returns back to baseline levels at 3 weeks. However, the effects of VEGF persist for weeks to months due to long term up-regulation of VEGF receptors (Adeoye *et al*., 2014).

Siques *et al*. evaluated the bioavailability of NO in the pulmonary artery, expression of phosphorylated eNOS, an active form of the enzyme and superoxide anion levels in rats exposed to chronic hypoxia for 46 days. They reported reduced availability of NO and decreased expression of phosphorylated NOS3 and increased the generation of superoxide anion radicals (Siques *et al*., 2014).

In the present study cilnidipine treated chronic hypoxia exposed rats demonstrated increased serum VEGF, serum NOS3 and improvement of serum NO. Improved serum NO levels in the group may be due to increased bioavailability and/or due to increased production. The reduced oxidative stress observed in cilnidipine treated rats (vide chapter: 5.8; table: 1) might have increased the bioavailability of NO. These results also support the antioxidant action of cilnidipine. Cilnidipine has also been demonstrated to enhance NOS3 expression and increase NO production (Fan *et al*., 2011). By improving serum NO cilnidipine ameliorates chronic hypoxia-induced endothelial dysfunction.

5.10 Cardiovascular Remodelling

5.10.1 RESULTS

- **Cardiosomatic index**
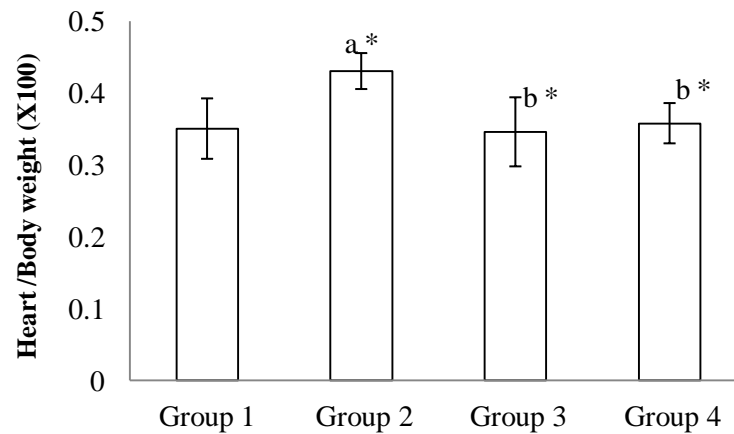
Figure 5.10.1: Comparison of the cardiosomatic index among groups (n=6 in each group)

Superscript a, b indicate a significant differences between groups. 'a' denotes comparison with Group 1; 'b' denotes comparison with group 2. $*p \leq 0.05$

Figure 5.10.1 shows a comparison of the cardiosomatic index among groups. The cardiosomatic index is significantly increased in group 2 (CH) compared to group 1 (control). In group 4 (CH+Cil) cardiosomatic index is comparable to group 1 (control).

- **Histopathological examination of the ventricles and intramyocardial coronary artery**
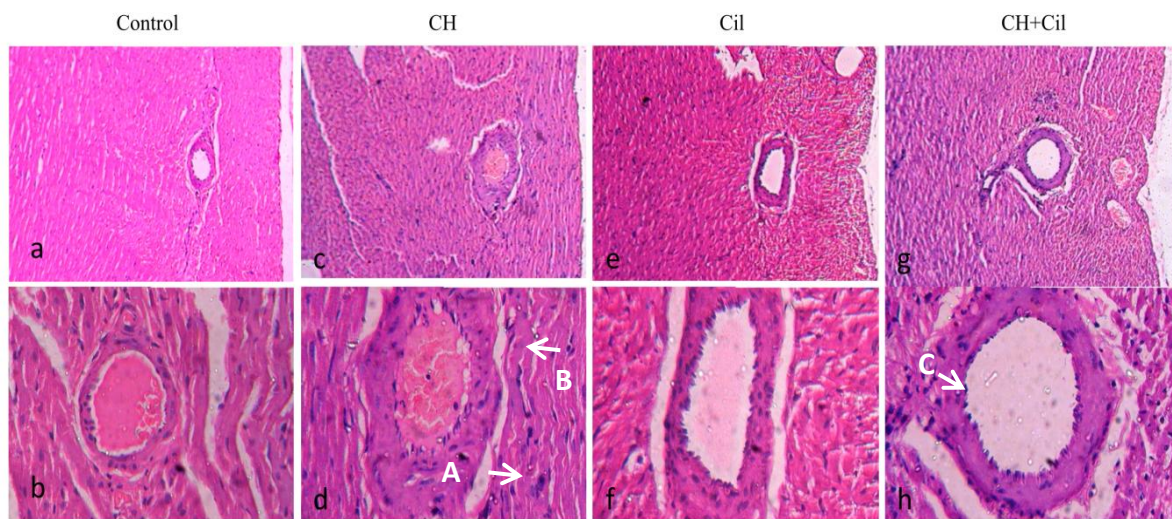
Figure 5.10.2: Photomicrograph of ventricular tissue with coronary artery stained with Haematoxylin & Eosin stain from a) group 1 (control) (x10), b) group 1 (control) (x40); c) group 2 (CH) (x10), d) group 2 (CH) (x40); e) group 3 (Cil) (x10), f) group 3 (Cil) (x40); g) group 4 (CH+Cil) (x10), h) group 4 (CH+Cil) (x40).
 'A': nuclear enlargement, 'B':myocardial hypertrophy, 'C': dilatation of coronary artery

Figure 5.10.2 represents a comparison of H & E stained sections of the ventricle with coronary microvasculature among groups. The microscopic examination of the myocardium stained with H & E gives the impression of normal myocardium in group 1 (control) and group 3 (Cil). Group 2 (CH) showed mild hypertrophy of cardiac myocytes with nuclear enlargement and capillary congestion. Coronary artery demonstrated moderate arteriosclerosis and congestion. Group 4 (CH+Cil) showed normal histology of myocardium with mild arteriosclerosis and dilatation of the coronary artery.

- **Normalised wall index (NWI) of coronary artery**

Table 5.10.1: Comparison of Normalized wall index (NWI) of the coronary artery among groups (n=6 in each group)

Parameter	Group 1 (Control)	Group 2 (CH)	Group 3 (Cil)	Group 4 (CH+Cil)	ANOVA F value	P-value
NWI	0.620 ± 0.02	0.71 ± 0.01^a	0.55 ± 0.02^{ab}	0.54 ± 0.02^{ab}	83.935	0.000*

Values are expressed as mean$\pm$SD. One way ANOVA followed by Post Hoc Tukey's multiple comparison tests. Superscript a, b, c indicates a significant difference between groups. 'a' denotes comparison with Group 1, 'b' denotes comparison with group 2, *p$\leq$0.05.

Table 5.10.1 shows a comparison of the normalised wall index (NWI) of the coronary artery among groups. NWI was significantly increased in group 2 (CH) pointing towards increased wall thickness. NWI was significantly reduced in group 4 (CH+Cil) compared to group 1 (control) and group 2 (CH+Cil).
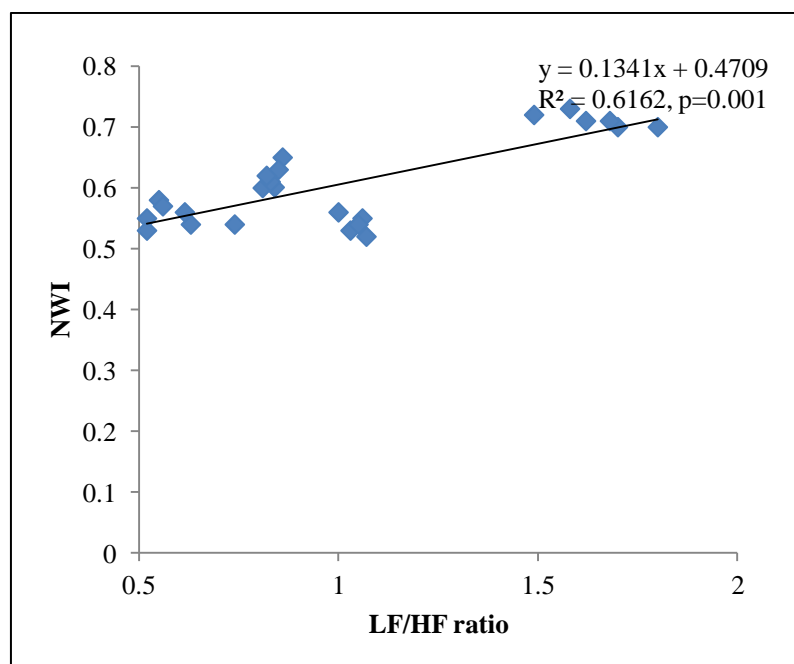
Figure 5.10.3: Correlation between NWI and LF/HF ratio

Figure 5.10.3 represents a statistically significant positive correlation between NWI and LF/HF ratio, an indicator of sympathovagal balance.
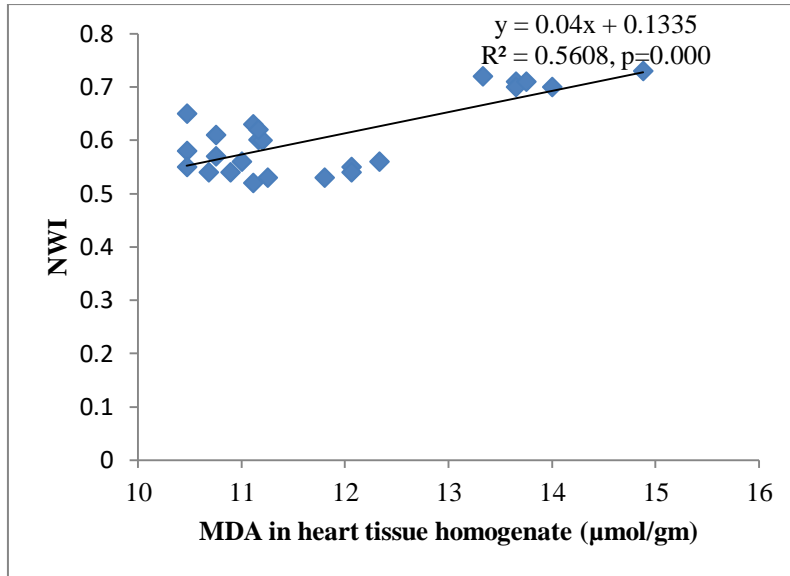
Figure 5.10.4: Correlation between NWI and MDA in ventricular tissue homogenate

Figure 5.10.4 represents a statistically significant positive correlation between NWI and

MDA in ventricular tissue homogenate.
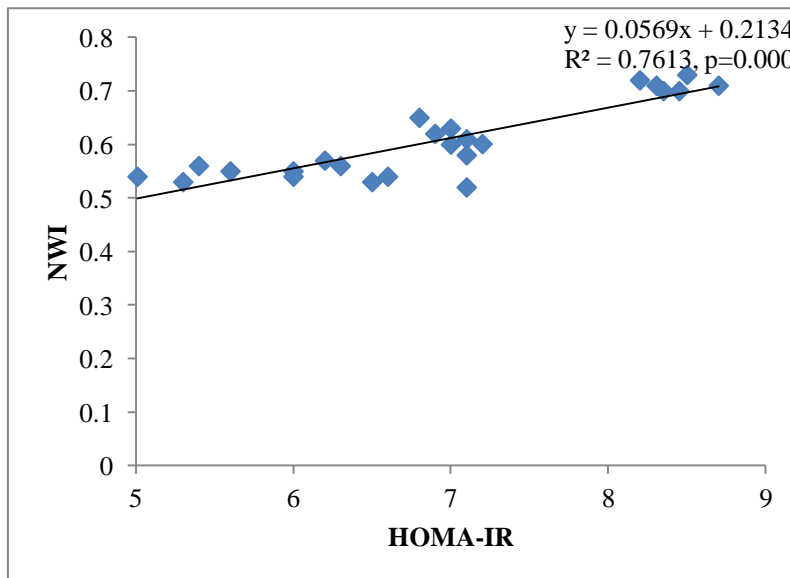
Figure 5.10.5: Correlation between NWI and HOMA-IR

Figure 5.10.5 represents a statistically significant positive correlation between NWI and

HOMA-IR ratio, an index of insulin resistance.
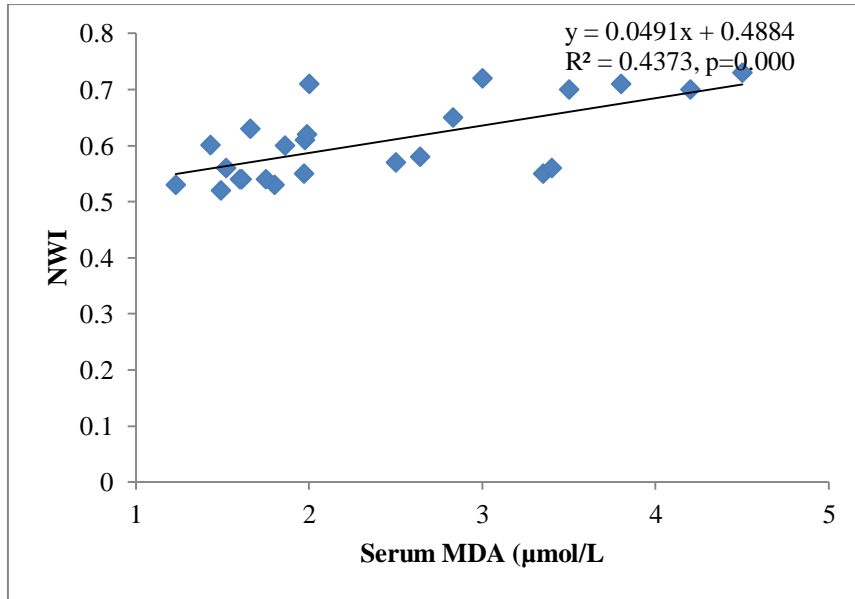
Figure 5.10.6: Correlation between NWI and Serum MDA

Figure 5.10.6 represents a statistically significant positive correlation between NWI and serum MDA.
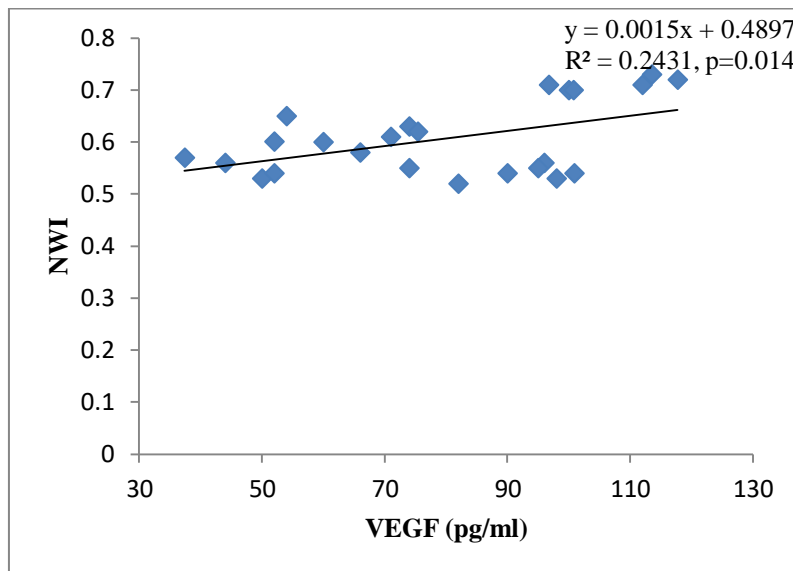
Figure 5.10.7: Correlation between NWI and VEGF

Figure 5.10.7 represents a statistically significant positive correlation between NWI and serum VEGF.

- **Histopathology of elastic artery**
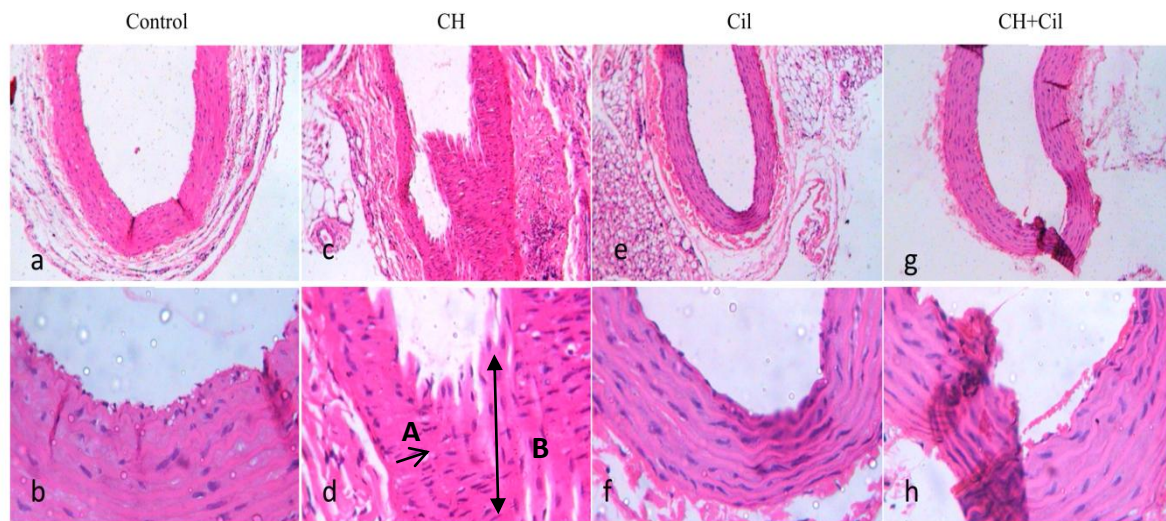
Figure 5.10.8: Photomicrograph of elastic artey stained with Haematoxylin & Eosin stain from a) group 1 (control) (x10); b) group 1 (control) (x40); c) group 2 (CH) (x10); d) group 2 (CH) (x40); e) group 3 (Cil) (x10); f) group 3 (Cil) (x40); g) group 4 (CH+Cil) (x10); h) group 4 (CH+Cil) (x40). **'A': Hyperplastic smooth muscle cells, B: increase in wall thickness**

Figure 5.10.8 depicts the comparison of H & E sections of elastic artery among groups. Group 2 (CH) demonstrated mild thickening of tunica intima, hyperplastic smooth muscle cells of tunica media and an overall increase in wall thickness of the elastic artery. Group 4 (CH+Cil) demonstrated mild thickening of tunica intima and aortic dilation. The rest of the groups showed normal histopathology.

- **Histopathology of muscular artery**
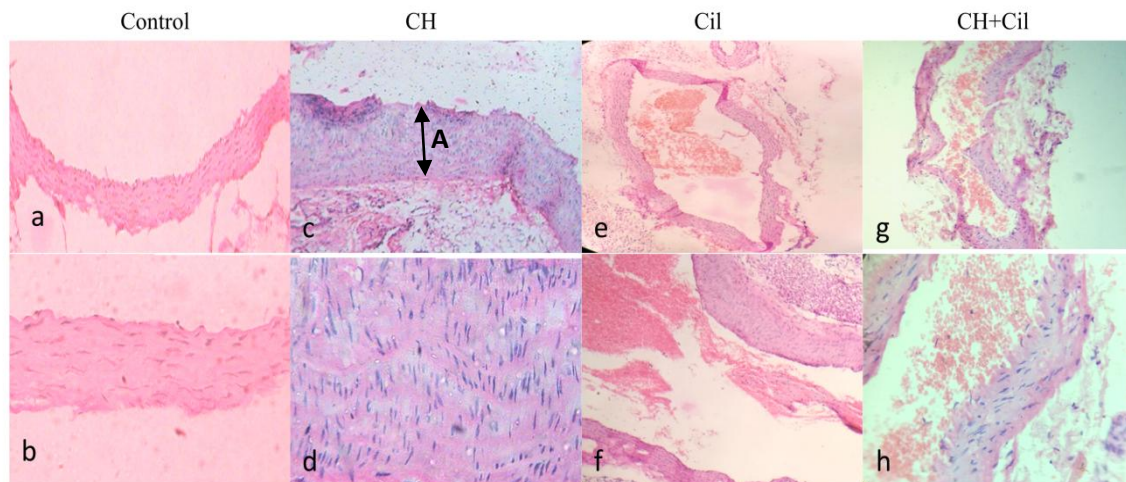
Figure 5.10.9: Photomicrograph of muscular artery stained with H & E stain from a) group 1 (control) (x10), b) group 1 (control) (x40); c) group 2 (CH) (x10), d) group 2 (CH) (x40); e) group 3 (Cil) (x10), f) group 3 (Cil) (x40); g) group 4 (CH+Cil) (x10), h) group 4 (CH+Cil) (x40).
'A': increased wall thickness

Figure 5.10.9 depicts the comparison of H & E sections of the muscular artery among groups. Group 2 (CH) demonstrated mild thickening of tunica intima, hyperplastic smooth muscle cells of tunica media and an increased wall thickness of the muscular artery. Group 4 (CH+Cil) demonstrated mild thickening of tunica intima. The rest of the groups showed normal histopathology.

5.10.2 DISCUSSION

Our study demonstrated an increased cardiosomatic index pointing towards cardiac hypertrophy (Corno *et al*., 2002). Histopathological examination of the ventricular myocardium also revealed hypertrophy of the cardiac myocytes in chronic hypoxia-exposed experimental animals. There are multiple factors implicated in the genesis of cardiac hypertrophy in chronic hypoxia. One of them may be a direct effect of hypoxia in inducing cardiac hypertrophy (Ito *et al*., 1996). Or maybe hypertrophy in response to increased mean arterial pressure (pressure overload) (vide chapter: 5.5, table: 5.5.1) (Hunter *et al*., 1999; Julian, 2007). Many studies have also delineated the role of increased sympathetic activity and oxidative stress (Kwon *et al.*, 2003; Li *et al.*, 2002; Higuchi *et al*., 2002; Pimentel *et al*., 2001) in chronic hypoxia-induced cardiac structural remodelling. Chronic stimulation of β-adrenergic receptors leads to activation of pro-hypertrophic genes triggering cardiac remodelling (Pare *et al.*, 2005). Oxidative stress is one of the major stimulants for signal transduction in cardiac myocytes which plays a key role in the development of cardiac hypertrophy (Rababa'h *et al*., 2018; Sabri *et al*., 2003). In the present study increased MDA in heart tissue homogenate (vide chapter 5.8; table: 1) may be a contributing factor in addition to the sympathetic overactivity. Thus chronic hypoxia induces cardiac remodelling via multiple mechanisms like alteration of cardiovascular hemodynamics, the direct impact of chronic hypoxia on heart phenotype, sympathetic overactivity and oxidative stress.

Fan *et al*. reported increased heart weight and size as reflected by heart weight to body weight ratio in neonatal mice exposed to chronic sustained hypoxia for 4 weeks. Further, they reported that increased heart weight was observed as early as 1 week after hypoxia exposure which was more marked at 2 and 4 weeks of exposure. Light microscopic examination of H & E stained sections of the heart revealed hypertrophy of the cardiomyocytes. They hypothesized that enhanced protein synthesis machinery contributed significantly in the

hypertrophy of the heart in CH exposed experimental animals. Enhanced protein synthesis has been viewed to be an adaptation of the organ to hypoxic stress. Further Fan et al. proposed that chronic hypoxia-induced cardiac remodelling and activation of proapoptotic genes may constitute an important mechanism for the future development of heart failure (Fan *et al*., 2005) (Rababa'h *et al*., 2018).

Corno *et al*. evaluated myocardial morphology in experimental animals exposed to chronic hypoxia for 2 weeks. They observed increased heart weight to body weight ratio indicating cardiac hypertrophy in chronic hypoxia exposure. Histopathological examination revealed hypertrophy of the right ventricular cardiomyocytes in response to pulmonary hypertension. However, the left ventricle appeared to be normal (Corno *et al*., 2004).

In the current study, cilnidipine treated chronic hypoxia-exposed rats demonstrated cardiosomatic index comparable to that of the control. Examination of H & E stained sections of the ventricles were comparable to control. In addition, the coronary artery demonstrated mild arteriosclerosis and dilatation. Thus cilnidipine ameliorated chronic hypoxia-induced cardiac remodelling. This effect of cilnidipine could be attributed to its ability to suppress sympathetic hyperactivity, increase NO, reduce oxidative stress and control the increase of arterial blood pressure induced by chronic hypoxia exposure (Takahara *et al*., 2002; Kobayashi *et al*., 2001). Cilnidipine has also been demonstrated to improve coronary microvascular remodelling (Kobayashi *et al*., 2001). This unique profile of cilnidipine makes it a potential drug against chronic hypoxia-induced cardiovascular pathophysiology.

The arterial wall is recognised as a dynamic structure capable of altering its size (Varnava, 1998). Under normal physiological conditions, arterial remodelling occurs as an adaptive response to changes in flow (Langille *et al*., 1996).

The heart is a highly aerobic organ and has the highest oxygen consumption. Hence regulation of coronary blood flow is crucial to maintain adequate perfusion to the heart. Short term regulation of coronary blood flow is achieved by autoregulation and alterations in perfusion pressure. Long term regulation of coronary blood flow involves vascular remodelling (Garcia-Canadilla *et al.*, 2019).

In the present study normalised wall index (NWI) of the coronary artery, a marker of arterial remodelling was significantly increased in chronic hypoxia. NWI was increased due to significantly reduced lumen size and thickened arterial wall. Further elastic artery and muscular artery also demonstrated an overall increase in wall thickness on histopathological examination. Normally, increased thickness of the arterial wall results from the multiplication of vascular smooth muscle cell (VSMC) and an increase in collagen. Mitogenic and fibrogenic growth factors like platelet-derived growth factor (PDGF) and endothelin-I and attenuated growth inhibitors like NO and transforming factor-β increase the proliferation of VSMC, collagen deposition and cross-linking thereby increasing arterial wall thickness (Zhao *et al.*, 2013).

Hypoxia has been thought to be a potent stimulus for the proliferation of VSMC. There is evidence indicating that chronic hypoxia promotes atherosclerosis, a process that occurs over decades and VSMC proliferation is considered to be an early event in the process of atherosclerosis (Schultz *et al.*, 2006). There are multiple factors implicated in chronic hypoxia-induced vascular remodelling. Sympathetic overactivity causes vascular remodelling that is independent of an increase in BP. It induces hypertrophy and proliferation of vascular smooth muscle cells (Fisher *et al.*, 2009). Oxidative stress (OS) is yet another important factor contributing to vascular remodelling (Fortuno *et al.*, 2005) (Azevedo *et al.*, 2016). The mechanism of oxidative stress-induced vascular remodelling is depicted in Figure 5.10.10. ROS stimulate the multiplication and hypertrophy of VSMC and fibroblasts, enhances the

expression of adhesion of molecules, activates matrix metalloproteinases, and induces the migration of VSMC. ROS also reduce the bioavailability of NO which in addition contributes to vascular remodelling (Campese *et al*., 2004). HIF-1 potentiates the growth-promoting effects of mitogens like PDGF, epidermal growth factor (EGF), fibroblast growth factor-2 (FGF-2) on VSMC (Schultz *et al*., 2006) thereby inducing vascular remodelling.

In cilnidipine treated chronic hypoxia-exposed rats, the cardiosomatic index was comparable with that of control. Histopathological examination revealed normal myocardium with a dilated coronary artery. Elastic artery and muscular artery demonstrated mild thickening of the tunica media. NWI of the coronary artery was reduced. Hence cilnidipine has demonstrated the potential to significantly alleviate chronic hypoxia-induced cardiovascular remodelling. **Probably this is one of the earliest studies reporting the impact of cilnidipine on cardiovascular remodelling in chronic hypoxia exposed experimental animals**. Again as previously stated the beneficial action of cilnidipine was because of its ability to control sympathetic overactivity due to its dual L/N type Ca^{2+} channel blocking actions, impact on cardiovascular hemodynamics, antioxidant property and by increasing the bioavailability of NO.
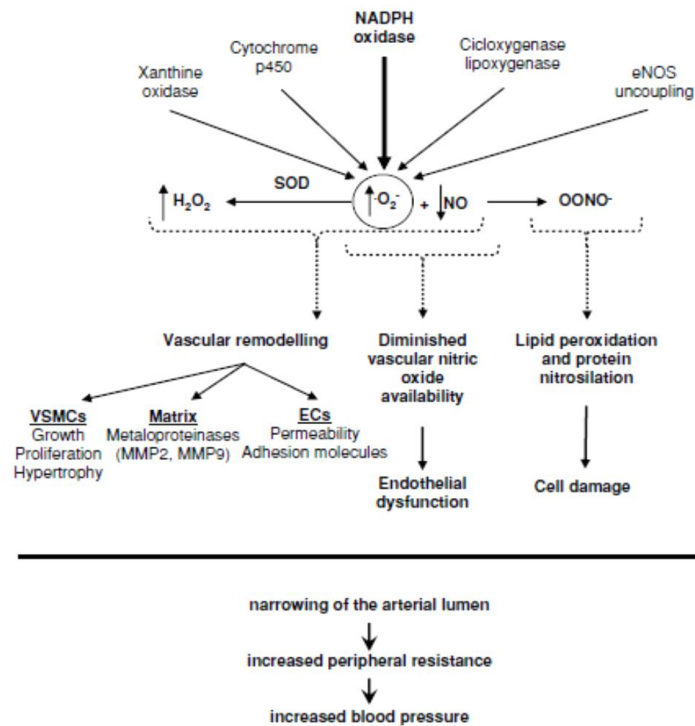
Figure 5.10.10: Oxidative stress and vascular remodelling

Source: Fortuno A, San Jose G, Moreno MU, Diez J, Zalba G. Oxidative stress and vascular remodelling. Exp Physiol. 2005; 90(4):457-62. DOI: 10.1113/expphysiol.2005.030098.

5.11 Histopathological examination of the lungs

5.11.1 RESULTS

- **Pulmonosomatic index (PSI)**
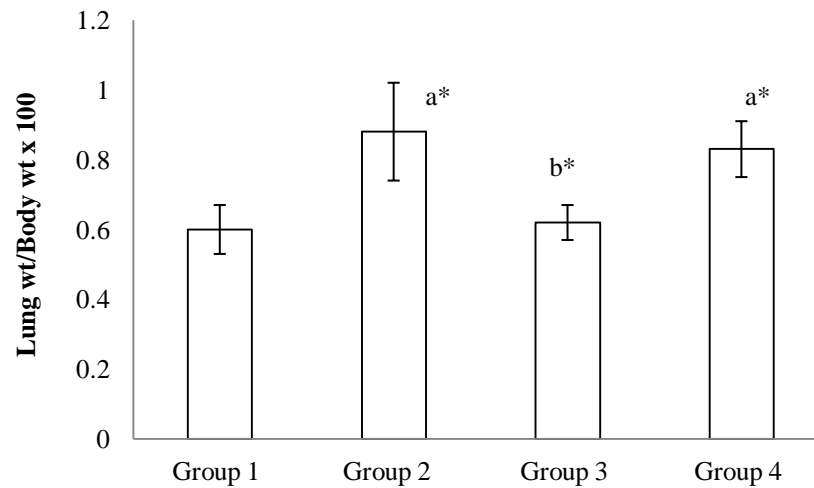
Figure 5.11.1 Comparison of pulmonosomatic index among groups
(n= 6 in each group)

Superscript a, b indicate a significant difference between groups. 'a' denotes comparison with Group 1, 'b' denotes comparison with group 2. *$p \leq 0.05$; Wt: weight

Figure 5.11.1 depicts the pulmonosomatic index (PSI) among groups. The PSI was significantly increased in group 2 (CH) and group 4 (CH+Cil) compared to group 1 (control).

- **Histopathological examination of the lungs**
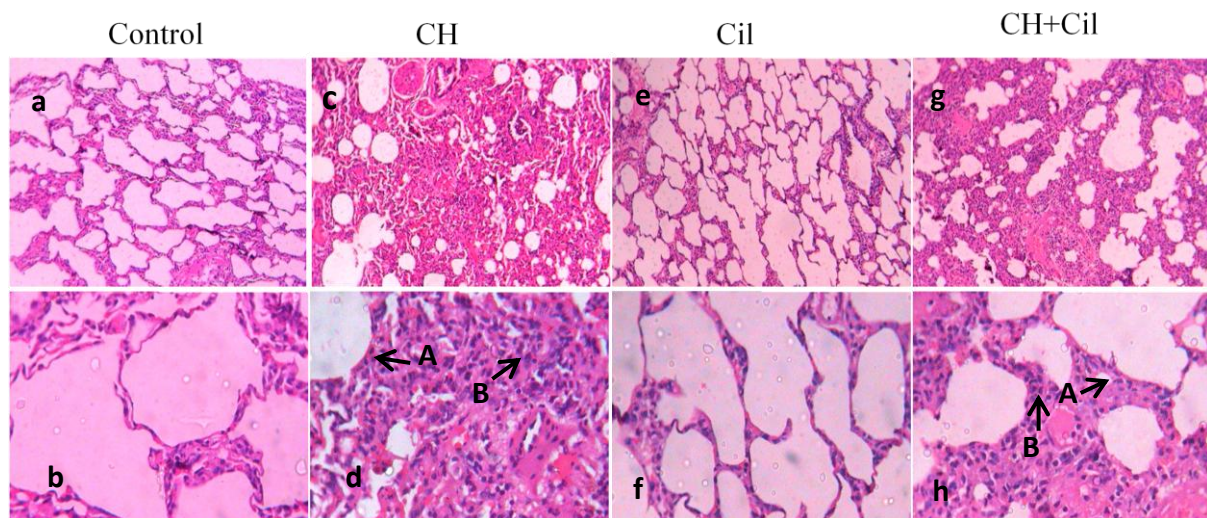
Figure 5.11.2 Photomicrograph of Lung stained with H & E from a) group 1 (control) (x10); b) group 1 (control) (x40); c) group 2 (CH) (x10); d) group 2 (CH) (x40); e) group 3 (Cil) (x10); f) group 3 (Cil) (x40); g) group 4 (CH+Cil) (x10); h) group 4 (CH+Cil) (x40).
A: Alveolar dilatation; B: mixed leucocytic inflammatory infiltrate.

Figure 5.11.2 depicts lung histopathological findings among groups.

Histopathology of the lungs in group 1 (control) and group 3 (Cil) shows normal lung parenchyma consisting of bronchi, bronchioles and thin-walled alveoli separated by intervening interstitial connective tissue containing small pulmonary capillaries.

Histopathology of the lungs in group 2 (CH) and group 4 (CH+Cil) demonstrated lung parenchyma consisting of bronchi, bronchioles and thin-walled alveoli separated by intervening interstitial connective tissue containing small pulmonary capillaries. Respiratory bronchioles were hyalinised. The alveolar spaces were dilated and filled with eosinophilic oedema fluid. The interstitial septa are thickened by oedema, congestion and haemorrhage and mixed inflammatory leucocytic infiltration.

5.11.2 DISCUSSION

Lungs are the first interface for O_2 between the environment and the body. Hence lungs could be one of the early organs to be impacted by alterations in the oxygen levels in the environment. In the present study, we evaluated the pulmonosomatic index and histopathology of the lungs in experimental animals exposed to chronic hypoxia and evaluated the effect of treatment with drug cilnidipine.

In the present study, the pulmonosomatic index (PSI) was increased in chronic hypoxia-exposed experimental animals irrespective of treatment with drug cilnidipine may be due to the accumulation of oedema fluid. Also, lung histopathology revealed dilated alveolar spaces filled with eosinophilic oedema fluid, thickened interstitial septa, congestion, haemorrhage and mixed inflammatory leucocytic infiltration in both groups of chronic hypoxia-exposed experimental animals irrespective of treatment with drug cilnidipine. Thus it appears that cilnidipine has no beneficial role in ameliorating chronic hypoxia-induced lung histopathological alterations.

Ciuclan *et al*. evaluated lung histopathology in experimental mice exposed to chronic hypoxia for 3 weeks. Examination of H & E stained sections of the lung revealed inflammatory infiltrate which are in accordance with the results of our study (Ciuclan *et al*., 2011).

Smita *et al*. evaluated lung histopathology in experimental animals exposed to sustained hypoxia for varying duration of 2 hrs, 4hrs, 8hrs, 12hrs, 16hrs, 24hrs and 48 hrs. 2 hrs and 4 hrs of hypoxia exposure revealed no significant alterations in the lung parenchyma. With further increase in the duration of exposure, there was a modest reduction of alveolar air space with moderately thickened inter-alveolar septa. With 24 hrs and 48 hrs of exposure,

lungs showed major histopathological changes with the build-up of oedema fluid and small alveolar space and severely thickened inter-alveolar septa (Smita *et al*., 2015).

Hunter *et al*. reported an increase in lung weight relative to body weight and thickening of the alveolar septa in rats and mice exposed to hypoxia (Hunter *et al*., 1974).

The results of Xu *et al*. are in accordance with the present study. They reported increased organosomatic index of the lung in experimental animals exposed to hypobaric hypoxia for 30 days (Xu *et al*., 2016).

5.12 Histopathological examination of the Liver

5.12.1 RESULTS

- **Hepatosomatic index (HSI)**
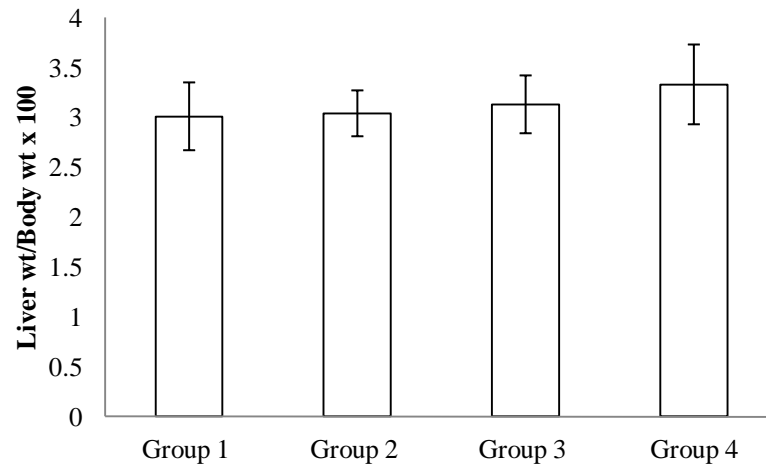
Figure 5.12.1 Comparison of hepatosomatic index among groups
(n= 6 in each group)

Figure 5.12.1 depicts a comparison of the hepatosomatic index among groups of experimental

animals. There were no significant differences in the hepatosomatic index between groups.

- **Histopathological examination of the liver**
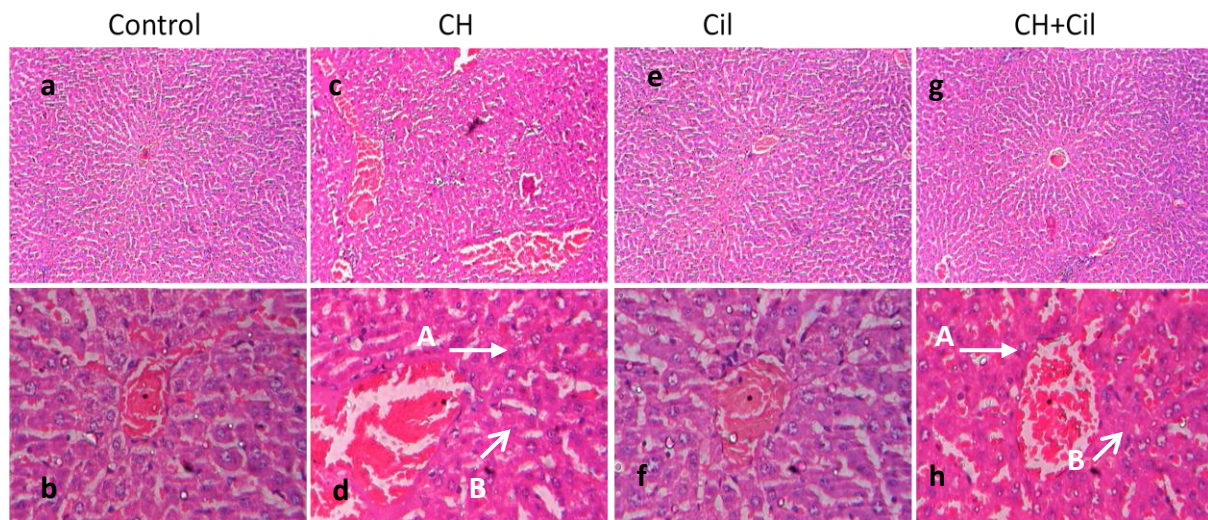
Figure 5.12.2 Photomicrograph of Liver stained with H & E from a) group 1 (control) (x10); b) group 1 (control) (x40); c) group 2 (CH) (x10); d) group 2 (CH) (x40); e) group 3 (Cil) (x10); f) group 3 (Cil) (x40); g) group 4 (CH+Cil) (x10), h); group 4 (CH+Cil) (x40).

A: distorted lobular architecture; B: swollen hepatocytes with ill-defined cell borders

Figure 5.12.2 represents a comparison of H & E stained sections of the liver among groups.

Histopathological examination of the liver in group 1 (control) and group 3 (Cil) gives a microscopic impression of a normal liver with normal hepatic architecture.

Group 2 (CH) and group 4 (CH+Cil) demonstrated hepatic parenchymal tissue with distorted '*Lobular*' architecture consisting of a central vein, hepatic plates, and portal areas containing branches of the bile duct, portal vein and hepatic artery. The hepatocytes appear to be little swollen having ill-defined cell borders with variation in cellular size and shape. The nuclei are large, more vesicular with variable size and shape and contain multiple 3 – 4 prominent nucleoli. The cytoplasm is vacuolated, microvesicular and appears more eosinophilic. There are foci of ballooning degeneration of hepatocytes in zone 3 (centrilobular) areas. The portal area appears mildly enlarged. The sinusoidal spaces are mildly widened. Central vein shows features of mild dilatation and congestion.

5.12.2 DISCUSSION

The liver is a unique organ with a dual blood supply receiving both oxygenated blood from the hepatic artery and a relatively deoxygenated blood from the portal vein. Hypoxia has been demonstrated to play a central role in the pathogenesis of several forms of liver diseases (Nath and Szabo, 2013). Hence hypoxia might have important consequences on liver histopathology.

Jusman *et al*. in their study did not observe any differences in the hepatosomatic index in experimental rats exposed to hypoxia for the varying duration (1, 3, 7 and 14 days) which is in accordance with the results of our study (Jusman *et al*., 2010).

Das *et al*. studied the histopathology of the liver in rats exposed to chronic sustained hypoxia for 21 days. They reported swollen hepatocytes, mild narrowing of the sinusoidal spaces and foci of necrosis and inflammatory reaction (Das *et al*., 2015; Das *et al*., 2019) which are in accordance with the results of the present study.

The results of Xu *et al*. are in accordance with the present study. They observed no significant changes in the hepatosomatic index in experimental animals exposed to hypobaric hypoxia for 30 days (Xu *et al*., 2016).

5.13 Effect of unilateral common carotid artery occlusion on brain histopathology in rats preconditioned to chronic hypoxia

5.13.1 RESULTS

Table 5.13.1: Comparison of neurological deficit score among groups of experimental animals (n=6 in each group)

Neurological Signs	Score (0-5 scale) for each rat	Total Score Group 1	Total Score Group 2	Total Score Group 3
Failure to extend affected forepaw fully	1	0	6	4
Circling movement	2	0	12	12
Falling	3	0	9	6
Did not walk spontaneously	4	0	8	4
Total Score	10x6 =60	0	35	26
Mean±SD		0	5.83 ± 3.43	4.33 ± 3.14*

Group 1, Sham-operated; group 2, Normoxia; group 3, Hypoxia preconditioned for 21 days. Mean $\pm$ SD values of group 2 and 3 are statistically significant from each other (*$p \leq 0.05$).

Table 5.13.1 depicts the comparison of neurological deficit score among groups. The score was lower in group 3 (hypoxia preconditioned) compared to group 2 (normoxia).
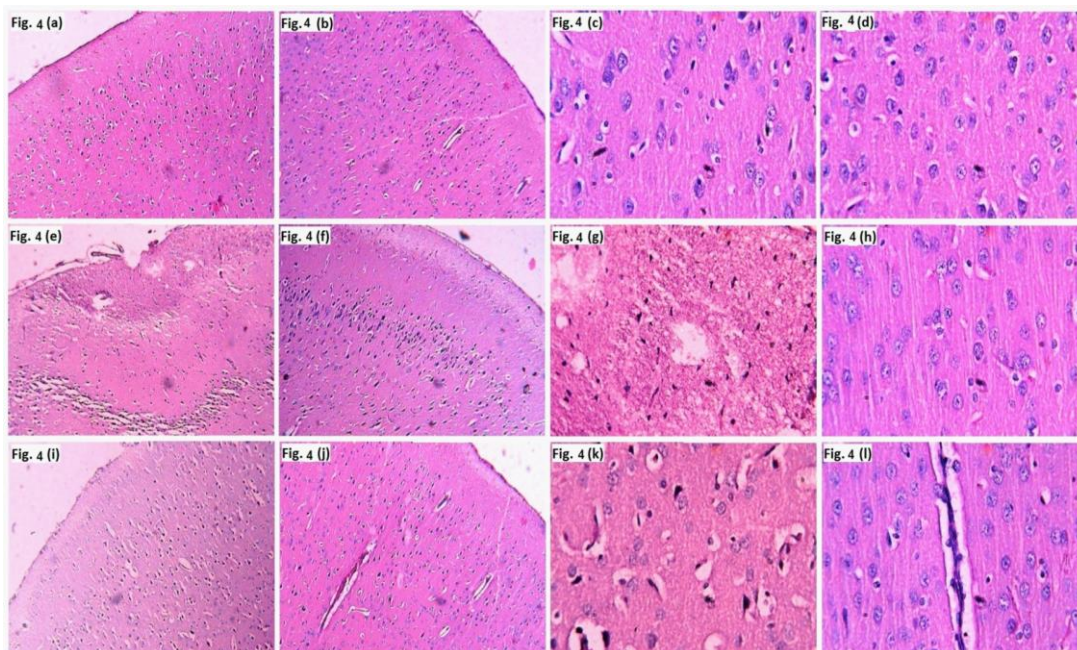
Figure 5.13.1: Photomicrograph of H&E stained section of left and right cerebral hemispheres showing (a) sham's left cerebral cortex (x10), (b)sham's right (x10), (c)sham's left cerebral cortex (x40), (d) sham's right cerebral cortex (x40), (e) normoxic left (occluded) cerebral cortex (x10), (f) normoxic right (non-occluded) (x10), (g) normoxic left (occluded) cerebral cortex (x40), (h) normoxic right (non-occluded) (x40), (i)hypoxia pre-treated left (occluded) cerebral cortex (x10), (j) hypoxia pre-treated right (occluded) (x10), (k) hypoxia pre-treated left (occluded) cerebral cortex (x40) and (l) hypoxia pre-treated right (non-occluded) (x40).

Figure 5.13.1 depicts H & E stained sections of the left and right cerebral hemispheres among groups.

Group 1 (Sham): H & E stained sections of the left and right cerebral hemisphere of the brain showed the normal cerebral cortex consisting of grey matter made of cell bodies of neurons along with their processes, neuroglia and blood vessels and white matter made up of bundles of axons. No pathology was noted in the group. The blood vessels appeared normal on both sides of the hemispheres.

Group 2 (normoxic with left-CCA occlusion): The grey matter of left cerebral cortex reveals a decrease in a number of pyramidal cells, stellate (granular) neurons appeared small, multipolar with pyknotic nuclei and vacuolated eosinophilic cytoplasm. Cerebrum demonstrated diffuse interstitial oedema and foci of wedge-shaped areas of cerebral infarcts. The junction between grey and white matter was blurred. The right cerebral hemisphere of the brain (non-occluded side) showed normal brain parenchyma.

Group 3 (hypoxia pre-conditioned with left-CCA occlusion): Grey matter of cerebral cortex revealed a decrease in number of pyramidal cells, small multipolar stellate (granular) neurons, with pyknotic nuclei and vacuolated eosinophilic cytoplasm having features of early neuronal damage (Red neurons) in the left cerebral hemisphere. Also, there were foci of interstitial oedema of the left cerebrum but without the features of cerebral ischemia which were observed in case of group 2 experimental animals. Besides these findings, blurring of the junction between grey and white matter was also noticed. The right cerebral hemisphere of the brain (non-occluded side) of group 3 rats showed normal brain parenchyma. Further, it has been observed dilated blood vessels, lined with prominent endothelial cells on the right side of the hemispheres.
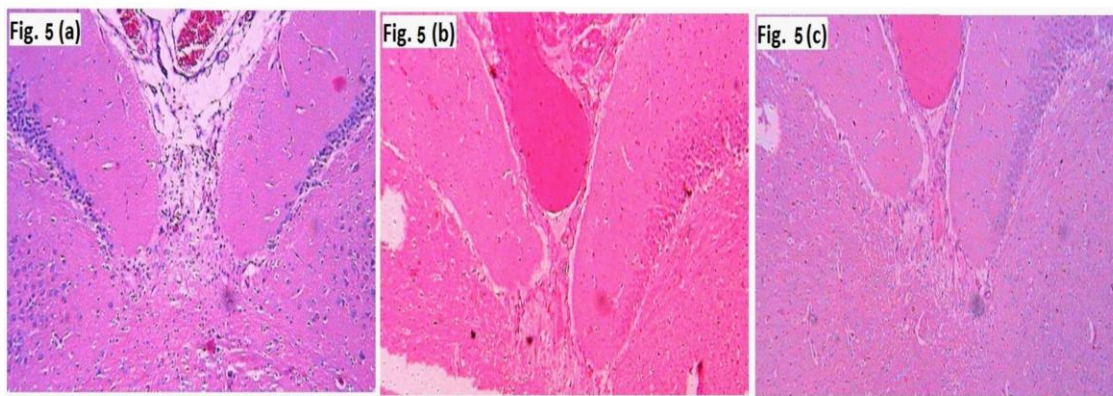
Figure 5.13.2: Photomicrograph of H & E stained sections of subcortical structures mainly the caudate nuclei, internal capsule, globus pallidus, substantia nigra and putamen of basal ganglia (x10) of (a); sham's left and right side, (b); normoxic left (occluded side) and right (nonoccluded) side and (c); chronic hypoxia pre-treated left (occluded side) and right (non-occluded) side.

Fig 5.13.2 depicts a comparison of H& E stained sections of subcortical structures among groups.

There were no changes in the subcortical structures of sham-operated rats. In the case of group 2 (normoxic), most of the caudate nuclei, internal capsule, globus pallidus, substantia nigra and putamen of basal ganglia showed small lacunar infarcts, whereas group 3 (hypoxia preconditioned) rats such small lacunar infarcts were found relatively less as compared to normoxic rats and showed pallor of staining and vacuolization of the white matter.

5.13.2 DISCUSSION

In the present study, the effect of unilateral common carotid artery occlusion on brain histopathology in hypoxia preconditioned rats was assessed. Following left CCA occlusion the H&E stained sections of the right and left cerebral cortex and subcortical structures were studied in sham-operated, normoxic and hypoxia preconditioned experimental animals.

There was a reduction in brain oedema and a smaller infarct volume in animals preconditioned to chronic hypoxia. This study demonstrates that rats preconditioned to chronic hypoxia could have reduced brain injury after focal ischemia. These observations

were further supported by neurological deficit scores (Das *et al*., 2018). The reduced brain injury in hypoxia preconditioned experimental animals may be because the brain has already initiated adaptive mechanisms during hypoxia exposure and hence could tolerate ischemia better (Rybnikova and Samoilov, 2015).

The brain requires a continuous supply of oxygen. In the event of any hypoxic stress, the blood flow and oxygen supply to the brain are maintained at the cost of the visceral organs. The experimental rats exposed to chronic normobaric hypoxia have demonstrated increased brain capillary density and decreased the intercapillary distance that is completed by 3 weeks of hypoxia exposure (Xu and LaManna, 2006).

Although further studies are needed to establish cerebrovascular pathophysiology in chronic hypoxia preconditioned experimental animals, yet it may be considered as a possible protective strategy to ameliorate ischemia/reperfusion brain injury from cerebral focal ischemia or stroke.

CHAPTER VI
SUMMARY AND CONCLUSION

6.1 SUMMARY

Most healthy organs live in 3-6% oxygen and conditions lower than 3% oxygen is referred to as hypoxia. Hypoxia could be acute or chronic and sustained or intermittent. Sustained hypoxia is observed in chronic obstructive pulmonary diseases (COPD), cystic fibrosis and any lung parenchymal diseases impairing alveolar gas exchange. Intermittent hypoxia is associated with obstructive sleep apnea (OSA), central hypoventilation syndrome. There is evidence of adverse cardiometabolic consequences in patients experiencing hypoxia. The hypoxia signalling molecules and alterations in the autonomic nervous balance may have a prime role in the initiation, development and progression of cardiometabolic disorders. Cilnidipine, a dual L/N type calcium channel blocker (CCB) is popular as an effective antihypertensive agent and its antioxidant actions are being widely recognised. This pharmacological profile of cilnidipine could open up new possibilities of its role in chronic hypoxia-induced cardiovascular pathophysiology.

The present study was undertaken to evaluate the cardiovascular autonomic functions and hypoxia signalling molecules after chronic hypoxia exposure and their impact on cardiovascular remodelling and glucose homeostasis and the role of cilnidipine, a dual L/N type calcium channel blocker. Further, the impact of unilateral common carotid artery occlusion on brain histopathology in experimental animals preconditioned to chronic hypoxia was assessed.

We hypothesized that chronic sustained hypoxia impacts glucose homeostasis induces cardiovascular remodelling that may be influenced by treatment with cilnidipine, a dual L/N type calcium channel blocker.

The study involved twenty-four adult male Wistar strain albino rats (*Rattus Norvegicus*), randomly allocated into four groups. Group 1: control; group 2: chronic hypoxia (10% O_2, 90% N_2) exposure for 21 days; group 3: cilnidipine treated (2.0mg/kg/day); group 4: chronic hypoxia exposed (10% O_2 and 90% N_2) and cilnidipine treated (2.0mg/kg/day) for 21 days. All the experimental animals were subjected to gravimetry and % body weight gain was calculated after 21 days. Haematological parameters like RBC count (million cells/mm^3 of blood), Hb (g/dl) and Hct (%) were estimated. The cardiovascular autonomic balance was assessed by HRV analysis. Hemodynamic parameters like heart rate and blood pressure were recorded. Oxidative stress and antioxidant defence were assessed by estimating MDA, vitamin C, vitamin E in the serum and MDA in heart, lung and liver tissue homogenate. Hypoxia signalling molecules like VEGF, NOS3 and NO were estimated in the serum. Glucose homeostasis was evaluated by estimation of fasting plasma glucose, oral glucose tolerance test (OGTT), fasting serum insulin. HOMA-IR was calculated as an index of insulin resistance. Cardiovascular remodelling was studied by calculation of cardiosomatic index, and histopathological examination of H & E stained sections of the ventricles, intramyocardial coronary artery, elastic artery and muscular artery. Further, the normalised wall index (NWI), an index of arterial remodelling was calculated for coronary artery. Lipid profile was assessed. Histopathological examination of the lung and liver were also done.

To study the impact of unilateral common carotid artery (CCA) occlusion on brain pathophysiology in chronic hypoxia preconditioned rats, the experimental animals were randomly allocated to one of the three groups: group 1: sham-operated; group 2: normoxia (21% oxygen), left CCA occlusion for 75 minutes and subsequent reperfusion for 12 hours; group 3: Hypoxia (10% O_2) preconditioned for 21 days prior to left CCA occlusion for 75 minutes and reperfusion for 12 hours. The experimental rats were assessed for neurologic

deficits before sacrifice. After reperfusion for 12 hours, the experimental animals were sacrificed and the brain was dissected out and subjected to histopathological examination.

Chronic hypoxia resulted in lower % body weight gain, elevated hematocrit. HRV analysis revealed sympathetic overactivity and shift in the sympathovagal balance. Assessment of cardiovascular hemodynamics showed decreased heart rate, increased mean arterial pressure (MAP). There were disturbances in oxidant-antioxidant balance indicating oxidative stress. Estimation of hypoxia signalling molecules revealed markedly elevated VEGF, NOS3, and decreased NO. Glucose homeostasis was disturbed with increased fasting plasma glucose and HOMA-IR. HOMA-IR and fasting plasma glucose were positively correlated with the LF/HF ratio. There were features suggestive of cardiovascular remodelling. Further, NWI of the coronary artery was positively correlated with LF/HF ratio, heart tissue MDA, HOMA-IR and VEGF. These findings suggest a possible link between hypoxia signalling, sympathetic overactivity, oxidative stress in cardiovascular remodelling and altering the glucose homeostasis on chronic hypoxia exposure.

Cilnidipine treatment was able to 1) control sympathetic overactivity 2) reduce MAP 3) decrease oxidative stress 4) increase the bioavailability of NO 5) improve glucose homeostasis and 6) ameliorate cardiovascular remodelling resulting from chronic hypoxia exposure. These effects of cilnidipine could be attributed to its dual L/N type calcium channel blocking action and partly to its antioxidant property. Thus the results of the present study suggest a possible use of cilnidipine as an adjunct therapy against hypoxia-related pathophysiology.

We studied the effect of unilateral left common carotid artery occlusion on brain histopathology in rats preconditioned to chronic hypoxia for 21 days. We observed a reduction in brain oedema, a smaller infarct volume and lesser neurological deficits in

experimental animals preconditioned to chronic hypoxia. This study demonstrates that rats preconditioned to chronic hypoxia could have reduced brain injury after focal ischemia as compared to normoxic (hypoxia unexposed) experimental animals. Further studies are needed to delineate cerebrovascular pathophysiology in chronic hypoxia preconditioned experimental animals.

6.2 CONCLUSION:

The present study demonstrates that chronic hypoxia exposure is accompanied by altered hypoxia signalling mechanism, impaired oxidant/antioxidant balance and shift in the sympathovagal balance towards the increased sympathetic activity. These alterations further proceed to impact glucose homeostasis and induce cardiovascular remodelling. Cilnidipine, owing to its dual L/N type calcium channel blocking properties probably has a beneficial role in improving chronic hypoxia-induced alterations in glucose homeostasis, cardiovascular remodelling suggesting a possible therapeutic use of cilnidipine against hypoxia-related pathophysiology.

GRAPHICAL ABSTRACT
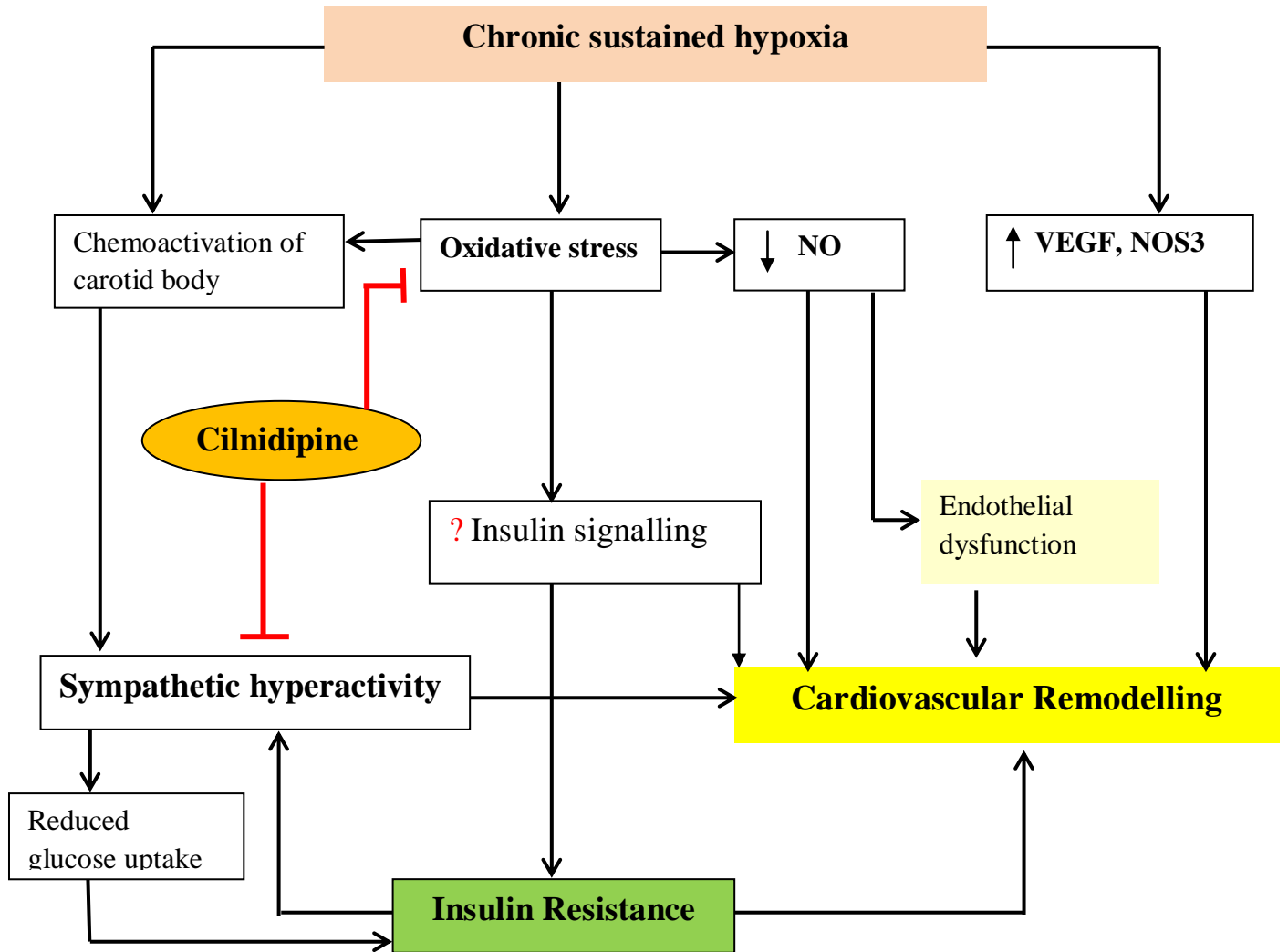
- **Limitations and future perspectives of the study**

Drug induced alterations in the pattern of DNA sequencing in response to hypoxia needs to be assessed by real time PCR.

BIBLIOGRAPHY

- Adeoye OO, Bouthors V, Hubbell MC, Williams JM, Pearce WJ. VEGF receptors mediate hypoxic remodelling of adult ovine carotid arteries. J Appl Physiol (1985). 2014; 117(7): 777-87. DOI:10.1152/japplphysiol.00012.2014.

- Allain CC, Poon LS, Chan CS, Richmond W, Fu PC. Enzymatic determination of total serum cholesterol. Clin Chem. 1974; 20(4):470-5.

- Arifin WN, Zahiruddin WM. Sample size calculation in animal studies using the resource equation approach. Malays JMed Sci.2017;24(5):101-105. doi: 10.21315/mjms2017.24.5.11.

- Ayala A, Munoz MF, Arguelles S. Lipid peroxidation: production, metabolism, and signalling mechanisms of malondialdehyde and 4-hydroxy-2-nonenal. Oxid Med Cell Longev. 2014; 2014: 360438. doi: 10.1155/2014/360438.

- Azevedo PS, Polegato BF, Minicucci MF, Paiva SA, Zornoff LA. Cardiac remodelling: Concepts, Clinical Impact, Pathophysiological Mechanisms and Pharmacologic treatment. Arq Bras Cardiol. 2016; 106 (1): 62-69. Doi: 10.5935/abc.20160005.

- Bagali S, Hadimani GA, Biradar MS, Das KK. Introductory chapter: Primary concept of hypoxia and anoxia. In: Das KK and Biradar MS. ed(s). Hypoxia and Anoxia. 1st ed. UK: Intech Open; 2018. p. 3-11.ISBN: 978-1-78984-828-1.

- Baron AD, Laakso M, Brechtel G, Hoit B, Watt C, Edelman SV. Reduced postprandial skeletal muscle blood flow contributes to glucose intolerance in human obesity. J Clin Endocrinol Metab. 1990; 70(6): 1525-33. DOI:10.1210/jcem-70-6-1525

- Barton CH, Ni Z, Vaziri ND. Blood pressure response to hypoxia: role of nitric oxide synthase. Am J Hypertens. 2003; 16(12): 1043-8. doi:10.1016/j.amjhyper.2003.07.021.

- Beeghly-Fadiel A, Shu XO, Lu W, Long J, Cai Q, Xiang YB, Zheng Y, Zhao Z, Gu K, Gao YT, Zheng W. Genetic variation in VEGF family genes and breast cancer risk: a report from

the Shanghai breast cancer genetics study. Cancer Epidemiol Biomarkers Prev. 2011; 20(1):33-41. Doi: 10.1158/1055-9965.

- Bhatia M, Karlenius TC, Di Trapani G, Tonissen KF. The interaction between redox and hypoxic signalling pathways in the dynamic oxygen environment of cancer cells. In Toniseen K, ed. Carcinogenesis. United Kingdom: Intech Open; 2013.p. 125-152 DOI: 10.5772/55185.

- Birben E, Sahiner UM, Sackesen C, Erzurum S, Kalayci O. Oxidative stress and antioxidant defence. World Allergy Organ J. 2012; 5(1): 9-19. doi: 10.1097/WOX.0b013e3182439613.

- Bisgard GE. Carotid body mechanism in acclimatization to hypoxia. Respir Physiol. 2000; 121(2-3):237-46.

- Borghetti G, von Lewinski D, Eaton DM, Sourij H, Houser SR, Wallner M. Diabetic Cardiomyopathy: Current and Future Therapies. Beyond Glycemic Control. Front Physiol. 2018; 9:1514. doi:10.3389/fphys.2018.01514.

- Bowe JE, Franklin ZJ, Hauge-Evans AC, King AJ, Persaud SJ, Jones PM. Metabolic phenotyping guidelines: assessing glucose homeostasis in rodent models. J Endocrinol 2014; 222(3): G13-25.

- Bryan-Brown CW. Blood flow to organs: parameters for function and survival in critical illness. Crit Care Med 1988; 16(2): 170-8.

- Buege JA, Aust SD. Microsomal lipid peroxidation. Methods Enzymol 1978; 52: 302-10. DOI:10.1016/s0076-6879(78)52032-6.

- Calbet JA. Chronic hypoxia increases blood pressure and noradrenaline spillover in healthy humans. J Physiol. 2003;551 (1): 379-386. DOI: 10.1113/jphysiol.2003.045112.

- Campese VM, Ye S, Zhong h, Yanamadala V, Ye Z, Chiu J. Reactive oxygen species stimulate central and peripheral sympathetic nervous system activity. Am J Physiol Heart Circ Physiol. 2004; 287(2): H695-703. DOI:10.1152/ajpheart.00619.2003.

- Cao R, Zhao X, Li S, Zhou H, Chen W, Ren L, Zhou X, Zang H, Shi R. Hypoxia induces dysregulation of lipid metabolism in HepG2 cells via activation of HIF-2α. Cell Physiol Biochem. 2014; 34(5):1427-41. doi: 10.1159/000366348.

- Carnagarin R, Matthews VB, Herat LY, Ho JK, Schlaich P. Autonomic regulation of glucose homeostasis: a specific role for sympathetic nervous system activation. Current Diabetes Reports 2018; 18: 107. Doi.org/10.1007/s11892-018-1069-2.

- Ceriello A, Motz E. Is oxidative stress the pathogenic mechanism underlying insulin resistance, diabetes and cardiovascular disease? The common soil hypothesis revisited. Arterioscler Thromb Vasc Biol. 2004;24:816-823.

- Chandra KS, Ramesh G. The fourth-generation calcium channel blocker: cilnidipine. Indian Heart J. 2013; 65(6):691-695. doi: 10.1016/j.ihj.2013.11.001.

- Chun YS, Kim MS, Park JW. Oxygen-dependent and independent regulation of HIF-1alpha. J Korean Med Sci. 2002; 17(5): 581-8. DOI:10.3346/jkms.2002.17.5.581.

- Ciuclan L, Bonneau O, Hussey M, Duggan N, Holmes AM, Good R, Stringer R, Jones P, Morrell NW, Jarai G, Walker C, Westwick J, Thomas M. A novel murine model of severe pulmonary hypertension. Am J Respir Crit Care Med. 2011; 184 (10):1171-82. doi: 10.1164/rccm.201103-0412OC.

- Clanton TL. Hypoxia-induced reactive oxygen species formation in skeletal muscle. J Appl Physiol. 2007; 102: 2379-2388.

- Cohn JN, Ferrari R, Sharpe N. Cardiac remodelling-concepts and clinical implications: A consensus paper from an international forum on cardiac remodelling. J Am Coll Cardiol 2000; 35: 569 – 8. https://doi.org/10.1016/S0735-1097(99)00630-0.

- Conde SV, Sacramento JF, Guarino MP, Gonzalez C, Obeso A, Diogo LN, Monteiro EC, Ribeiro MJ. Carotid body, insulin, and metabolic diseases: unravelling the links. Front Physiol. 2014; 5: 418. doi: 10.3389/fphys.2014.00418

- Corno AF, Milano G, Morel S, Tozzi P, Genton CY, samaja M, von Segesser LK. Hypoxia: unique myocardial morphology? J Thorac Cardiovasc Surg. 2004; 127(5):1301-8. DOI: 10.1016/j.jtcvs.2003.06.012.

- Corno AF, Milano G, Samaja M, Tozzi P, von Segesser LK. Chronic hypoxia: a model for cyanotic congenital heart defects. J Thorac Cardiovasc Surg. 2002; 124(1): 105-12. doi:10.1067/mtc.2002.121302.

- Cortas NK, Wakid NW. Determination of inorganic nitrate in serum and urine by a kinetic cadmium-reduction method. Clin Chem. 1990; 36(8 Pt 1): 1440-3.

- Das KK, Honnutagi R, Mullur L, Reddy RC, Das S, Majid DSA, Biradar MS. Heavy metals and low oxygen microenvironment-Its impact on liver metabolism and dietary supplementation. In: Watson RR, Preedy VR, ed(s). Dietary Interventions in Liver Disease: Foods, Nutrients and Dietary Supplements. 1st ed. United Kingdom: Academic Press Elsevier; 2019. p. 315-329. ISBN: 978-0-12-814466-4.

- Das KK, Jargar JG, Saha S, Yendigeri SM, Singh SB. α-tocopherol supplementation prevents lead acetate and hypoxia-induced hepatic dysfunction. Indian J Pharmacol. 2015; 47(3): 285-91. doi: 10.4103/0253-7613.157126.

- Das KK, Saha S. Hypoxia, Lead Toxicities and Oxidative Stress: Cell Signaling, Molecular Interactions and Antioxidant (Vitamin C) Defense. Current Signal Transduction Therapy 2014; 9 (3): 113-122. Doi:10.2174/1574362410666150225232258.

- Das KK, Yendigeri SM, Patil BS, Bagoji IB, Reddy RC, Bagali S, Biradar MS, Saha S. Subchronic hypoxia pretreatment on brain pathophysiology in unilateral common carotid

artery occluded albino rats. Indian J Pharmacol. 2018; 50 (4): 185-191. doi: 10.4103/ijp.IJP_312_17.

- Das KK, Nemagouda SR, Patil SG, Saha S. Possible hypoxia signalling induced alteration of glucose homeostasis in rats exposed to chronic intermittent hypoxia - Role of antioxidant (vitamin C) and Ca^{2+} channel blocker (cilnidipine). Current Signal Transduction Therapy 2016; 11: 49-55.

- Debevec T, Millet GP, Pialoux V. Hypoxia-Induced Oxidative Stress Modulation with Physical Activity. Front Physiol. 2017; 8: 84. Published 2017 Feb 13. doi:10.3389/fphys.2017.00084.

- Debevec T, Pialoux V, Mekjavic IB, Eiken O, Mury P, Millet GP. Moderate exercise blunts oxidative stress induced by normobaric hypoxic confinement. Med Sci Sports Exerc. 2014; 46(1): 33-41. doi: 10.1249/MSS.0b013e31829f87ef.

- Dorsa Pontes HB, Viera Pontes JCD, E de Azevedo Neto, Zangari AH, Cunha Miranda JV, Moreira Gomes O. Cardiac remodelling: General aspects and mechanisms. Curr Res Cardiol 2016; 3(3):79-82.

- Dosek A, Ohno H, Acs Z, Taylor AW, Radak Z. High altitude and oxidative stress. Respir Physiol Neurobiol. 2007; 158 (2-3): 128-31. DOI:10.1016/j.resp.2007.03.013

- Dulak J, Jozkowicz A. Regulation of vascular endothelial growth factor synthesis by NO: facts and controversies. Antioxid Redox Signal. 2003; 5 (1): 123-32. DOI:10.1089/152308603321223612.

- Dweik RA. Nitric oxide, hypoxia, and superoxide: the good, the bad, and the ugly! Thorax 2005; 60: 265-267.

- El Guerrab A, Cayre A, Kwiatkowski F, Privat M, Rossignol JM, Rossignol F, Penault-Llorca F, Bignon YJ. Quantification of hypoxia-related gene expression as a potential

approach for clinical outcome prediction in breast cancer. PLoS ONE 2017;12(4):e0175960. Doi.0rg/10.1371/journal.pone.0175960.

- Essop MF. Cardiac metabolic adaptations in response to chronic hypoxia. J Physiol. 2007; 584 (Pt 3):715-26. DOI:10.1113/jphysiol.2007.143511.

- Faiss R, Pialoux V, Sartori C, Faes C, Deriaz O, Milet GP. Ventilation, oxidative stress, and nitric oxide in hypobaric versus normobaric hypoxia. Med Sci Sports Exerc. 2013; 45(2): 253-60. doi: 10.1249/MSS.0b013e31826d5aa2.

- Fan C, Iacobas DA, Zhou D, Chen Q, Lai JK, Gavrialov O, Haddad GG. Gene expression and phenotypic characterization of mouse heart after chronic constant or intermittent hypoxia. Physiol Genomics. 2005; 22 (3): 292-307. Doi: 10.1152/physiolgenomics.00217.2004.

- Fan L, Yang Q, Xiao XQ, Grove KL, Huang Y, Chen ZW, Furnary A, He GW. Dual actions of cilnidipine in human internal thoracic artery: inhibition of calcium channels and enhancement of endothelial nitric oxide synthase. J Thorac Cardiovasc Surg. 2011; 141(4): 1063-9. doi: 10.1016/j.jtcvs.2010.01.048.

- Fernandez-Aguera MC, Gao L, Gonzalez-Rodrigues P, Pintado CO, Arias-Mayenco, Garcia-Flores P et al. Oxygen sensing by arterial chemoreceptors depends on mitochondrial complex I signalling. Cell Metab. 2015; 22 (5): 825-37. DOI:10.1016/j.cmet.2015.09.004

- Fisher JP, Young CN, Fadel PJ. Central sympathetic overactivity: maladies and mechanisms. Auton Neurosci. 2009; 148 (1-2):5–15. doi:10.1016/j.autneu.2009.02.003.

- Flaa A, Aksnes TA, Kjeldsen SE, Eide I, Rostrup M. Increased sympathetic reactivity may predict insulin resistance: an 18-year follow- up study. Metabolism 2008; 57(10):1422-7. doi: 10.1016/j.metabol.2008.05.012.

- Forstermann U, Sessa WC. Nitric oxide synthases: regulation and function. Eur Heart J. 2012; 33(7): 829-37. DOI:10.1093/eurheartj/ehr304.

- Fortuno A, San Jose G, Moreno MU, Diez J, Zalba G. Oxidative stress and vascular remodelling. Exp Physiol. 2005; 90(4): 457-62. DOI:10.1113/expphysiol.2005.030098.

- Fossati P, Prencipe L. Serum triglycerides determined colorimetrically with an enzyme that produces hydrogen peroxide. Clin Chem. 1982; 28(10): 2077-80.

- Friedewald WT, Levy RI, Fredrickson DS. Estimation of the concentration of low-density lipoprotein cholesterol in plasma, without the use of the preparative ultracentrifuge. Clin Chem. 1972; 18(6): 499-502.

- Garcia-Canadilla P, de Vries T, Gonzalez-Tendero A, Bonnin A, Gratacos E, Crispi F, et al. Structural coronary artery remodelling in the rabbit fetus as a result of intrauterine growth restriction. Plos One 2019; 14(6): e0218192. doi.org/10.1371/journal.pone.0218192.

- Giaccia AJ, Simon MC, Johnson R. The biology of hypoxia: the role of oxygen sensing in development, normal function, and disease. Genes Dev. 2004;18(18):2183-2194. doi: 10.1101/gad.1243304.

- Green LC, Wagner DA, Glogowski J, Skipper PL, Wishnok JS, Tannenbaum SR. Analysis of nitrate, nitrite and [15N] nitrate in biological fluids. Anal Biochem. 1982; 126(1): 131-8. DOI:10.1016/0003-2697(82)90118-x.

- Haase VH. Regulation of erythropoiesis by hypoxia-inducible factors. Blood Rev. 2013; 27(1): 41-53. doi: 10.1016/j.blre.2012.12.003.

- Han HS, Kang G, Kim JS, Choi BH, Koo SH. Regulation of glucose metabolism from a liver-centric perspective. Exp Mol Med. 2016; 48(3):e218. doi:10.1038/emm.2015.122.

- Hanaa Ali Hassan Mostafa Abd El-Aal. Lipid Peroxidation End-Products as a Key of Oxidative Stress: Effect of Antioxidant on Their Production and Transfer of Free Radicals. In: Catala A, ed. Lipid Peroxidation. UK: IntechOpen: 2012. p. 63-88. DOI: 10.5772/45944.

- Harada N, Ohnaka M, Sakamoto S, Niwa Y, Nakaya Y. Cilnidipine improves insulin sensitivity in the Otsuka Long-Evans Tokushima Fatty rat, a model of spontaneous NIDDM. Cardiovasc Drugs Ther. 1999; 13(6): 519-23.

- Harteveld AA, Denswil NP, Van Hecke W, Kuijf HJ, Vink A, Spliet WGM et al. Data on vessel wall thickness measurements of intracranial arteries derived from the human circle of Willis specimens. Data Brief 2018; 19: 6-12. DOI:10.1016/j.dib.2018.04.116.

- Higuchi Y, Otsu K, Nishida K, Hirotani S, Nakayama H, Yamaguchi O, Matsumura Y, Ueno H, Tada M, Hori M. Involvement of reactive oxygen species-mediated NF-kappa β activation in TNF-alpha-induced cardiomyocyte hypertrophy. J Mol Cell Cardiol. 2002; 34(2):233-40. DOI:10.1006/jmcc.2001.1505.

- Hirooka Y, Kishi T, Sakai K, Takeshita A, Sunagawa K. Imbalance of central nitric oxide and reactive oxygen species in the regulation of sympathetic activity and neural mechanisms of hypertension. Am J Physiol Regul Integr Comp Physiol. 2011; 300(4): R818-26. doi: 10.1152/ajpregu.00426.2010.

- Hishikawa Keiichi, Takase O, Idei M, Fujito T. Comparison of antioxidant activity of cilnidipine and amlodipine. Kidney International 2009; 76: 230-231. doi:10.1152/japplphysiol.01298.2006.

- Huang HY, Appel LJ, Croft KD, Miller ER 3rd, Mori TA, Puddey IB. Effects of vitamin C and vitamin E on in vivo lipid peroxidation: results of a randomised controlled trial. Am J Clin Nutr. 2002; 76(3):549-55.

- Hunter C, Barer GR, Shaw JW, Clegg EJ. Growth of the heart and lungs in hypoxic rodents: a model of human hypoxic disease. Clin Sci Mol Med. 1974; 46(3): 375-91.

- Hunter JJ and Chien KR. Signalling pathways for cardiac hypertrophy and failure. N Engl J Med 1999; 341:1276–1283.

- Hurrle S, Hsu WH. The aetiology of oxidative stress in insulin resistance. Biomed J. 2017;40(5):257–262. doi:10.1016/j.bj.2017.06.007

- Ito H, Adachi S, Tamamori M, Fujisaki H, Tanaka M, Lin M et al. Mild hypoxia induces hypertrophy of cultured neonatal rat cardiomyocytes: a possible endogenous endothelin-1-mediated mechanism. J Mol Cell Cardiol 1996; 28:1271–1277.

- Janus A, Szahidewicz-Krupska E, Mazur G, Doroszko A. Insulin Resistance and Endothelial Dysfunction Constitute a Common Therapeutic Target in Cardiometabolic Disorders. Mediators Inflamm. 2016;2016:3634948. doi:10.1155/2016/3634948.

- Jargar JG, Hattiwale SH, Das S, Dhundasi SA, Das KK. A modified simple method for determination of serum α-tocopherol (vitamin E). J Basic Clin Physiol Pharmacol. 2012; 23(1): 45-8. doi: 10.1515/jbcpp-2011-0033.

- Jiang BH, Semenza GL, Bauer C, Marti HH. Hypoxia-inducible factor 1 levels vary exponentially over a physiologically relevant range of O2 tension. Am J Physiol 1996;271: C1172–C1180. DOI:10.1152/ajpcell.1996.271.4.C1172.

- Julian RJ. The Response of the Heart and Pulmonary Arteries to Hypoxia, Pressure, and Volume. A Short Review. Poult Science 2007; 86:1006–1011.

- Julius S, Gybbrandsson T, Jamerson K, Andersson O. The interconnection between sympathetic, microcirculation, and insulin resistance in hypertension. Blood Press.1992; 1(1): 9-19.

- Jun J, Savransky V, Nanayakkara A, Bevans S, Li J, Smith PL, Polotsky VY. Intermittent Hypoxia has organ-specific effects on oxidative stress. Am J Physiol Regul Integr Comp Physiol. 2008; 295 (4): R1274-81. doi: 10.1152/ajpregu.90346.2008.

- Jusman SW, Halim A, Wanandi SI, Sadikin M. Expression of hypoxia-inducible factor-1alpha (HIF-1alpha) related to oxidative stress in liver of rat-induced by systemic chronic normobaric hypoxia. Acta Med Indones.2010; 42(1):17-23.

- Kaab S, Miguel-Velado E, Lopez-Lopez JR, Perez-Garcia MT. Downregulation of Kv3.4 channels by chronic hypoxia increases acute oxygen sensitivity in rabbit carotid body. J Physiol. 2005; 566 (Pt 2):395-408. DOI:10.1113/jphysiol.2005.085837.

- Kacimi R, Richalet JP, Corsin A, Abousahl I, Crozatier B. Hypoxia-induced downregulation of beta-adrenergic receptors in rat heart. J Appl Physiol. 1985; 73(4): 1377-82. DOI:10.1152/jappl.1992.73.4.1377.

- Kammer AR, Orcezwska JI, O'Brien KM. Oxidative stress is transient and tissue specific during cold acclimation of three spine stickleback. The Journal of Experimental Biology 2011; 214: 1248-1256.

- Kang J, Li Y, Hu K, Lu W, Zhou X, Yu S, Xu L. Chronic intermittent hypoxia versus continuous hypoxia: Same effect on hemorheology? Clin Hemorheol Microcirc. 2016; 63(3):245-55. doi: 10.3233/CH-151973.

- Kijima S, Shida M, Yokoyama H. Comparison between cilnidipine and amlodipine besilate with respect to proteinuria in hypertensive proteinuria in hypertensive patients with renal diseases. Hypertens Res 2004; 27:379-385.

- Kimura H, Esumi H. Reciprocal regulation between nitric oxide and vascular endothelial growth factor in angiogenesis. Acta Biochim Pol. 2003; 50 (1): 49-59. DOI: 035001049.

- Kobayashi N, Mori Y, Mita S, Nakano S, Kobayashi T, Tsubokou Y, Matsuoka H. Effects of cilnidipine on nitric oxide and endothelin-1 expression and extracellular signal-regulated kinase in hypertensive rats. Eur J Pharmacol. 2001; 422 (1-3):149-57. DOI: 10.1016/s0014-2999(01)01067-6.

- Kontos A, Lushington K, Martin J, Schwarz Q, Green R, Wabnitz D et al. Relationship between Vascular Resistance and Sympathetic Nerve Fiber Density in Arterial Vessels in Children With Sleep Disordered Breathing. J Am Heart Assoc. 2017;6(7):e006137. doi:10.1161/JAHA.117.006137.

- Kwon SH, Pimentel DR, Remondino A, Sawyer DB, Colucci WS. H(2)O(2) regulates cardiac myocyte phenotype via concentration-dependent activation of distinct kinase pathways. J Mol Cell Cardiol. 2003; 35(6):615-21.

- Lahiri S, Roy A, Baby SM, Hoshi T, Semenza GL, Prabhakar NR. Oxygen sensing in the body. Prog Biophys mol biol. 2006; 91: 249-286. doi: 10.1016/j.pbiomolbio.2005.07.001

- Lahiri S. Historical perspectives of cellular oxygen sensing and responses to hypoxia. J Appl Physiol. 2000; 88: 1467-1473. https://doi.org/10.1152/jappl.2000.88.4.1467.

- Landsberg L, Young JB. Catecholamines and adrenal medulla. In: Wilson JD, Foster DW, editors. Williams textbook of endocrinology. 8th ed. Philadelphia: W. B. Saunders; 1992. p. 621–706.

- Langille BL. Arterial remodelling: relation to hemodynamics. Can J Physiol Pharmacol 1996; 74: 834-841.

- Lavie L, Lavie P. Molecular mechanisms of cardiovascular disease in OSAHS: the oxidative stress link. Eur Respir J. 2009; 33(6): 1467-84. doi: 10.1183/09031936.00086608.

- Le Moine CM, Morash AJ, McClelland GB. Changes in HIF-1α protein, pyruvate dehydrogenase phosphorylation, and activity with exercise in acute and chronic hypoxia. Am J Physiol Regul Integr Comp Physiol. 2011; 301(4):R1098-104. doi: 10.1152/ajpregu.00070.2011.

- Li JM, Gall NP, Grieve DJ, Chen M, Shah AM. Activation of NADPH oxidase during progression of cardiac hypertrophy to failure. Hypertension. 2002; 40(4):477-84.

- Longa EZ, Weinstein PR, Carlson S, Cummins R. Reversible middle cerebral artery occlusion without craniectomy in rats. Stroke 1989; 20 (1): 84-91. doi: 10.1161/01.STR.20.1.84.

- Lopez-Barneo J, Gonzalez-Rodriguez P, Gao L, Fernandez-Aguera MC, Pardal R, Ortega-Saenz P. Oxygen sensing by the carotid body: mechanisms and role in adaptation to hypoxia. Am J Physiol Cell Physiol. 2016; 310 (8): C629-42. DOI:10.1152/ajpcell.00265.2015.

- Luneburg N, Siques P, Brito J, Arriaza K, Pena E, Klose H, Leon-Velarde F, Boger RH. Long-Term chronic intermittent hypobaric hypoxia in rats causes an imbalance in the asymmetric dimethylarginine/nitric oxide pathway and ROS activity: A possible synergistic mechanism for altitude pulmonary hypertension. Pulm Med. 2016; 2016: 6578578. doi: 10.1155/2016/6578578.

- Macarthur H, Westfall TC, Wilken GH. Oxidative stress attenuates NO-induced modulation of sympathetic neurotransmission in the mesenteric arterial bed of spontaneously hypertensive rats. Am J Physiol Heart Circ Physiol. 2008; 294(1): H183-9. DOI:10.1152/ajpheart.01040.2007.

- Magalhaes J, Ascensao A, Soares JM, Ferreira R, Neuparth MJ, Marques F, Duarte JA. Acute and severe hypobaric hypoxia increases oxidative stress and impairs mitochondrial function in mouse skeletal muscle. J Appl Physiol (1985). 2005; 99(4): 1247-53. DOI:10.1152/japplphysiol.01324.2004.

- Magalhaes J, Ascensao A, Viscor G, Soares J, Oliveira J, Marques F, Duarte J. Oxidative stress in humans during and after 4 hours of hypoxia at a simulated altitude of 5500 m. Aviat Space Environ Med. 2004; 75(1): 16-22.

- Malpas SC. Sympathetic nervous system overactivity and its role in the development of the cardiovascular disease. Physiol Rev. 2010; 90(2): 513-57. doi: 10.1152/physrev.00007.2009.

- McDonagh MS, Eden KB, Peterson K. Drug Class Review: Calcium Channel Blockers: Final Report [Internet]. Portland (OR): Oregon Health & Science University; 2005 Mar. Available from: https://www.ncbi.nlm.nih.gov/books/NBK10474/

- McGowan MW, Artiss JD, Strandbergh DR, Zak B. A peroxidase-coupled method for the colorimetric determination of serum triglycerides. Clin Chem. 1983; 29(3): 538-42.

- Messina G, De Luca V, Viggiano A, Ascione A, Iannaccone T, Chieffi S, Monda M. Autonomic nervous system in the control of energy balance and body weight: personal contributions. Neurol Res Int. 2013; 2013:639280. doi:10.1155/2013/639280.

- Michiels C. Physiological and pathological responses to hypoxia. *Am J Pathol*. 2004; 164(6):1875–1882. Doi: 10.1016/S0002-9440(10)63747-9.

- Mittal B, Mishra A, Srivastava A, Kumar S, Garg N. Matrix metalloproteinases in coronary artery disease. Adv Clin Chem. 2014; 64:1-74.

- Miyata T, Takizawa S, van Yperselede Strihou C. Hypoxia. 1. Intracellular sensors for oxygen and oxidative stress: novel therapeutic targets. Am J Physiol Cell Physiol. 2011; 300(2): C226-31. doi: 10.1152/ajpcell.00430.2010.

- Moraes DJ, Bonagamba LG, Costa KM, Costa –Silva JH, Zoccal DB, Machado BH. Short term sustained hypoxia induces changes in the coupling of sympathetic and respiratory activities in rats. J Physiol. 2014; 592(9): 2013-33. doi: 10.1113/jphysiol.2013.262212.

- Moreira MCS, Pinto ISJ, Mourão AA, Fajemiroye JO, Colombari E, Reis ÂAS, Freiria-Oliveira AH, Ferreira-Neto ML and Pedrino GR. Does the sympathetic nervous system contribute to the pathophysiology of metabolic syndrome? Front. Physiol. 2015; 6:234. doi: 10.3389/fphys.2015.00234

- Moshage H, Kok B, Huizenga JR, Jansen PLM. Nitrite and Nitrate determinations in plasma: A critical evaluation. Clin Chem. 1995; 41(6): 892-896.

- Musicki B, Kramer MF, Becker RE, Burnett AL. Inactivation of phosphorylated endothelial nitric oxide synthase (Ser-1177) by O-GlcNAc in diabetes-associated erectile dysfunction. Proc Natl Acad Sci U.S.A. 2005; 102(33): 11870-5. DOI:10.1073/pnas.0502488102.

- Nair AB, Jacob S. A simple practice guide for dose conversion between animals and human. J Basic Clin Pharm. 2016;7(2):27–31. doi:10.4103/0976-0105.177703.

- Nakanishi K, Tajima F, Nakamura A, Yagura S, Ookawara T, Yamashita H, Suzuki K, Taniguchi N, Ohno H. Effects of hypobaric hypoxia on antioxidant enzymes in rats. J Physiol.1995; 489(Pt) 3: 869-76. DOI:10.1113/jphysiol.1995.sp021099.

- Nath B, Szabo G. Hypoxia and hypoxia inducible factors: diverse roles in liver diseases. Hepatology. 2012; 55 (2): 622-633. doi: 10.1002/hep.25497.

- Nonogaki K. New insights into sympathetic regulation of glucose and fat metabolism. Diabetologia. 2004; 43(5): 533-49. doi:10.1007/s001250051341

- Olson EB Jr, Dempsey JA. Rat as a model for human-like ventilator adaptation to chronic hypoxia. J Appl Physiol Respir Environ Exerc Physiol. 1978; 44(5):763-9. DOI: 10.1152/jappl.1978.44.5.763

- Pare GC, Bauman AL, McHenry M, Michel JJ, Dodge-Kafka KL, Kapiloff MS. The mAKAP complex participates in the induction of cardiac myocyte hypertrophy by adrenergic receptor signalling. J Cell Sci. 2005; 1 18 (Pt23):5637-46. DOI: 10.1242/jcs.02675.

- Patil BS, Kanthe PS, Reddy RC, Das KK. Emblica Officinalis (Amla) ameliorates high-fat diet induced alteration of cardiovascular pathophysiology. Cardiovasc Hematol Agents Med Chem. 2019 (ahead of print). doi: 10.2174/1871525717666190409120018.

- Phaniendra A, Jestadi DB, Periyasamy L. Free radicals: properties, sources, targets, and their implication in various diseases. Indian J Clin Biochem. 2015;30(1):11–26. doi:10.1007/s12291-014-0446-0.

- Pimentel DR, Amin JK, Xiao L, Miller T, Viereck J, Oliver-Krasinski J, Baliga R, Wang J, Siwik DA, Singh K, Pagano P, Colucci WS, Sawyer DB. Reactive oxygen species mediate

amplitude-dependent hypertrophic and apoptotic responses to mechanical stretch in cardiac myocytes. *Circ. Res.* 2001; 89: 453–460. DOI:10.1161/hh1701.096615

- Pisani T, Gebski CP, Leary ET, Warnick GR, Ollington JF. Accurate determination of low-density lipoprotein cholesterol using an immunoseparation reagent and enzymatic cholesterol assay. Arch Pathol Lab Med. 1995; 119(12): 1127-35.

- Powell FL, Huey KA, Dwinell MR. Central nervous system mechanisms of ventilatory acclimatization to hypoxia. Respir Physiol. 2000; 121 (2-3): 223-36.

- Powell FL, Milson WK, Mitchell GS. Time domains of the hypoxic ventilatory response. Respir Physiol. 1998; 112(2):123-34.

- Prabhakar NR, Jacono FJ. Cellular and molecular mechanisms associated with carotid body adaptations to chronic hypoxia. High Alt Med Biol. 2005; 6(2): 112-20. DOI:10.1089/ham.2005.6.112.

- Pulgar-Sepulveda R, Varas R, Iturriaga R, Del Rio R, Ortiz FC. Carotid body type-I cells under chronic sustained hypoxia: Focus on metabolism and membrane excitability. Front Physiol. 2018; 9: 1282. doi: 10.3389/fphys.2018.01282.

- Qutub AA, Popel AS. Reactive oxygen species regulate hypoxia-inducible factor 1alpha differentially in cancer and ischemia. Mol Cell Biol. 2008; 28(16):5106-19. Doi: 10.1128/MCB.00060-08.

- Rababa'h AM, Guillory AN, Mustafa R, Hijjawi T. Oxidative stress and cardiac remodelling: An updated edge. Curr Cardiol Rev. 2018; 14(1): 53-59. doi: 10.2174/1573403X14666180111145207.

- Ramakrishnan A, Anand V, Roy S. Vascular endothelial growth factor signalling in hypoxia and inflammation. J Neuroimmune Pharmacol. 2014; 9 (2): 142-160. Doi: 10.1007/s11481-014-9531-7.

- Ramirez TA, Jourdan-Le Saux C, Joy A, Zhang J, Dai Q, Mifflin S, Lindsey ML. Chronic and intermittent hypoxia differentially regulate left ventricular inflammatory and extracellular matrix responses. Hypertens Res. 2012; 35(8): 811-8. doi: 10.1038/hr.2012.32.

- Rankin EB, Giaccia AJ. The role of hypoxia-inducible factors in tumorigenesis. Cell Death Differ. 2008; 15(4): 678-685. doi:10.1038/cdd.2008.21.

- Richalet JP. The heart and the adrenergic system. In: Hypoxia, the Adaptations, edited by J. R. Sutton, G. Coates, and J. E. Remmers. Philadelphia, PA: Dekker, 1990, p. 231-245.

- Rodriguez-Diaz R, Speier S, Molano RD, Formoso A, Gans I, Abdulreda MH, et al. Noninvasive in vivo model demonstrating the effects of autonomic innervation on pancreatic islet function. Proc Natl Acad Sci USA. 2012; 109: 21456–61. DOI:10.1073/pnas.1211659110.

- Rodriguez-Miguelez P, Lima-Cabello E, Martinez-Florez S, Almar M, Cuevas MJ, Gonzalez-Gallego J. Hypoxia-inducible factor-1 modulates the expression of vascular endothelial growth factor and endothelial nitric oxide synthase induced by eccentric exercise. J Appl Physiol. (1895). 2015; 118(8):1075-83. doi: 10.1152/japplphysiol.00780.2014.

- Roe JH, Koether CA. The determination of ascorbic acid in whole blood and urine through the 2, 4-dinitrophenylhydrazine derivative of dehydroascorbic acid. J Biol Chem. 1943; 147:399–407.

- Roever L, Palandri Chagas AC. Editorial: Cardiac Remodeling: New Insights in Physiological and Pathological Adaptations. Front Physiol.2017;8:751. doi:10.3389/fphys.2017.00751.

- Rose GW, Ikebukoro H. Cilnidipine as effective as benazepril for control of blood pressure and proteinuria in hypertensive patients with benign nephrosclerosis. Hypertens Res. 2001; 24: 377-383.

- Ryan MJ, Dudash HJ, Docherty M, Geronilla KB, Baker BA, Haff GG, Cutlip RG, Alway SE. Vitamin E and C supplementation reduces oxidative stress, improves antioxidant enzymes and positive muscle work in chronically loaded muscles of aged rats. Exp Gerontol. 2010; 45(11):882-95. doi: 10.1016/j.exger.2010.08.002.

- Rybnikova E, Samoilov M. Current insights into the molecular mechanisms of hypoxic pre- and postconditioning using hypobaric hypoxia. Front Neurosci. 2015; 9: 388. doi: 10.3389/fnins.2015.00388.

- Sabri A, Hughie HH, Lucchesi PA. Regulation of hypertrophic and apoptotic signalling pathways by reactive oxygen species in cardiac myocytes. Antioxid Redox Signal. 2003; 5(6): 731-40. DOI:10.1089/152308603770380034.

- Samanta D, Prabhakar NR, Semenza GL. Systems biology of oxygen homeostasis. Wiley Interdiscip Rev Syst Biol Med. 2017;9(4):10.1002/wsbm.1382. doi:10.1002/wsbm.1382.

- Sarada SK, Sairam M, Dipti P, Anju B, Pauline T, Kain AK, Sharma AK, Bagawat S, Ilavazhagan G, Kumar D. Role of selenium in reducing hypoxia-induced oxidative stress: an in vivo study. Biomed Pharmacother. 2002; 56(4):173-8.

- Schultz K, Fanburg BL, Beasley D. Hypoxia and hypoxia-inducible factor-1alpha promote growth factor-induced proliferation of human vascular smooth muscle cells. Am J Physiol Heart Circ Physiol. 2006; 290 (6): H2528-34. DOI: 10.1152/ajpheart.01077.2005.

- Shaffer F, Ginsberg JP. An overview of heart rate variability metrics and norms. Front Public Health. 2017;5: 258. doi: 10.3389/fpubh.2017.00258.

- Shibuya M. Vascular Endothelial Growth factor (VEGF) and its receptor (VEGFR) signalling in angiogenesis: A crucial target for Anti- and Pro- angiogenic therapies. Genes Cancer. 2011; 2 (12): 1097-1105. Doi:10.1177/1947601911423031.

- Sies H. The concept of oxidative stress after 30 years. In: Gelpi R., Boveris A., Poderoso J., editors. Advances in biochemistry in health and disease. Springer; New York: 2016. pp. 3–11.

- Siques P, Brito J, Naveas N, Pilido R, de La Cruz JJ, Mamani M, Leon-Velarde F. Plasma and liver lipid profiles in rats exposed to chronic hypoxia: changes in metabolic pathways. High Alt Med Biol. 2014; 15 (3):388-95. doi: 10.1089/ham.2013.1134.

- Siques P, Lopez de Pablo AL, Brito J, Arribas SM, Flores K, Arriaza K, Naveas N, Gonzalez MC, Hoorntje A, Leon-Velarde F, Lopez MR. Nitric oxide and superoxide anion balance in rats exposed to chronic and long term intermittent hypoxia. Biomed res Int. 2014; 2014: 610474. doi: 10.1155/2014/610474.

- Smita K, Pasha Qadar MA, Jain SK. Oxidative stress and histopathological evaluation of rat lung tissue during hypobaric hypoxia. Journal of Proteomics and Bioinformatics 2015; 8(6): 108-115. doi:10.4172/jpb.1000358.

- Soderlund DM. Toxicology and mode of action of pyrethroid insecticides. In: Krieger R ed. Haye's handbook of pesticide toxicology. 3rd ed. United Kingdom: Academic Press Elsevier; 2010. P. 1665-1686. ISBN: 978-0-12-374367.

- Szablewski L. Glucose Homeostasis. In: Zhang W, ed. Gluconeogenesis. United Kingdom: Intech Open; 2017.p.5-20. ISBN: 978-953-51-3324-7

- Takahara A, Koganei H, Takeda T, Iwata S. Antisympathetic and hemodynamic property of a dual L/N- type Ca (2+) channel blocker cilnidipine in rats. Eur J Pharmacol. 2002 Jan 2; 434(1-2):43-7. DOI: 10.1016/s0014-2999(01)01521-7.

- Takahara A. Cilnidipine: A new generation calcium channel blocker with inhibitory action on sympathetic neurotransmitter release. Cardiovasc Ther. 2009; 27 (2): 124-139. doi: 10.1111/j.1755-5922.2009.00079.x.

- Takashi M, Misao O, Tatsumi M, Matsumoto T, Kutsuna T, Hara M, Aiba N, Noda C, Izumi T. Beneficial effects of L- and N-type calcium channel blocker on glucose and lipid metabolism and renal function in patients with hypertension and type II diabetes mellitus. Cardiovasc Ther. 2011; 29(1): 46-53. DOI:10.1111/j.1755-5922.2009.00126.x.

- Takeda S, Ueshiba H, Hattori Y, Irie M. Cilnidipine, the N- and L-type calcium channel antagonist, reduced on 24-h urinary catecholamines and C-peptide in hypertensive non-insulin dependent diabetes mellitus. Diabetes Res Clin Pract. 1999; 44:197-205.

- Thorp AA, Schlaich MP. Relevance of sympathetic nervous system activation in obesity and metabolic syndrome. J Diabetes Res. 2015; 2015:341583. doi: 10.1155/2015/341583.

- Touyz RM, Montezano AC, Rosendorff C. Vascular function in health and diseases. In: Caplan M, ed. Reference Module in Biomedical Sicences. Elsevier; 2014. p. ISBN 9780128012383.

- Trimbake SB, Sontakke AN, Dhat VV. Oxidative stress and antioxidant vitamins in leprosy. Int J Res Med Sci. 2013; 1(3):101-104. DOI: 10.5455/2320-6012.ijrms20130804.

- Trinder P. Determination of glucose in blood using glucose oxidase with an alternative oxygen acceptor. Ann Clin Biochem 1969; 6: 24-27.

- Tsuchihashi T, Ueno M, Tominaga M, Kajioka T, Onaka U, Eto K, Goto K. Anti-proteinuric effect of an N-type calcium channel blocker, cilnidipine. Clin Exp Hypertens. 2005; 27: 583-591.

- Uchida T, Rossignol F, Matthay MA, Mounier R, Couette S, Clottes E, Clerici C. Prolonged hypoxia differentially regulates hypoxia-inducible factor (HIF)-1alpha and HIF-2 alpha expression in lung epithelial cells: implication of natural antisense HIF-1alpha. J Biol Chem. 2004; 279(15):14871-8. DOI: 10.1074/jbc.M400461200.

- Ueshiba H, Miyachi Y. Effects of cilnidipine on adrenocortical steroid hormones and insulin resistance in hypertensive patients with obesity. Ther Res 2002; 23:2493-2497.

- Umbrello M, Dyson A, Feelisch M, Singer M. The key role of nitric oxide in hypoxia: hypoxic vasodilation and energy supply-demand matching. Antioxid Redox Signal. 2013; 19(14): 1690-710. DOI:10.1089/ars.2012.4979.

- Van Puyvelde K, Mets T, Njemini R, Beyer I, Bautmans I. Effect of advanced glycation end-product intake on inflammation and ageing: a systematic review. Nutr Rev.2014;72(10): 638-50. DOI:10.1111/nure.12141.

- Varnava A. Coronary artery remodelling. Heart 1998; 79**:**109-110.

- Viglino D, Julian-Desayes I, Minoves M, Aron-Wisnewsky J, Leroy V, Zarski JP et al. Non-alcoholic fatty liver disease in chronic obstructive pulmonary disease. Eur Respir J 2017; 49(6).pii:1601923. DOI: 10.1183/13993003.01923-2016.

- Walsh MP, Marshall JM. The early effects of chronic hypoxia on the cardiovascular system in the rat: role of nitric oxide. J Physiol 2006; 575:263-75. DOI:10.1113/jphysiol.2006.108753.

- Werner M, Gabrielson DG, Eastman J. Ultramicro determination of serum triglycerides by bioluminescent assay. Clin Chem. 1981; 27(2): 268-71.

- Xiang L, Mittwede PN, Clemmer JS. Glucose homeostasis and cardiovascular alterations in diabetes. Compr Physiol. 2015; 5(4): 1815-39. doi: 10.1002/cphy.c150001.

- Xu C, Qiao X, Zhao Y, Sun R, Shang X, Niu W. Resveratrol ameliorates chronic high altitude exposure-induced oxidative stress and suppresses lipid metabolism alteration in rats. Eur J Lipid Sci Technol. 2016; 118(4): 612-621. doi:10.1002/ejlt.201400426.

- Xu K, Lamanna JC. Chronic hypoxia and cerebral circulation. J Appl Physiol (1985). 2006; 100(2):725-30. DOI:10.1152/japplphysiol.00940.2005.

- Yin HL, Luo CW, Dai ZK, Shaw KP, Chai CY, Wu CC. Hypoxia-inducible factor-1α, vascular endothelial growth factor, inducible endothelial nitric oxide synthase, and

endothelin-1 expression correlates with angiogenesis in congenital heart disease. Kaohsiung J Med Sci. 2016; 32(7): 348-55. doi: 10.1016/j.kjms.2016.05.011.

- Yoon G, Oh CS, Kim HS. Distinctive expression patterns of hypoxia-inducible factor-1α and endothelial nitric oxide synthase following hypergravity exposure. Oncotarget 2016; 7 (23): 33675-33688. doi: 10.18632/oncotarget.9372.

- Zang W, Carreno FR, Cunningham JT, Mifflin SW. Chronic sustained hypoxia enhances both evoked EPSCs and norepinephrine inhibition of glutamatergic afferent inputs in the nucleus of the solitary tract. J Neurosci. 2009; 29 (10): 3093-102. doi: 10.1523/JNEUROSCI. 2648-08.2009.

- Zhao H, Chen H, Li H, Li D, Wang S, Han Y. Remodelling of small intramyocardial coronary arteries distal to total occlusions after myocardial infarction in pigs. Coron Artery Dis. 2013; 24(6):493-500. doi: 10.1097/MCA.0b013e328363244b.

- Zhu C, Teng Z, Sadat U, Young VE, Graves MJ, Li ZY, Gillard JH. Normalized wall index specific and MRI-based stress analysis of atherosclerotic carotid plaques: a study comparing acutely symptomatic and asymptomatic patients. Circ J. 2010; 74(1): 2360-4.

ANNEXURES

ANNEXURE I

PLAGIARISM VERIFICATION CERTIFICATE

BLDE (DEEMED TO BE UNIVERSITY)

PLAGIARISM VERIFICATION CERTIFICATE

1. Name of the Student:..Shrilaxmi Bagali.............Reg No..15PHD006

2. Title of the Thesis:..Hypoxia and Cell Signalling: Cardiovascular Remodelling Glucose Homeostasis and Role of Calcium Channel Blocker (Cilnidipine)

3. Department:..Physiology.

4. Name of the Guide & Designation:..Prof Kusal K. Das, Professor

5. Name of the Co Guide & Designation:..Dr Akram Naikwadi, Professor and Head

The above thesis was verified for similarity detection. The report is as follows:

Software used......ITHENTICATE....... Date:2nd August 2019

Similarity Index(%):........8%............. Total word Count.32700

The report is attached for the review by the Student and Guide.

The plagiarism report of the above thesis has been reviewed by the undersigned.

The similarity index is below accepted norms.

The similarity index is above accepted norms, because of following reasons:

....

....

....

The thesis may be considered for submission to the University. The software report is attached.

Signature of the Guide
Name & Designation
Prof. Kusal K. Das PhD
Laboratory of Vascular Physiology & Medicine
Department of Physiology
BLDE(DU) Shri B M Patil Medical College
Vijayapur-586103 Karnataka India

Signature of Co-Guide
Name & Designation
DR. Akram A.Naikawadi

Professor & HOD
Dept. of Pharmacology
BLDEU's Shri B. M. Patil
Medical College VIJAYAPUR

Signature of Student

6.8.19
Verified by (Signature)
Name & Designation
Librarian
B.L.D.E. University's
Shri B.M. Patil Medical College
Bijapur.

ANNEXURE II

INSTITUTIONAL ANIMAL ETHICAL CLEARANCE CERTIFICATE

BLDE Association's

SHRI SANGANABASAVA MAHASWAMIJI COLLEGE OF PHARMACY & RESEARCH CENTRE

Post Box No. 40, BLDE University Campus, Solapur Road, **VIJAYAPUR**-586 103

Approved by Pharmacy Council of India(PCI), All India Council for Technical Education(AICTE), New Delhi.

Recognised by. Govt. of Karnataka & Affiliated to RGUHS, Bengaluru

Dr. Navanath V. Kalyane
Professor & Principal

Phone : (O) 08352-264004 (R)265206 Cell : 9448947496 Fax : 08352-262643
Website : www.bldeapharmacy.ac.in   e-mail : bldeascop@yahoo.com

Ref. : BLDE/ BPC/641/2016-17

Date : 26)10/16

Reg. No. 1076/PO/ERs/S/07 CPCSEA, Dated: 20th Aug, 2014 under the rules of 5 (a) of "Breeding of and Experiments on Animal (Control, Supervision) Rules 1998"

This is to certify that the research project entitled **"Hypoxia and cell signaling: cardiovascular remodeling, glucose homeostasis and role of calcium channel blocker (Cilnidipine)"** has been approved by the IAEC.

Dr. N V Kalyane

Name of Chairman/Memb. Secretary IAEC

IAEC CHAIRMAN

Signature with date 11olub

Chairman/Memb. Secretary IAEC

Mr. Mallikarjun S Kolhar

Name of CPCSEA Nominee

CPCSEA Nominee

(Kindly make sure that minutes of meeting duly signed by all the participants are maintained by office.)

ANNEXURE III

PRESENTATIONS AND AWARDS

Presentations

1. "Effect of Ca^{2+} channel blocker on chronic hypoxia induced alteration of glucose homeostasis" at ASSOPICON-2016 during 15th -17th September, 2016, organized by Department of Physiology, Shri B. M. Patil Medical College, Hospital & Resaerch Centre, Vijayapur, Karnataka, India.

2. "Effect of Ca^{2+} channel blocker on chronic hypoxia induced alteration of cardiac electrophysiology"at VII Congress of the Federation of Indian Physiological Societies (FIPS) & XXIX Annual Conference of the Physioogical Society of India (PSI) (FIPSPHYSIOCON-2017), during 5th -7th November, 2017, organized by Defence Institute of Physiology & Allied Sciences (DRDO), Delhi.

3. "Chronic Hypoxia and Cardiovascular electrophysiology: Signal transduction and role of drug cilnidipine" during one day seminar on 'Research Trends in Science and Technology'organized by BLDEA's V P G Halakatti College of Engineering and Technology, Vijayapur on 29th May 2019.
Received **Best Poster Award.**

4. "Hypoxia induced cell signal transduction on cardiovascular pathophysiology in experimental rats" on Research Day, 6th June 2018, organized by BLDE (Deemed to be University), Vijayapur, Karnataka.
Received **'Research Day Medal'**

PUBLICATIONS

1. **Bagali S**, Naikwadi A, Das KK. Tissue specific effects of chronic sustained hypoxia on oxidative streee: Role of Cilnidipine, a dual L/N type calcium channel blocker. JKIMSU 2019; 1(8): 31-36. (Scopus).

2. Reddy RC, Devarnavadagi B, Yendigeri SM, **Bagali S**, Kulkarni RV, Das KK. Effect of L-Ascorbic acid on nickel-induced alteration of cardiovascular pathophysiology in Wistar rats. Biol Trace Elem Res. 2019. doi: 10.1007/s12011-019-01829-w. [Epub ahead of print]. **(IF-2.43).**

3. Das KK, Yendigeri SM, Patil BS, Bagoji IB, Reddy RC, **Bagali S**, Biradar MS, Saha S. Subchronic hypoxia pretreatment on brain pathophysiology in unilateral common carotid artery occluded albino rats. Indian J Pharmacol. 2018; 50(4): 185-91. doi: 10.4103/ijp.IJP_312_17. **(IF-1.03)**

4. Das KK, Reddy RC, Bagoji IB, Das S, **Bagali S**, Mullur L, Khodnapur JP, Biradar MS. Primary concept of nickel toxicity – an overview. J Basic Clin Physiol Pharmacol. 2018; 30(2): 141-152. doi: 10.1515/jbcpp-2017-0171. (Scopus/Pubmed)

Book Chapter

1. **Bagali S**, Hadimani GA, Biradar MS, Das KK. Introductory chapter: Primary concept of hypoxia and anoxia. In: Das KK and Biradar MS. ed(s). Hypoxia and Anoxia. UK: Intech Open; 2018. p. 3-11. ISBN: 978-1-78984-828-1.

2. Ray J, **Bagali S,** Basu S. Vitamin E for Children: From neonates to adolscents. In: Berhardt LV. Ed. Advances in Medicine and Biology, Vol 146. USA: Nova publishers; 2019. ISBN: 978-1-53615-961-5.

ORIGINAL ARTICLE

Tissue Specific Effects of Chronic Sustained Hypoxia on Oxidative Stress: Role of Cilnidipine, a Dual L/N Type Calcium Channel Blocker

Shrilaxmi Bagali[1], Akram Naikwadi[2], Kusal K Das[1]*

[1]Laboratory of Vascular Physiology and Medicine, Department of Physiology, [2]Department of Pharmacology, Shri B. M. Patil Medical College, Hospital and Research Centre, BLDE (Deemed to be University), Vijayapura-586103(Karnataka) India

Abstract:

Background: Blood flow, metabolic rate and oxygen requirements of an organ guide the extent of oxidative stress experienced by any tissue in response to chronic hypoxia. Currently cilnidipine is used in the management of hypertension and its antioxidant actions are gaining wide interest. *Aim and Objectives:* To evaluate the tissue specific effects of chronic sustained hypoxia with regards to oxidative stress in the context of cilnidipine. *Material and Methods:* Twenty four adult male Wistar strain albino rats were randomly assigned into four groups: group 1, control, normoxia (21% O_2); group 2, chronic hypoxia (CH) (10% O_2) for 21 days; group 3, normoxia + cilnidipine (Cil) for 21 days; group 4, chronic hypoxia + cilnidipine (CH+Cil) for 21 days. Following 21 days of intervention blood was collected and animals were sacrificed and liver, lung and heart were collected. Serum MDA and MDA in tissue homogenate of liver, lung and heart were estimated. *Results:* Our results demonstrate the elevated serum MDA levels in chronic hypoxia exposed rats (group 2). We also observed increased MDA in liver followed by lung and least in the heart in chronic hypoxia exposed rats (group 2). Treatment with cilnidipine reduced serum MDA and heart MDA levels in cilnidipine treated chronic hypoxia exposed rats (group 4). However cilnidipine did not have any influence on MDA levels in the liver and lung in same group of rats. *Conclusion:* The results demonstrate tissue specific effects of chronic sustained hypoxia with the highest oxidative stress observed in the liver followed by the lung. Although oxidative stress is also observed in the heart it is the least in comparison to the liver and the lung. Cilnidipine, a dual L/N type calcium channel blocker demonstrated beneficial antioxidant actions only in the heart supporting the cardioprotective role of cilnidipine.

Keywords: Chronic Hypoxia, Oxidative stress, Cilnidipine

Introduction:

Oxygen is indispensable for life. Accordingly the cells have evolved mechanisms to detect and to react to alterations in the oxygen levels in the microenvironment. Both low and high oxygen levels disturb oxygen homeostasis and endanger cell survival [1, 2]. Hypoxia is lack of oxygen at the tissue level. Hypoxia may be acute or chronic and sustained or intermittent. Irrespective of its type, hypoxia is associated with increased generation of free radicals and consumption of the antioxidants disturbing the oxidant/antioxidant balance in favor of oxidants [3, 4]. The generated free radicals damage the constituents that make up the cell like nucleic acids, proteins, lipids and carbohydrates causing oxidative stress [5].

Blood flow and oxygen requirements of different organs are not uniform. Additionally the antioxidant reserves in different tissues also vary [6]. Consequently oxidative stress induced by hypoxia may be tissue and organ specific. This

understanding may be of significance in the management of various clinical conditions resulting from occurrence or exposure to hypoxia e.g. Chronic Obstructive Pulmonary Disease (COPD), congenital heart disease, high altitude etc. Hence the present study was undertaken to explore the organ specific effects of chronic sustained hypoxia particularly liver, heart and lung with regards to oxidative stress.

Cilnidipine is a Calcium Channel Blocker (CCB) belonging to the dihydropyridine class. Cilnidipine is unique owing to its dual L/N type calcium channel blocking property [7]. It has also been demonstrated to have some antioxidant properties owing to its strong lipophilic nature. Cilnidipine due to its pharmacological profile is being widely used in the treatment of hypertension and its antioxidant actions have currently gained wide attention [8]. The present study also intends to explore the antioxidant property of cilnidipine and its impact on the chronic hypoxia induced oxidative stress of various organs.

Material and Methods:

Experimental Animals:

Twenty four adult male Wistar strain albino rats (*Rattus norvegicus*), weighing 180 to 250 g were procured from the animal house of BLDE (Deemed to be University). All the animals were maintained at 22-24^{0}C and exposed to 12 hours light/dark cycle with food and water made available to them *ad libitum.* The animals were allowed to adapt to the laboratory conditions for a week before the onset of the experimental protocol.

Ethical considerations:

Institutional Animal Ethics Committee (IAEC) clearance was obtained for the study (Ref: BLDE/BPC/641/2016-2017 dated 21.10.2016) and all the experimental procedures were done in accordance with the guidelines of Committee for the Purpose and Control and Supervision of Experiments on Animals (CPCSEA), Government of India.

Experimental groups:

The experimental animals were randomly assigned to one of the four groups as depicted in Table 1. The body weight of all rats was recorded on day 1 and after 21 days of intervention using electronic balance (Practum 1102-10IN, Sartorius Lab Instruments, Germany). The rats of all groups were matched for weight at the onset of the experimental protocol.

Table 1: Experimental Groups of Rats (n=6 in Each Group)

Groups	Intervention
Group 1 (Control)	Vehicle (0.5% Na CMC) by oral gavage for 21 days
Group 2 (CH)	Chronic hypoxia (CH) for 21 days + Vehicle (0.5% Na CMC) by oral gavage for 21 days
Group 3 (Cil)	Cilnidipine (2mg/Kg body wt.) in 0.5% Na CMC by oral gavage for 21 days
Group 4 (CH+Cil)	Chronic hypoxia (CH) for 21 days + cilnidipine (2 mg/Kg body wt.) in 0.5% Na CMC by oral gavage for 21 days

CH-Chronic Hypoxia, Cil-Cilnidipine, CH+Cil- Chronic Hypoxia+Cilnidipine, Na CMC- Sodium Carboxymethyl Cellulose

Experimental Protocol:

The experimental protocol followed has been summarized in Fig 1.

```
┌─────────────────────────────┐
│   Random allocation into    │
│           groups            │
└─────────────────────────────┘
              │
              ▼
┌─────────────────────────────┐
│         Gravimetry          │
└─────────────────────────────┘
              │
              ▼
┌─────────────────────────────┐
│  Intervention for 21 days   │
│     (CH, Cilnidipine)       │
└─────────────────────────────┘
              │
              ▼
┌─────────────────────────────┐
│        Gravimetry,          │
│    Collection of Blood for  │
│     Biochemical analysis    │
└─────────────────────────────┘
              │
              ▼
┌─────────────────────────────┐
│      Sacrifice followed by  │
│ collection of liver, lung, heart │
│      for OS assessment      │
└─────────────────────────────┘
```
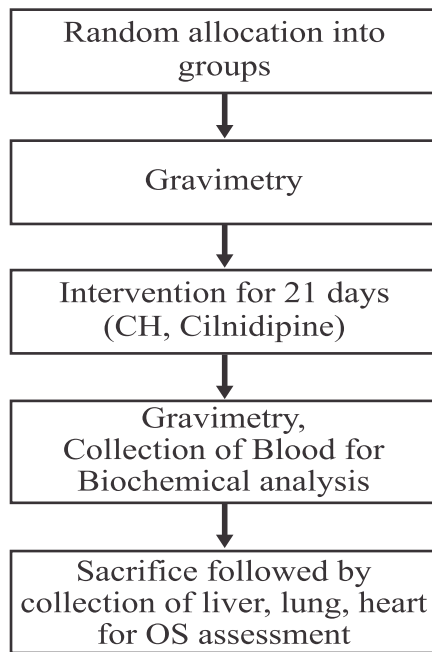
Fig 1: Experimental Protocol followed

CH=Chronic Hypoxia; OS=oxidative stress

Exposure of animals to Chronic (Normobaric) Hypoxia/CH:

Chronic sustained hypoxia was induced by placing caged rats (4 per cage) inside a acrylic chamber of 300-liter capacity, that can hold up to 4 cages (16 rats), and were exposed to inspired Oxygen (O_2) (10%) and Nitrogen (N_2) (90%) to induce normobaric hypoxia. The hypoxic environment was created with an inflow of mixture of room air and nitrogen. CO_2 was absorbed by soda lime (27 granules), and a desiccator removed excess humidity. The temperature was maintained at 22-26°C. The chamber was opened for 1 hour, two times a week to clean the cages and to replenish food and water [9]. In our study rats were exposed to chronic sustained hypoxia for a period of 21 days.

Administration of drug:

Cilnidipine is dual L/N type CCB. Cilnidipine was procured from Laksh Finechem Pvt. Limited, Gujarat, India. Cilnidipine was stored in the refrigerator until further use. The dose of cilnidipine for rats was calculated using the formula:

Rats (mg/kg) = Human dose×0.018×5 [10].

The dose was calculated to be 2 mg/kg body weight. A suspension of cilnidipine in 0.5% sodium Carboxymethyl Cellulose (0.5% Na CMC) was freshly prepared every day and was administered by oral gavage once daily in the morning to group 3 (Cil) and group 4 (CH+Cil) rats for 21 days.

Assessment of oxidative stress

Malondialdehyde is a product of lipid peroxidation and a frequently used marker of oxidative stress. MDA concentration (conc.) was estimated in the serum and tissue homogenate of liver, lung, and heart by the method of Buege and Aust (1978) [11]. 10% tissue homogenate was prepared in 0.1M phosphate buffer using tissue homogenizer (REMI MOTORS, Bombay, India) and supernatant was used for the assay. MDA reacts with Thiobarbituric Acid (TBA) to give a pink colour and the absorbance of was read at 535 nm using spectrophotometer (Schimadzu UV 800, Schimadzu corporation, Japan).

Statistical Analysis:

All the statistical analysis was done using SPSS 16.0 (SPSS Inc., Chicago, USA). The parameters are presented as Mean ± SD. Statistical significance of data across multiple groups was analyzed using One-way analysis of variance (ANOVA) followed by Post hoc Tukey's multiple comparison test to determine significant difference between groups. A p-value < 0.05 was considered as statistically significant.

Table 2: Comparison of Biomarkers of Oxidative Stress in Serum and Tissue Homogenate among Groups (n=6 in Each Group)

Parameter	Group 1 (Control)	Group 2 (CH)	Group 3 (Cil)	Group 4 (CH+Cil)	p-value
Serum MDA (µmol/L)	1.95±0.53	3.39±0.70[a]	1.48±0.15[b]	2.13±0.29[b]	0.000*
Liver MDA (µmol/gm of tissue)	27.27±3.68	43.68±3.50[a]	28.36±3.94[b]	41.31±1.81[ac]	0.000*
Heart MDA (µmol/gm of tissue)	10.79±0.51	13.89±0.59[a]	11.18±0.63[b]	11.66±0.83[b]	0.000*
Lung MDA (µmol/gm of tissue)	27.01±2.97	37.12±2.57[a]	28.88±3.33[b]	31.74±5.40	0.003*

Values are expressed as Mean ± SD. One way ANOVA followed by Post Hoc Tukey's multiple comparison test. Superscript a, b, c indicate significant difference between groups. 'a' denotes comparison with Group 1, 'b' denotes comparison with group 2, 'c' denotes comparison with group 3. *p<0.05. CH-Chronic Hypoxia; Cil-cilnidipine; CH+Cil- Chronic Hypoxia+Cilnidipine; MDA-Malondialdehyde

Results:

Table 2 shows significant increase in serum MDA levels in chronic hypoxia exposed rats (group 2) compared to control rats (group 1). Also MDA levels in tissue homogenate of liver, heart and lung were significantly increased in chronic hypoxia exposed rats (group 2) compared to control rats (group 1). There was a 60% increase in liver MDA, 37% increase in lung MDA, 28% increase in heart MDA in chronic hypoxia exposed rats (group 2) compared to control rats (group 1). Chronic hypoxia exposed cilnidipine treated rats (group 4) did not demonstrate significant differences in liver MDA and lung MDA levels when compared to group 2 rats. However serum MDA, heart MDA were significantly reduced in group 4 (CH+Cil) compared to group 2 (CH).

Discussion:

The blood flow, oxygen requirements and antioxidant reserves in different tissues varies. Consequently there may be differences in the susceptibility of tissues to oxidative stress [6]. MDA is product of lipid peroxidation and has been used as an indirect biomarker of oxidative stress [11]. In the present study we assessed oxidative stress by estimating MDA levels both in the serum and tissue homogenate of liver, heart and lung to explore the organ specific effects of chronic hypoxia with regards to oxidative stress. We observed increased serum MDA levels in chronic hypoxia exposed rats compared to control rats indicating higher oxidative stress in the former. Among the tissues studied liver demonstrated the highest oxidative stress followed by the lung and least oxidative stress in the heart. This observation indicates that highest brunt of hypoxia is borne by the liver despite the fact that it has high antioxidant reserve. There are several factors contributing to this. Tissues like heart and brain are considered as

supply dependent and tissues like kidneys, skin, resting muscle and splanchnic area are considered as supply independent [12]. Whenever the body is challenged with any stressful condition like hypoxia, the blood flow is diverted to supply dependent vital organs like heart and brain at the expense of the visceral organs [13]. In addition, Reactive Oxygen Species (ROS) formation is decided by the levels of free iron, hemoproteins and Polyunsaturated fatty acids (PUFAs) all of them promoting its formation. Liver has more iron and free iron reacts with hydrogen peroxide via Fenton reaction producing hydroxyl radicals. Heme released from the hemoproteins also contributes to the formation of ROS via the same Fenton reaction. High levels of Cytochrome P450 in the liver have a role in the generation ROS [14]. Chronic hypoxia induced hepatic oxidative stress may play a vital role in the pathogenesis of liver diseases in patients experiencing hypoxia. Studies have reported higher prevalence of Nonalcoholic Fatty Liver Disease (NAFLD) in patients with Chronic Obstructive Pulmonary Disease (COPD) [15].

Lungs are the gate way for oxygen in the environment and the cells of the body. Accordingly lungs may be one of the early organs to experience adverse consequences of hypoxia. However, in the present study lung experienced lesser oxidative stress when compared to the liver. This could be due to tolerance of the alveolar epithelial cells to hypoxia due to which they can maintain adequate cellular ATP on exposure to prolonged hypoxia [16].

Cilnidipine is a dihydropyridine calcium channel blocker with dual L/N type calcium channel blocking property [7]. Cilnidipine is lipophilic and acts as a lipophilic chain breaking antioxidant. Among all the dihydropyridine derivatives cilnidipine demonstrates strongest lipophilicity and has highest antioxidant actions [8]. Although our study did not demonstrate any beneficial effects of cilnidipine on the oxidative stress levels in the liver and lung but was successful in reducing oxidative stress in the heart and serum MDA levels. This demonstrates the cardioprotective role of cilnidipine.

Implications of the study:

The results of our study demonstrate that liver is the one to suffer highest oxidative stress followed by the lung and the heart due to hypoxia. Hence the early markers of liver diseases should be monitored to identify their onset in patients experiencing hypoxia. Cilnidipine, a dual L/N type calcium channel blocker has been found to have a beneficial role to counteract hypoxia induced alteration of oxidant/antioxidant balance. Further study on the role of different antioxidant supplementation on disease progression can be undertaken.

References

1. Giaccia AJ, Simon MC, Johnson R. The biology of hypoxia: the role of oxygen sensing in development, normal function, and disease. *Genes Dev* 2004; 18(18):2183-94.

2. Zhao HW, Haddad GG. Review: Hypoxia and oxidative stress resistance in Drosophila melanogaster. *Placenta* 2011; 32(Suppl 2):S104-8.

3. Das KK, Nemagouda SR, Patil SG, Saha S. Possible hypoxia signaling induced alteration of glucose homeostasis in rats exposed to chronic intermittent hypoxia-Role of antioxidant (vitamin C) and Ca^{2+} channel blocker (Cilnidipine). *Curr Sign Transduc Thera* 2016;11(1):49-55.

4. Bagali S, Hadimani GA, Biradar MS, Das KK. Introductory Chapter: Primary Concept of Hypoxia and Anoxia. In: Das KK, Biradar MS (ed) Hypoxia and Anoxia, Vol 1. Intech Open, London. 2018:3-11.

5. Birben E, Sahiner UM, Sackesen C, Erzurum S, Kalayci O. Oxidative stress and antioxidant defense. *World Allergy Organ* J 2012; 5(1):9-19.

6. Cao G, Giovanoni M, Prior RL. Antioxidant capacity in different tissues of young and old rats. *Proc Soc Exp Biol Med* 1996; 211(4):359-65.

7. Takahara A. Cilnidipine: A new generation calcium channel blocker with inhibitory action on sympathetic neurotransmitter release. *Cardiovasc Ther* 2009; 27(2):124-39.

8. Hishikawa Keiichi, Takase O, Idei M, Fujito T. Comparison of antioxidant activity of cilnidipine and amlodipine. *Kidney Int* 2009; 76(2):230-1.

9. Das KK, Jargar G, Saha S, Yendigeri SM, Singh SB. -tocopherol supplementation prevents lead acetate and hypoxia – induced hepatic dysfunction. *Indian J Pharmacol* 2015; 47(3):285-91.

10. Paget GE and Barnes JM. Toxicity tests in evaluation of drug activities pharmacometrics (Laurence, D. R. and Bacharach, A. L. eds) Academic Press, London and New York, 1964.

11. Buege JA, Aust SD. Microsomal Lipid peroxidation. *Methods Enzymol* 1978; 52:302-10.

12. Bryan-Brown CW. Blood flow to organs: parameters for function and survival in critical illness. *Crit Care Med* 1988; 16(2):170-8.

13. Jun J, Savransky V, Nanayakkara A, Bevans S, Li J, Smith PL, *et al*. Intermittent Hypoxia has organ – specific effects on oxidative stress. *Am J Physiol Regul Integr Comp Physiol* 2008; 295(4): R1274-81.

14. Kammer AR, Orcezwska JI, O'Brien KM. Oxidative stress is transient and tissue specific during cold acclimation of three spine stickleback. *J Exp Biol* 2011; 214(Pt 8): 1248-56.

15. Viglino D, Julian-Desayes I, Minoves M, Aron-Wisnewsky J, Leroy V, Zarski JP *et al*. Nonalcoholic fatty liver disease in chronic obstructive pulmonary disease. *Eur Respir J* 2017; 49(6).pii:1601923.

16. Kumari S, Qadar PMA, Jain SK. Oxidative stress and histopathological evaluation of rat lung tissue during hypobaric hypoxia. *J Proteo Bioinform* 2015; 8(6):108-15.

Author for Correspondence: Shrilaxmi Bagali, PhD Scholar, Laboratory of Vascular Physiology and Medicine, Department of Physiology, Shri B. M. Patil Medical College, BLDE (Deemed to be University), Vijayapura-586103, Karnataka, India. Email: shrikots@yahoo.in Cell: 09481632615

Subchronic hypoxia pretreatment on brain pathophysiology in unilateral common carotid artery occluded albino rats

Kusal K. Das, Saeed M. Yendigeri[1], Bheemshetty S. Patil[2], Ishwar B. Bagoji[2], R. Chandramouli Reddy, Shrilaxmi Bagali, M. S. Biradar[3], Sikha Saha[4]

Abstract:

OBJECTIVE: This study was aimed to assess the effect of unilateral common carotid artery occlusion on brain pathophysiology in rats pretreated with subchronic hypoxia.

MATERIALS AND METHODS: Rats (200 ± 20 g) were randomized into three groups: Group 1 served as sham, Group 2 were normoxic (21% O_2 and 79% N_2), and Group 3 were hypoxia preconditioned (10% O_2 and 90% N_2) for 21 days before left common carotid artery occlusion (LCCAO). The LCCAO was done for 75 min followed by reperfusion for 12 h. Neurological scores were recorded. Serum malondialdehyde (MDA) and nitric oxide (NO) levels at pre- and 12 h post-LCCAO were measured. Brain histopathological assessments were also done.

RESULTS: Higher neurological deficits scores in Group 2 as compared to Group 3 rats were noticed. Serum MDA and NO levels at 12 h post-LCCAO in Group 2 rats showed significant elevation as compared to preocclusion levels. Group 3 rats did not show such elevations. On histopathology of left and right cerebral hemispheres of Group 1 (sham) did not show any specific changes. In Group 2 rats, the right cerebral hemisphere (nonoccluded) showed no areas of ischemia-induced brain changes, but in the left side (occlusive), there were features of ischemic brain damage including cerebral edema. In the case of Group 3 rats, there were less ischemic damages in the left occluded side as compared to the left side of the Group 2 rats.

CONCLUSION: This study clearly demonstrates that subchronic hypoxia pretreatment can reduce ischemic brain injury by unilateral common carotid artery occlusion in rats.

Keywords:

Brain histopathology, cerebral edema, left common carotid artery occlusion, neurological scores, pretreated hypoxia

Department of Physiology, Laboratory of Vascular Physiology and Medicine, Shri B. M. Patil Medical College, Hospital and Research Centre, BLDE (Deemed to be University), Departments of [2]Anatomy and [3]Medicine, Shri B. M. Patil Medical College, Hospital and Research Centre, BLDE (Deemed to be University), [1]Department of Pathology, Al Ameen Medical College, Bijapur, Karnataka, India, [4]Division of Cardiovascular and Diabetes Research, Leeds Institute of Cardiovascular and Metabolic Medicine, University of Leeds, Leeds, UK

Address for correspondence:
Prof. Kusal K. Das, Department of Physiology, Laboratory of Vascular Physiology and Medicine, Shri B. M. Patil Medical College, Hospital and Research Centre, BLDE (Deemed to be University), Bijapur - 586 103, Karnataka, India.
E-mail: kusaldas@yahoo.com

Submission: 24-09-2017
Accepted: 16-08-2018

Introduction

The significance of cerebrovascular ischemia in medical practices made medical scientists to take up preparation of various experimental ischemic models on rodents.[1] It is reported that after occlusion of extracranial or common carotid artery the functional competence of the intracranial collateral circulation through internal carotid artery and basilar artery protects further ischemic brain damages except some preexisting vascular irregularities or exposure of hypoxia.[2] It is also evidenced that the duration to tolerate cerebral ischemia depends on the severity of ischemia, duration of reperfusion, and many other conditions including metabolic reserves. It is further stated that different areas of brain differentially tolerate ischemia.[3] Studies reported that rats engaged in exercise for 2 weeks before

transient forebrain experimental ischemia show marked improvement in neuronal damages.[4] Hypoxia leads to altered intracellular chemical microenvironment by increasing calcium concentration, lipooxygenase, lipid peroxidation, and cyclooxygenase.[5] Cells exposed to hypoxia follow adaptive changes for its survival. One such response is to activate hypoxia-inducible factors 1α. Hypoxia microenvironment stimulates cell signaling mechanism to stabilize many proteins such as signal transducer and activator of transcription (STAT3) and protein kinase B (Akt) to adapt against ischemic assaults.[6]

The study was aimed to evaluate the consequences of the left common carotid artery occlusion for 75 min and subsequent reperfusion for 12 h on brain histopathology in normoxic (21% O_2) and subchronic hypoxia pretreated (10% O_2 for 21 days) rats.

Materials and Methods

Animals

Adult male Wistar-strain albino rats (*Rattus norvegicus*; 180–200 g, b.wt.) from central animal house of BLDE Deemed to be University Vijayapur, Karnataka, were obtained. Rats were divided into the three groups (*n* = 6 in each group) under 12 h light: 12 h dark cycle to avoid diurnal rhythm. Metabolic wire cage (60 cm × 30 cm × 20 cm) is used to keep maximum 3 rats in each one. Standard pellets (Hindustan Lever, Mumbai, India) were used as normal diet, and drinking water were provided *ad libitum* during the entire experimental protocol.

Experimental groups

Table 1 shows the study design of experimental groups of rats which are divided into three groups with six rats in each group.

Subchronic hypoxia exposure

The hypoxia was set up with the inflow of a combination of air (oxygen 10% and nitrogen 90%) that was regulated by an oxygen analyzer (model 175518A, Gold Edition, Vacuum Med, Sanchung, Taipei). CO_2 was absorbed by soda lime (27 granules), and excess

humidity was removed by a desiccators. The room temperature was maintained at 24°C–26°C. Twice in a week for 1 h, the hypoxia chamber was opened to clean the cages and provide food and water. The exposure to low oxygen in all the rats of Group 3 was continued for 21 days.[7]

Experimental protocol

Group 1 served as sham, Group 2 was normoxic, and Group 3 served as hypoxic. Electrocardiography (ECG) and pneumogram were recorded using Biopac (MP 45) before, during the surgical procedure and after 12 h of reperfusion. Data were evaluated and analyzed with SPSS version 16.0 (SPSS Inc., Chicago, USA).

Group 1 (sham) was taken as a control group; Group 2 (normoxic) was exposed with normal atmospheric oxygen under normal pressure, and Group 3 (hypoxic) was exposed to subchronic sustained hypoxia by keeping the rats in 10% oxygen and 90% nitrogen for 21 days as per the standard protocol before left CCA occlusion. The occlusion (genuine and sham) of the left common carotid artery at carotid triangle level was performed in all the rats of Group 1, Group 2, and Group 3 under proper anesthesia (Ketamine, 60 mg/kg b.wt and Xylazine, 6 mg/kg b.wt.).[8] Sham operations in Group 1 rats were performed by similar left common carotid artery occlusion (LCCAO) technique except occlusion and allowing instant reperfusion.[9] Once the left carotid artery at the carotid triangle was exposed, it was occluded for 75 min in all the rats of Group 2 and Group 3 [Figure 1]. After 75 min, carotid occlusion was slowly released, surgical incision was closed with catgut, and reperfusion was allowed for 12 h till sacrifice.[10] Utmost postoperative care was taken for each rat. At the end of 12 h, all three groups of rats were euthanized by deep anesthesia. Before the sacrifice, blood samples were collected from retro-orbital plexus. Blood samples were also collected in a similar way before LCCAO from

Table 1: Experimental groups of rats (*n*=6 in each group)

Groups	Experimental protocols
Group 1	Sham operation (surgical incision at carotid triangle, no occlusion and immediate allow for instant reperfusion)
Group 2	Normoxia, 21% oxygen (75 min LCCAO and subsequent reperfusion for 12 h)
Group 3	Hypoxia (10% oxygen) pretreatment for 21 days (subchronic) before 75 min LCCAO and reperfusion for 12 h

LCCAO=Left common carotid artery occlusion
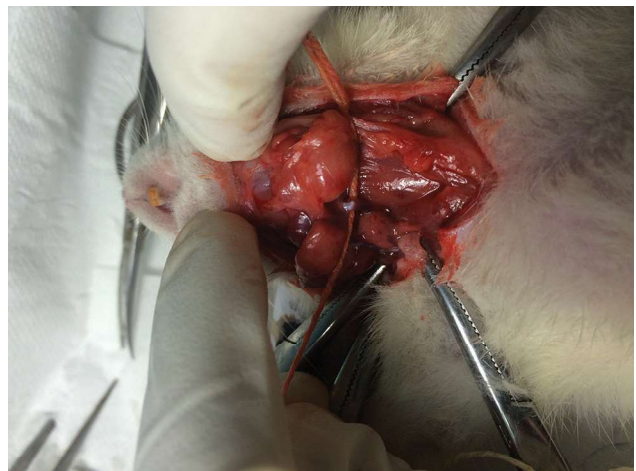
Figure 1: Ligation of the left common carotid artery with silicon thread

all the rats of Group 1, Group 2, and Group 3. The brain was carefully dissected out and immersion fixed in 10% formalin for 2 days. Serum malondialdehyde (MDA) levels as a marker of oxidative stress were assessed in all the three groups of rats before the occlusion and after 12 h of reperfusion by Kei Satoh method.[11] Similarly, serum nitric oxide (NO), a nitrosative stress marker, and also a regulator of oxidative stress were estimated using Griess reagents spectrophotometrically.[12]

Neurological scores

Neurologic examinations were performed on all the rats in Group 1, Group 2, and Group 3 in just before the sacrifice. Neurological scores were evaluated as per standard protocol.[13]

Histopathological procedure

Cerebral hemispheres were sliced into coronal slices of 2-mm thickness. The brain stem was cut vertical to its long axis. The cerebellum also cut into two slices perpendicularly to the folia of the dorsal angle of each hemisphere. Bilateral blocks of the brain were embedded in paraffin wax and sections were cut on a rotary microtome from 2.0 μ to 3.0 μ and stained with routine hematoxylin and eosin (H and E) stains. The brain sections of all animals were examined under a conventional light microscopy (Olympus CH20i) with Samsung Digital Color Camera, Model No. SDC-242, N. J 07094, U. S. A.

Statistical analysis

Results were obtained as mean ± standard deviation values for each group. To determine the significance of intergroup differences, one-way analysis (ANOVA) followed by "*post hoc t*-test" were done.

Ethics

Animal experiments were conducted as per the ethical norms approved by CPCSEA, the Ministry of Social Justice and Empowerment, Government of India (Reg. No. 1076/PO/ERs/S/07 CPCSEA dated Aug 20.,2014), and Institutional Animal Ethical Committee, BLDE University, Vijayapur (BLDE/BPC/641/2016-17 dated Aug 22, 2016).

Results and Discussion

Physiological and biochemical parameters

The ECG pattern (heart rate [HR]), pneumogram (respiratory rate [RR]), and blood pressure (systolic blood pressure [BP], diastolic BP, and mean arterial pressure) were also found within normal ranges during the entire experimental protocol in all the animals of all the groups till sacrifice [Table 2]. Results suggested that no vital parameters such as HR, BP, and RR were affected in all the three groups during the entire experimental procedure. After 12 h of reperfusion and just before sacrifice, we observed cognitive and neurological impairments in Group 2 and Group 3 rats [Table 3]. Results showed the maximum neurological deficit scores in Group 2 (normoxia) rats (35/60; 58%) followed by Group 3 (subchronic hypoxia pretreatment) rats (26/60; 43%). Oxidative and nitrosative stress levels were measured by assessing serum MDA, and NO in Group 2 (normoxic) rats following 12 h of reperfusion showed a significant increase compared to preocclusion levels. In the case of subchronic hypoxia pretreated rats (Group 3), no such significant alteration of MDA and NO levels (pre vs post) were observed [Figures 2 and 3]. Higher MDA and NO levels in Group 3 rats before surgery (pre-LCCAO) may be due to hypoxia-induced lipid peroxidation, and subsequently, the formation of peroxynitrites due to exposure of subchronic hypoxia but such preconditioning actually facilitate greater adaptation from cerebral ischemic stress (post-LCCAO) induced lipid peroxidation. The increase of lipid peroxidation or rise of reactive oxygen species and reactive nitrogen species may probably induce neuronal injury from apoptosis and further contribute to ischemic brain injuries. Our results indicate a greater protection from oxidative stress-induced inflammatory response due to LCCAO in rats preconditioned with hypoxia.[14]

**Table 2: Cardiovascular and respiratory parameters of all the group of rats**

Group	Status	HR (bpm)	SBP (mmHg)	DBP (mmHg)	RR (cycles/min)
Group 1	Before occlusion	273.45±45.34	100.23±13.23	75.50±15.50	14.34±5.35
	During occlusion	289.45±40.50	96.78±20.50	70.56±10.50	12.50±7.60
	Re-perfusion after 12 h	280.56±47.00	99.00±19.50	73.50±19.00	12.70±5.70
Group 2	Before occlusion	270.25±35.45	104.23±20.45	73.45±11.54	15.50±5.00
	During occlusion	290.45±54.50	105.56±21.34	78.00±18.50	15.50±5.20
	Re-perfusion after 12 h	285.00±67.00	98.90±18.00	70.68±12.50	13.75±7.50
Group 3	Before occlusion	290.25±76.50	100.45±15.34	69.50±12.45	14.45±5.50
	During occlusion	291.45±6.50	103.34±20.00	73.92±18.34	15.50±6.00
	Re-perfusion after 12 h	285.00±67.00	98.50±20.00	72.23±11.02	15.70±7.00
P		0.095	0.120	0.085	0.110

Values are mean±SD of each group (*n*=6). Group 1=Sham operated, Group 2=Normoxic, Group 3=Subchronic hypoxia pretreated, HR=Heart rate, SBP=Systolic blood pressure, DBP=Diastolic blood pressure, RR=Respiratory rate, SD=Standard deviation

Table 3: Neurological deficit scores after 12 h reperfusion and before sacrifice

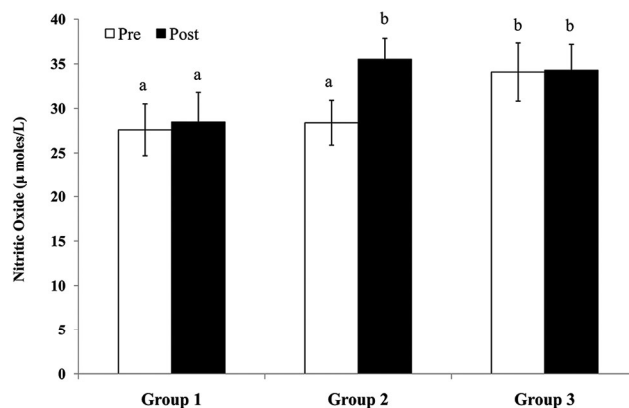| Neurological signs	Score (0-5 scale) for each rat	Total scores (*n*=6)		
		Group 1	Group 2	Group 3
Failure to extend left forepaw fully	1	0	6	4
Circling to the left	2	0	12	12
Falling to the left	3	0	9	6
Did not walk spontaneously	4	0	8	4
Grand total score	10 × 6=60	0	35 (58%)	26 (43%)
Mean±SD		0	5.833±3.430	4.333±3.141*

Mean±SD values of Group 2 and Group 3 are statistically significant from each other (*$P<0.05$). Group 1=Sham operated, Group 2=Normoxia, Group 3=Hypoxia pretreatment for 21 days, SD=Standard deviation
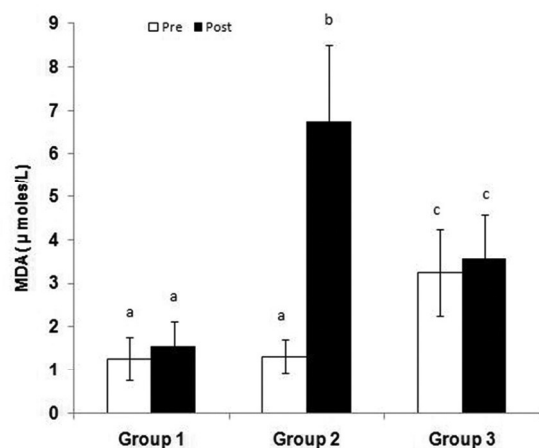
Figure 2: Serum malondialdehyde levels in Group 1 (sham), Group 2 (normoxia), and Group 3 (subchronic hypoxia pretreated) rats before (pre) left common carotid artery occlusion and 12 h after reperfusion (post). *n* = 6 rats in each group. Values with different superscripts (a and b) are significantly differ from each other (*P* < 0.05)


Figure 3: Serum nitric oxide levels in Group 1 (sham), Group 2 (normoxia), and Group 3 (subchronic hypoxia pretreated) rats before (pre) left common carotid artery occlusion and 12 h after reperfusion (post). *n* = 6 rats in each group. Values with different superscripts (a and b) are significantly differ from each other (*P* < 0.05)

Histopathological observations in cerebral cortex

Sections of all the three groups under H and E stain were studied serially on the left and right cerebral hemispheres of the brain (*n* = 6), from the frontoparietal cortex and dorsolateral portion of the neostriatum. Figure 4a to l shows H- and E-stained sections of the left and right cerebral hemispheres of the brain. The sections from sham animals showed normal cerebral cortex consisting of gray matter made of cell bodies of neurons and glial cells along with their processes blood vessels and white matter made up of bundles of axons. No visible pathology was noted in the group. The blood vessels appeared normal on both sides of the hemispheres [Figure 4c and d]. Group 2 (normoxic with left-CCA occlusion) reveals histopathological changes in gray matter of left cerebral cortex with a decrease in number of pyramidal cells and stellate (granular) cells which appear to be small, multipolar, and vacuolated to eosinophilic cytoplasm and pyknotic nuclei [Figure 4e]. There were foci of wedge-shaped areas of cerebral infarcts with diffuse interstitial edema of the cerebrum [Figure 4g]. The junction between gray and white matter was blurred. Right cerebral hemisphere of the brain (nonoccluded side) showed normal brain

parenchyma [Figure 4f and h]. Group 3 (subchronic hypoxia pretreated rats with left-CCA occlusion subsequently sacrifice after 12 h) shows in the gray matter of cerebral cortex, a decrease in number of pyramidal cells, small multipolar stellate (granular) neurons, and vacuolated eosinophilic cytoplasm with pyknotic nuclei having features of early cellular damage (Red cells) in the left cerebral hemisphere [Figure 4i]. There were also foci of interstitial edema of the left cerebrum but without the features of cerebral ischemia which were observed in case of Group 2 experimental animals [Figure 4k]. Besides these findings, blurring of the junction between gray and white matter was also noticed in Group 3 rats (subchronic hypoxia pretreated). Right cerebral hemisphere of brain (nonoccluded side) of Group 3 rats showed normal brain parenchyma. Dilated blood vessels, lined with prominent blood vessels cells on the right side of the hemispheres, were also observed in Group 3 rats [Figure 4j and l].

Histopathological observations in subcortex

There were no changes in the subcortical structures of sham-operated rats [Figure 5a]. In case of Group 2 (normoxic), most of the caudate nuclei, internal capsule, globus pallidus, substantia nigra, and putamen of basal ganglia showed small lacunar infarcts [Figure 5b],
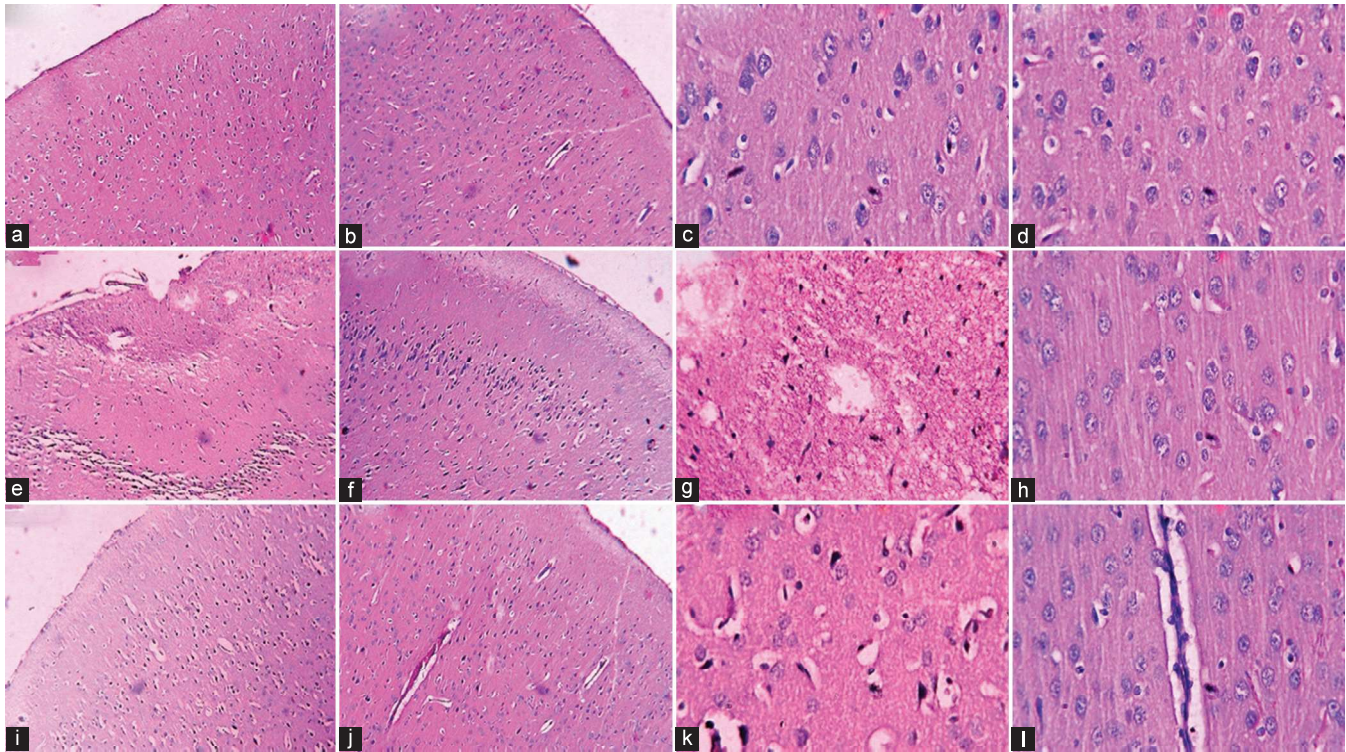
Figure 4: Hematoxylin and Eosin stain showing (a) sham's left cerebral cortex (×10), (b) sham's right (×10), (c) sham's left cerebral cortex (×40), (d) sham's right (×40), (e) normoxic left (occluded) cerebral cortex (×10), (f) normoxic right (nonoccluded) (×10), (g) normoxic left (occluded) cerebral cortex (×40), (h) normoxic right (nonoccluded) (×40), (i) hypoxia pretreated left (occluded) cerebral cortex (×10), (j) hypoxia pretreated right (non occluded) (×10), (k) hypoxia pretreated left (occluded) cerebral cortex (×40), and (l) hypoxia pretreated right (nonoccluded) (×40)
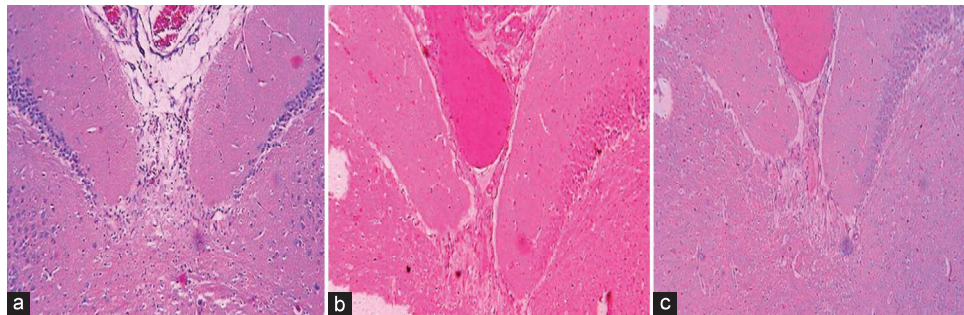
Figure 5: Photomicrograph stained with hematoxylin and eosin stain showing subcortical structures mainly the caudate nuclei, internal capsule, globus pallidus, substantia nigra, and putamen of basal ganglia (×10) of (a); sham's left and right side, (b); normoxic left (occluded side) and right (nonoccluded) side, and (c); subchronic hypoxia pretreated left (occluded side) and right (nonoccluded) side

whereas Group 3 (subchronic hypoxia pretreated) rats such small lacunar infarcts were found relatively less as compared to normoxic rats. This group showed pallor of staining and vacuolization of the white matter [Figure 5c].

The partial/incomplete infarct section, defined as the area with lack of staining (pallor or failure to perfuse) of the cortex, brain edema, cell body degeneration, and suggestive of early focal neuronal damage (red neurons), was determined from serially cut sections from the frontoparietal cortex and dorsolateral portion of the neostriatum of both left (ischemia-induced) and right brain hemispheres of all the sham, normoxic, and subchronic hypoxia pretreated rats ($n = 6$). In normoxic rats, there were no areas of ischemia-induced brain changes in the right side of the (nonoccluded) cerebral hemisphere and left side (left occluded side), there were features of diffuse global ischemic brain damage involving mainly frontal, frontoparietal regions of the cortex, and basal ganglia (striatum), particularly in the lateral segment of the caudate.[15] The striking feature in both sides of the brain in subchronic hypoxia pretreated rat was the dilated blood vessels lined by prominent endothelial cells signifying a compensatory mechanism in response to subchronic hypoxia. The reduced brain damage in subchronic hypoxic pretreated rats was well correlated morphologically with vascular adaptive

changes whereas the changes of occipital cortex and medial striatum were concerned only uncommonly and variable elsewhere. In contrast to the left side of the subchronic hypoxia pretreated rats with less ischemic damages, the left side of the normoxic rats showed more extensive damages.[16]

Our study demonstrated a reduction in brain edema associated with reduced infarct volume in animals preconditioned (21 days) to subchronic hypoxia by comparing the infarct size difference in brain between the left (ischemic site) and right (nonischemic) hemispheres [Figure 4e-k]. Hypoxia preconditioned for 21 days before cerebral ischemia possibly reduced the ischemic alterations and decreased ischemic brain damage after focal ischemia.[17] These observations are further supported by neurological deficit scores and serum MDA and NO levels while comparing in both Group 2 and Group 3 rats. Results also showed that subchronic hypoxia preconditioning (Group 3) increases both serum MDA and NO levels at pre-LCCA occlusions as compared to respective normoxic Group 2 experimental animals [Figures 2 and 3]. Interestingly, both serum MDA and NO levels of Group 3 did not further change after occlusion from preocclusion values at the end of 12 h reperfusion (post) period. Nonsignificant changes of both serum MDA and NO between pre- and post-LCCA occlusion in Group 3 (subchronic hypoxia pretreated) reflects lesser LCCA occlusion induced oxidative and nitrosative stresses in Group 3 (subchronic hypoxia pretreated) as compared to Group 2 (normoxia). Some studies on mice showed acute hypoxia preconditioning protect against transient focal cerebral ischemia, but our study demonstrated for the first time that subchronic preconditioning with hypoxia protects the brain injury against transient focal ischemia induced by unilateral carotid artery occlusion.[18]

This hypoxic model could serve as a helpful plan to remodel ischemic brain injury from cerebral ischemia including stroke. The exact mechanism underlying this neuroprotective effect of preconditioned/pretreated subchronic hypoxia remains obscure. Although further studies are needed to establish true cerebrovascular pathophysiology on unilateral common carotid artery occlusion with reference to subchronic hypoxia pretreatment, it may be considered as a possible protective strategy to ameliorate ischemic brain injury from cerebral focal ischemia or stroke. Further, it has been reported from a clinical study that hypoxia preconditioning provides more protective cardiometabolic profile.[19] Hypoxia preconditioning was also found to be beneficial to promote mesenchymal stem cells proliferation which facilitates intrastriatal transplantation and support therapeutically to fight against Parkinson's disease.[20]

Conflicts of interest

There are no conflicts of interest.

References

1. Ding YH, Ding Y, Li J, Bessert DA, Rafols JA. Exercise pre-conditioning strengthens brain microvascular integrity in a rat stroke model. Neurol Res 2006;28:184-9.
2. Tamura A, Graham DI, McCulloch J, Teasdale GM. Focal cerebral ischaemia in the rat: 1. Description of technique and early neuropathological consequences following middle cerebral artery occlusion. J Cereb Blood Flow Metab 1981;1:53-60.
3. Payabvash S, Souza LC, Wang Y, Schaefer PW, Furie KL, Halpern EF, *et al.* Regional ischemic vulnerability of the brain to hypoperfusion: The need for location specific computed tomography perfusion thresholds in acute stroke patients. Stroke 2011;42:1255-60.
4. Hossmann KA. Experimental models for the investigation of brain ischemia. Cardiovasc Res 1998;39:106-20.
5. Stummer W, Weber K, Tranmer B, Baethmann A, Kempski O. Reduced mortality and brain damage after locomotor activity in gerbil forebrain ischemia. Stroke 1994;25:1862-9.
6. Das KK, Saha S. Hypoxia, lead toxicities and oxidative stress: Molecular interactions and antioxidant (Vitamin C) defense. Curr Signal Transduct Ther 2014;9:113-22.
7. Das KK, Jargar JG, Saha S, Yendigeri SM, Singh SB. A-tocopherol supplementation prevents lead acetate and hypoxia-induced hepatic dysfunction. Indian J Pharmacol 2015;47:285-91.
8. Bronner G, Mitchell K, Welsh FA. Cerebrovascular adaptation after unilateral carotid artery ligation in the rat: Preservation of blood flow and ATP during forebrain ischemia. J Cereb Blood Flow Metab 1998;18:118-21.
9. Engel O, Kolodziej S, Dirnagl U, Prinz V. Modeling stroke in mice - middle cerebral artery occlusion with the filament model. J Vis Exp 2011. pii: 2423.
10. Thanvi B, Robinson T. Complete occlusion of extracranial internal carotid artery: Clinical features, pathophysiology, diagnosis and management. Postgrad Med J 2007;83:95-9.
11. Satoh K. Serum lipid peroxide in cerebrovascular disorders determined by a new colorimetric method. Clin Chim Acta 1978;90:37-43.
12. Moshage H, Kok B, Huizenga JR, Jansen PL. Nitrite and nitrate determinations in plasma: A critical evaluation. Clin Chem 1995;41:892-6.
13. Longa EZ, Weinstein PR, Carlson S, Cummins R. Reversible middle cerebral artery occlusion without craniectomy in rats. Stroke 1989;20:84-91.
14. Shi S, Yang W, Tu X, Chen C, Wang C. Ischemic preconditioning reduces ischemic brain injury by suppressing nuclear factor kappa B expression and neuronal apoptosis. Neural Regen Res 2013;8:633-8.

15. Uluç K, Miranpuri A, Kujoth GC, Aktüre E, Başkaya MK. Focal cerebral ischemia model by endovascular suture occlusion of the middle cerebral artery in the rat. J Vis Exp 2011. pii: 1978.

16. Das KK, Das S, Ambekar JG. Hypoxia and oxidative stress: Cell signalling mechanisms and protective role of Vitamin C and cilnidipine. In: Catala A, editors. Lipid Peroxidation: Inhibition, Effects and Mechanisms. 1st ed. New York: Nova Publishers; 2017. p. 249-62.

17. Guo M, Cox B, Mahale S, Davis W, Carranza A, Hayes K, *et al.* Pre-ischemic exercise reduces matrix metalloproteinase-9 expression and ameliorates blood-brain barrier dysfunction in stroke. Neuroscience 2008;151:340-51.

18. Bernaudin M, Nedelec AS, Divoux D, MacKenzie ET, Petit E, Schumann-Bard P, *et al.* Normobaric hypoxia induces tolerance to focal permanent cerebral ischemia in association with an increased expression of hypoxia-inducible factor-1 and its target genes, erythropoietin and VEGF, in the adult mouse brain. J Cereb Blood Flow Metab 2002;22:393-403.

19. Glazachev O, Kopylov P, Susta D, Dudnik E, Zagaynaya E. Adaptations following an intermittent hypoxia-hyperoxia training in coronary artery disease patients: A controlled study. Clin Cardiol 2017;40:370-6.

20. Wang Y, Yang J, Li H, Wang X, Zhu L, Fan M, *et al.* Hypoxia promotes dopaminergic differentiation of mesenchymal stem cells and shows benefits for transplantation in a rat model of parkinson's disease. PLoS One 2013;8:e54296.